Technische Universität München
TUM School of Management

The cost of renewable energy and battery electricity storage

Lukas Enno Kemmer

Vollständiger Abdruck der von der TUM School of Management der Technischen Universität München zur Erlangung des akademischen Grades eines Doktors der Wirtschafts- und Sozialwissenschaften (Dr. rer. pol.) genehmigten Dissertation.

Vorsitz:	Prof. Dr. Hanna Hottenrott
Prüfende der Dissertation:	1) Prof. Dr. Gunther Friedl
	2) Prof. Dr. Sebastian Schwenen

Die Dissertation wurde am 09.09.2024 bei der Technischen Universität München eingereicht und durch die TUM School of Management am 15.11.2024 angenommen.

Acknowledgements

I'm extremely grateful to . . .

. . . my supervisor Gunther Friedl for his invaluable guidance and feedback and for providing a work environment that has enabled me to make these years some of the most enriching of my academic and professional live yet.

. . . my partner Katrin Schnürle for her relentless and unconditional love, companionship, and support throughout this journey.

. . . my parents, my sister, and my family for raising me to be determined, open-minded, and curious, and for always supporting me and my decisions.

. . . my office colleagues Maximilian Blaschke and Yanis Gamarra for the countless laughs we shared.

. . . and all of my other colleagues at the Technical University of Munich for the inspiring discussions and the open-minded and positive atmosphere at our chair.

Abstract

To reduce the adverse effects of climate change, decarbonization efforts are required across all sectors. The energy and transportation sectors play an important role in this effort but the high investment costs of low carbon technologies can lead to challenges in cost competitiveness. Subsequently, in the energy sector the Levelized Cost of Electricity (LCOE), which aggregate investment expenditures and operating costs, have emerged as the dominant unit cost measure to assess the cost-competitiveness of different electricity generation technologies. The first essay of this dissertation reviews the literature on Levelized Cost (LC). It shows that today, LC is mostly applied in electricity generation and -storage, hydrogen, and carbon capture, and suggests further use cases, e.g. in transportation. In the transportation sector, high purchase cost driven by battery prices are an important barrier to the widespread adoption of Electric Vehicles (EVs). This challenge is addressed by the second essay which introduces a bottom-up cost model for EV batteries and compares the production cost of two state-of-the-art battery designs. It also introduces the Levelized Cost of Battery Production (LCBP) and shows that they can be a more accurate cost measure compared to Full Cost (FC) and Marginal Cost (MC). Besides differences in production cost, different battery designs also have different performance characteristics, e.g. their capacity degradation. The third essay takes these performance characteristics into account and analyzes their influence on the optimal system size and cost competitiveness of residential rooftop Solar Photovoltaic (PV) and Battery Electricity Storage (BES) systems. It finds that modern lithium- and sodium-based batteries are significantly more economical than traditional sodium-calcium or lead-based batteries and shows that a large-scale roll-out of residential PV and BES systems could reduce the electricity produced from fossil fuels in Germany. The three essays contribute to existing literature by highlighting the importance of cost models and -measures to select technologies for a cost-efficient decarbonization of the energy and transportation sector.

Contents

List of Figures

List of Tables

Abbreviations

BatPac Argonne National Laboratories Battery Performance and Cost Model

BES Battery Electricity Storage

CAES Compressed Air Energy Storage

CCS Carbon Capture and Sequestration

CCU Carbon Capture and Utilization

COP Conference of Parties

COP21 2015 United States Climate Change Conference

DAC Direct Air Capture

DOD Depth of Discharge

EFC Equivalent Full Cycles

EU European Union

EV Electric Vehicle

FC Full Cost

FIT Feed-In Tariff

G Graphite

GHG Greenhouse Gases

ICE Internal Combustion Engine

ITC Investment Tax Credit

LA Lead Acid

LC Levelized Cost

LCBP Levelized Cost of Battery Production

LCOC Levelized Cost of Carbon

LCOE Levelized Cost of Electricity

LCOH Levelized Cost of Hydrogen

LCOS Levelized Cost of Energy Storage

LCXM Levelized Cost per X-mile

LFP Lithium-Iron-Phosphate

LIB Lithium-Ion Batteries

MC Marginal Cost

NAE Net Additional Electricity

NCX Sodium-Calcium Exchanger

NDC Nationally Determined Contribution

NPV Net Present Value

OCV Open-Circuit-Voltage

OEM Original Equipment Manufacturer

PBCM Process-Based-Cost-Modelling

PHS Pumped-Hydro Storage

PV Solar Photovoltaic

RES Renewable Energy Sources

RTE Round-Trip Efficiency

SEI Solid Electrolyte Interface

SIB Sodium-Ion Battery

SOC State of Charge

TCO Total Cost of Ownership

WEF World Economic Forum

1 | Introduction

1.1 Motivation

Climate change is one of the biggest challenges of the 21st century. It describes changes in the Earth's climate system, such as global warming or shifts in precipitation and wind patterns. Climate change is primarily the result of human activities that lead to the emission of Greenhouse Gases (GHG) into the atmosphere, for example, from burning fossil fuels for electricity generation or in the Internal Combustion Engines (ICEs) of cars (Intergovernmental Panel on Climate Change, 2023). As shown in Figure 1.1a, GHG emissions from human activity have increased materially since 1850 with a notable acceleration after 1950. As a result of these emissions, the atmospheric concentrations of some of the most important GHGs, carbon dioxide (CO_2), methane (CH_4), and nitrous oxcide (N_2O), have increased, as depicted in Figure 1.1b. In the same time frame, the global surface temperature has increased by around 1.1°C in 2011-2020 compared to 1850-1900 levels (Intergovernmental Panel on Climate Change, 2023). To put this temperature increase into perspective and highlight its magnitude, it can be compared with the estimated temperature during the warmest multi-century period in the last 100,000 years which was around 0.2 to 1.0°C above the 1850-1900 levels and occurred ca. 6,500 years ago. Overall, detection and attribution studies show that the best explanation for the temperature increases is human activity (Intergovernmental Panel on Climate Change, 2023). Apart from increases in temperature levels, other effects of climate change that can already be seen today are increasing amounts of extreme weather events such as heatwaves, droughts, floods, or wildfires.

In the future, climate change could lead to rising sea levels, water scarcity, and the disruption of entire ecosystems. Therefore, as depicted in Figure 1.2, the World Economic Forum (WEF) expects climate-related risks to be the predominant and highest-ranked risk factors both in the short- and long-term (World Economic Forum, 2023).

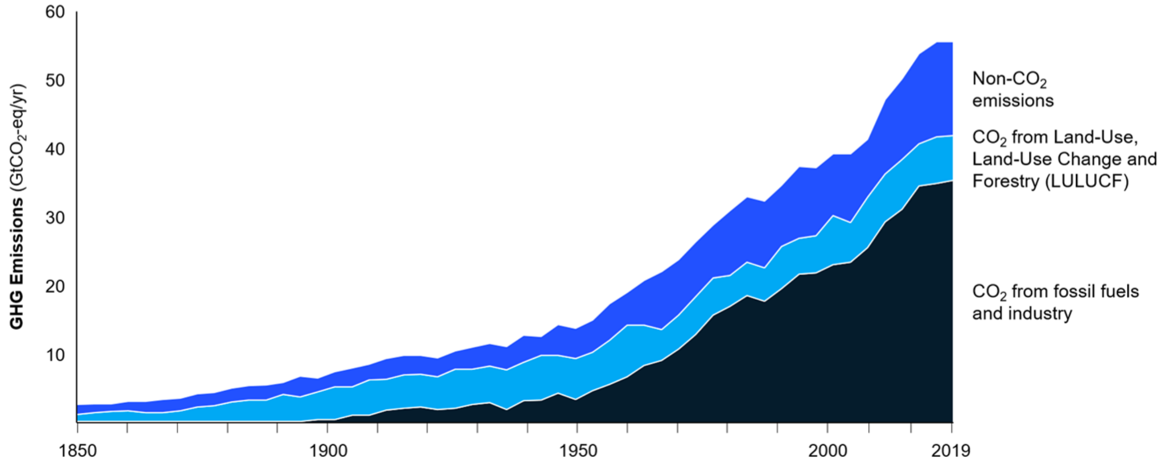

(A) GHG emissions (from human activity) since 1850.

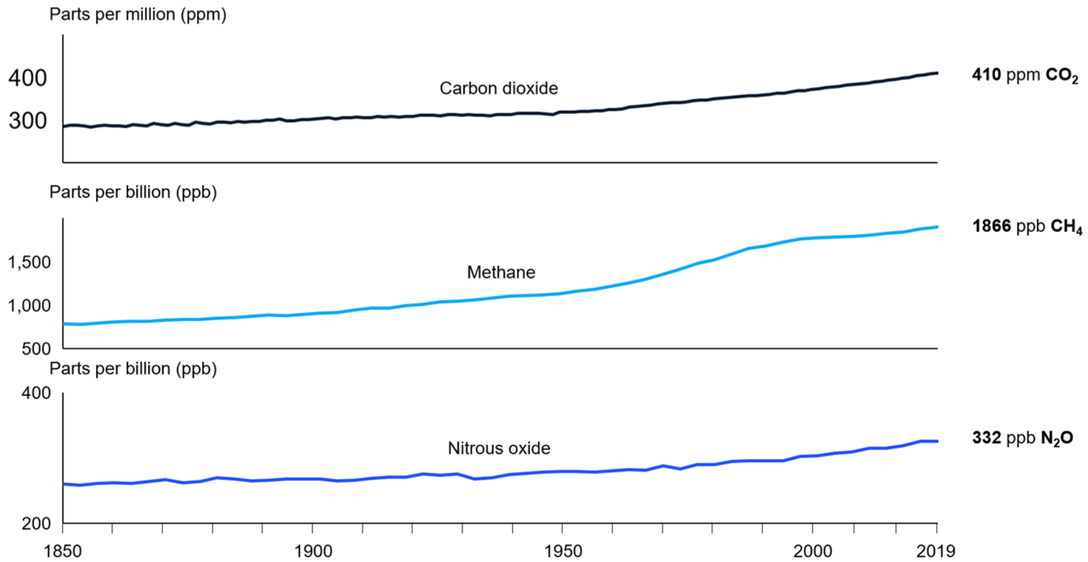

(B) Concentration of CO_2, CH_4, and N_2O since 1850.

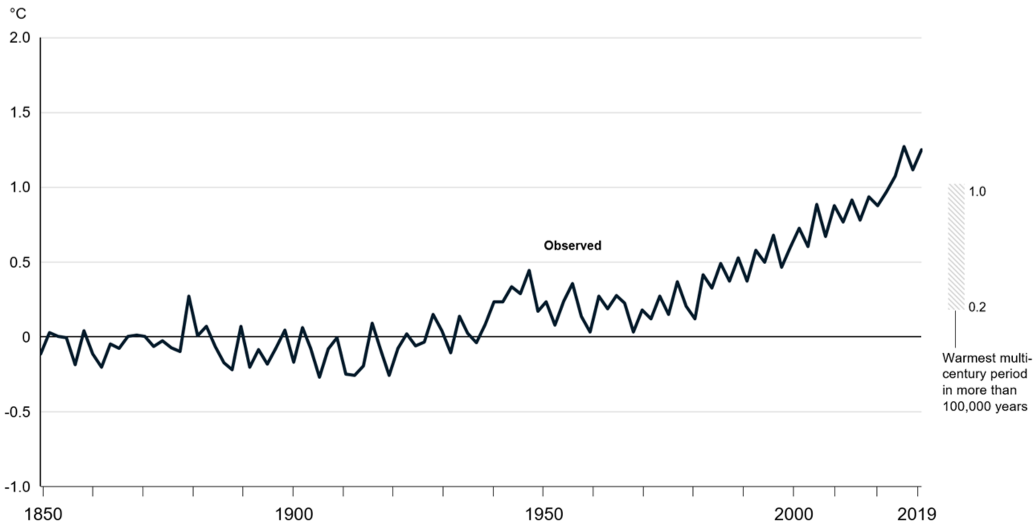

(C) Increase in global surface temperatre since 1850.

FIGURE 1.1: The relation between human caused CO_2 emissions and global warming (own representation after Intergovernmental Panel on Climate Change, 2023)

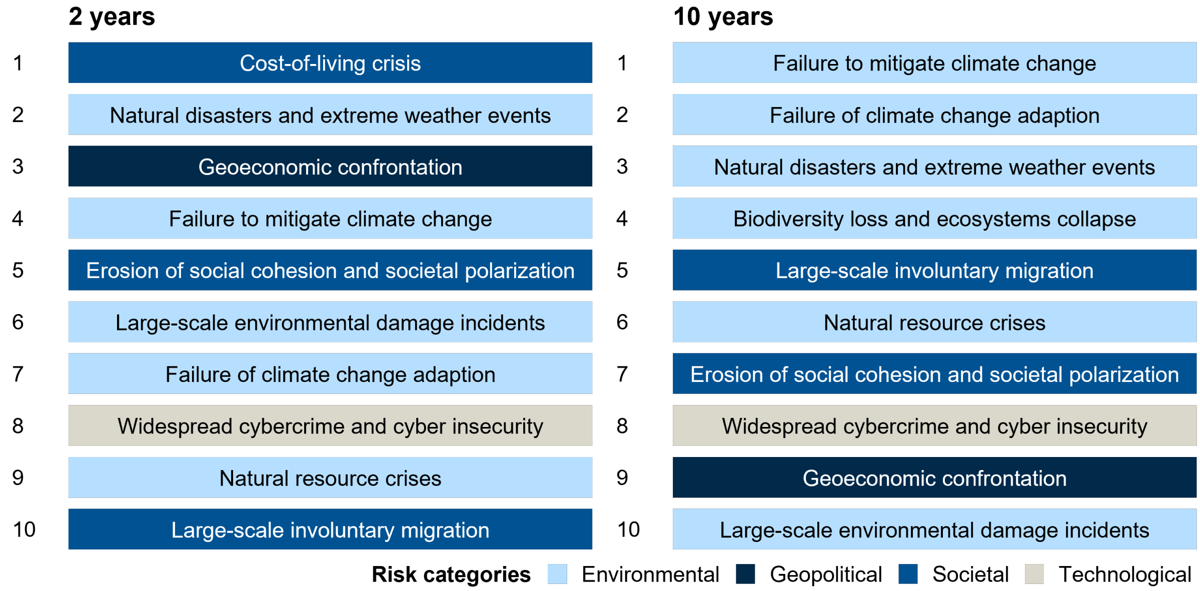

FIGURE 1.2: Global risks ranked by severity over the short and long term (own representation after World Economic Forum, 2023)

In addition to the magnitude of the challenge, several factors make climate change a complex and hard-to-tackle problem: (1) Climate change is a global problem that requires all countries to collectively reduce their GHG emissions, regardless of geopolitical conflicts and international competition. (2) It includes many interrelated factors across sectors. For example, electrification could help reduce direct emissions in the transport sector, but the additional electricity demand could increase emissions in the energy sector, and the need for batteries could increase emissions from mining and manufacturing. (3) In many sectors, there are already viable low-carbon technologies, such as solar PV, wind energy, or hydrogen, but implementing them requires significant investments. (4) Many actions necessary to tackle climate change could lead to significant economic and social challenges. For instance, the introduction of carbon prices could increase the cost of energy and goods and place a serious burden on low-income households. Furthermore, they could increase the production cost of companies from energy-intensive industries and reduce their competitiveness compared to companies in areas that are not subject to such policies. (5) Even though the first effects of climate change can already be seen today, many of its more severe implications will only be fully visible in the future.

Local and regional solutions to a global problem

Due to the scale and complexity of the problem, in 1992, the UN Framework Convention on Climate Change was adopted. It stipulates that the signing parties should meet regularly to address climate change at the Conference of Parties (COP). After a series of failed attempts to negotiate a global agreement on GHG emissions reductions, during the 2015 United States Climate Change Conference (COP21) in Paris, the so-called Paris Agreement was negotiated to find a global solution to climate change. The Paris Agreement is an international treaty signed by 195 countries and the European Union (EU) to keep global warming to well below 2°C above pre-industrial levels and to preferably limit the temperature increase to 1.5°C above pre-industrial levels, which would substantially reduce the adverse effects of climate change.

Limiting global warming to 1.5°C requires GHG emissions to peak in the early 2020s, to decline by at least 43% by 2030, and to achieve net zero emissions in the early 2050s (Intergovernmental Panel on Climate Change, 2023). To achieve this goal, each country that has signed the Paris Agreement must regularly determine individual, Nationally Determined Contributions (NDCs) for decarbonization, set up a plan to achieve them and report on their progress. In this process, each update of the NDCs should be more ambitious than the previous one, but there are no rules to set specific emission targets and no mechanism to ensure that the collective NDCs suffice to achieve the goals of the Paris Agreement. Subsequently, current NDCs likely do not suffice to limit global warming to 1.5°C and make it hard to limit global warming to 2 °C (Intergovernmental Panel on Climate Change, 2023).

One signatory that has been very vocal about its ambitions to limit climate change is the EU. Despite being only the third largest GHG emitter (after China and the United States) with a contribution of 8% of global GHG emissions (European Environment Agency, 2020), the EU has set ambitious GHG reduction targets. After an initial NDC pledging a 40% reduction of GHG emissions[1], the EU submitted an updated and enhanced NDCs in December 2020, pledging to reduce GHG emissions by 55% in 2030[1]. To support this effort, in 2020, the EU approved the European Green Deal, a set of policy initiatives by the European Commission, aiming to reduce GHG emissions by at least 55% by 2030[1] and to become the first climate-neutral continent by 2050. To deliver the Green Deal, multiple initiatives with sector-specific targets, for example, for energy and transportation, were launched. In the energy sector, a binding target of at least

[1] Compared to 1990 levels.

40% renewables in the energy mix and a reduction of 36-39% for final and primary energy consumption by 2030 were set (Council of the European Union, 2022). In the transport sector, a 55% emission reduction target is set for cars in 2030. In addition, from 2035 on, all new cars must be EVs or use combustion engines fueled by zero-emission fuels (European Parliament, 2023).

Germany is the largest GHG emitter in the EU (Statista GmbH, 2022a). Therefore, to achieve the EUs NDCs, it is crucial to reduce German emissions significantly. Notably, climate protection is anchored in Article 20a of the German Basic Law which the German Federal Constitutional Court interprets as achieving the targets of the Paris Agreement (Bundesverfassungsgericht, 2021). In 2021, the Federal Constitutional Court ruled that the previous climate law, which aimed to reduce GHG emissions by at least 55% by 2030, was incompatible with fundamental rights because it did not provide sufficient specifications for emissions reductions from 2031 onwards. More specifically, the court reasoned that the challenged climate law would postpone severe emissions reductions into periods after 2030 which would then affect the basic freedom rights of the, in some cases, still very young complainants. This is because achieving the emissions reductions necessary to comply with the Paris Agreement after 2030 could require severe restrictions in every aspect of human life (Bundesverfassungsgericht, 2021). Reacting to this, the governing centre-left-green-liberal coalition increased and pulled forward the GHG reduction targets to a reduction of 65% by 2030, 88% by 2040, and net zero by 2045, compared to 1990 levels (KSG, 2021). For the transport sector, this is translated into a reduction of 49% until 2030. To achieve this, among others, the number of registered EVs is planned to increase from one million in 2022 to between seven and ten million in 2030 (ADAC, 2023, Bundesministerium für Umwelt, Naturschutz, nukleare Sicherheit und Verbraucherschutz). For the energy sector, a reduction of 65% until 2030 needs to be achieved. To do so, a significant expansion of solar PV and wind energy to 215 GW and 145 GW[2] respectively is planned to aid in achieving an 80% share of Renewable Energy Sourcess (RESs) (Die Bundesregierung, 2023) in the electricity mix.

Decarbonization is a cross-sectoral task

As depicted in Figure 1.3, significant efforts to reduce GHG emissions must be made across all sectors to achieve net zero emissions by 2050 to limit global warming to 1.5 °C. Depending on the sector, these efforts include transitioning to RES, increasing circularity, or replacing

[2] 30 GW of offshore and 115 GW of onshore wind capacity.

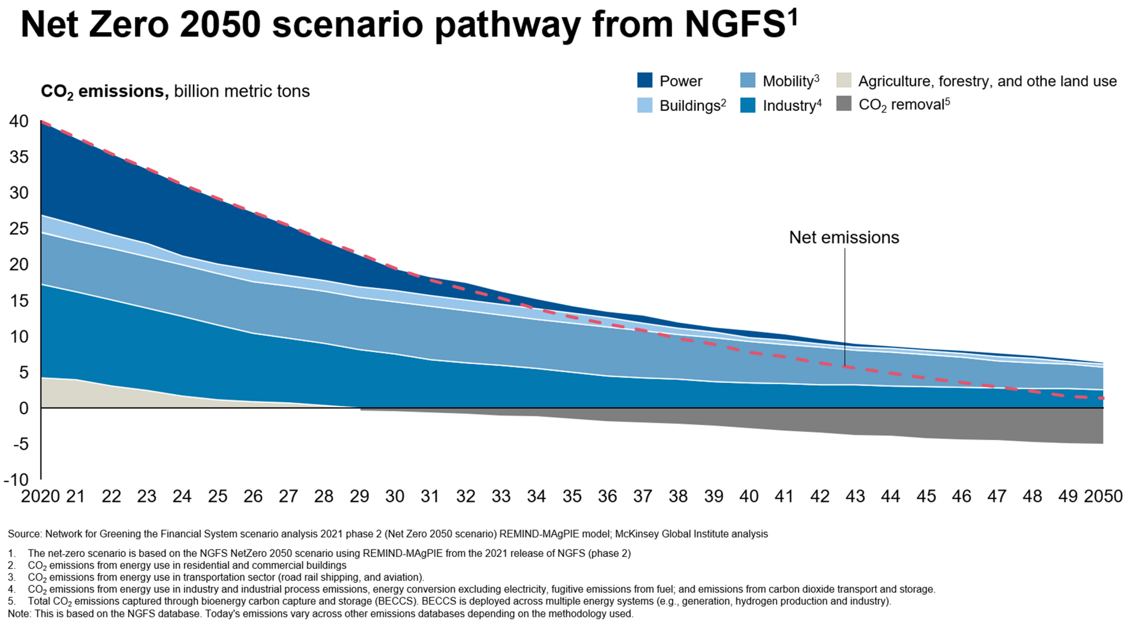

FIGURE 1.3: Net Zero 2050 pathway based on Network for Greening the Financial System scenario (own representation after McKinsey & Company, 2022)

GHG emissions-intensive processes with sustainable ones. The transition often requires large investments, for example, into wind turbines, electrolyzers for hydrogen production, or the development and production of new, low-emission products like EVs. McKinsey & Company (2022) estimates that in a 1.5 °C scenario 3.5 trillion \$ additional annual investment in physical assets for energy and land-use systems[3] are required between 2021 and 2050.

Even though all sectors need to reduce their carbon emissions, some sectors, such as the energy and transportation sector, will transition earlier than others. In both cases, an earlier transition is facilitated by the availability of competitive decarbonization technologies such as RES or EVs, making the transition easier and cheaper compared to, for example, steel production, where potential decarbonization technologies such as hydrogen are much less established (McKinsey & Company, 2022). A swift transformation of the energy sector is also necessary due to the electrification of other sectors, such as transportation, heating, or industry[4], where the availability of low or zero emission energy is a pre-requisite.

[3] Includes energy supply, e.g., power systems, hydrogen, and biofuel, energy demand, e.g., for vehicles, or alternate methods of steel and cement production, and various forms of land use, such as GHG-efficient farming practices.
[4] For example, green steel production, which uses green hydrogen produced from RES.

Renewable generation and storage can help decarbonize the energy sector

In the energy sector, which has accounted for about 30% of CO_2 emissions in 2019 (McKinsey & Company, 2022), a substantial increase in RES combined with the phase-out of fossil fuels such as hard coal or lignite is required to reduce GHG emissions while satisfying the additional demand from the electrification of other sectors and economic growth. In the past, RES costs have fallen dramatically, often making them the most economical type of electricity generation (Kost et al., 2021). However, because the sun does not always shine and the wind does not always blow, a high share of RES in the power system can create challenges due to their inherent intermittency. To create a stable generation that can satisfy demand and lead to stable prices, flexibility options are required to increase supply during times of low renewable generation or to increase demand during times of oversupply[5]. Flexibility options include dispatchable generation that can be ramped up or down when demand exceeds or subceeds supply, or electricity storage that can be charged and discharged to balance supply and demand.

A frequently used option for dispatchable generation capacity are gas-fired power plants. Their short ramp-up and -down times and lower CO_2 emissions compared to other technologies, such as coal-fired power plants, have made them popular in countries like Germany. But even though emissions from gas-fired power plants are lower than from other fossil fuels, they are not zero and cannot lead to an entirely decarbonized energy system. Therefore, additional gas-fired power must be either paired with Carbon Capture and Sequestration (CCS) / Carbon Capture and Utilization (CCU) or operated with hydrogen. Furthermore, geopolitical crises like the war in Ukraine have highlighted the supply risks that a significant dependence on energy imports can cause. Due to the high cost of carbon capture and hydrogen production, as well as the potential supply risks from energy imports, to enable large shares of renewable generation, it is crucial to not only rely on dispatchable generation capacity but to also leverage electricity storage.

Similar to dispatchable generation, electricity storage can be used to create additional demand by charging electricity during periods of oversupply, for example, midday, when solar generation is high, and to create additional supply by discharging electricity, for instance, in the evening, when demand often peaks but renewable generation from solar PV is decreasing. Due to the importance of electricity storage, multiple technologies with different cost profiles and applications have emerged. Pumped-Hydro Storage (PHS) or Compressed Air Energy Storage (CAES)

[5] When renewable generation is high due to favorable weather conditions but demand is low, for instance during vacations.

in salt caverns are economical options for long-term storage due to their low relative investment cost (Schmidt et al., 2019). However, their implementation in many countries is limited due to geographic requirements. Other technologies, such as hydrogen storage, could also be used for long-term electricity storage, but the low Round-Trip Efficiency (RTE) of today's systems makes them costly in the near term. Furthermore, hydrogen is essential for decarbonizing many industrial applications, such as chemicals or green steel production. Therefore, supply shortages of green hydrogen are likely, and it is expected that it will first be used for applications outside of electricity storage where there are no technological alternatives.

Batteries are increasingly researched and used for electricity storage. EV uptake has led to the continued development of new, more efficient, durable, and cheaper batteries, and the significant increase in production volume has reduced battery costs. But large-scale battery storage capacity is still expensive compared toPHS and CAES. Therefore, they are often employed in short-term use cases, for example, to shift overgeneration from the day to the night. And while grid-scale examples of BES are still rare, many households in developed countries such as Germany have already adopted small-scale BES systems.

Cheaper batteries can support the uptake of EVs to decarbonize the transportation sector

The transportation sector is the third largest emitting sector globally. It has contributed 19% of CO_2 emissions in 2019, out of which about 75% are caused by road transportation (McKinsey & Company, 2022). To decrease the GHG emissions from road transportation, ICE vehicles powered by fossil fuels must be replaced by EVs[6], fuel cell EVs, or vehicles that run on zero-emission fuels. Today, BEVs comprise the largest share of low-emissions vehicles, and most major automotive Original Equipment Manufacturers (OEMs) offer multiple BEV models. Therefore, many countries aim to reduce GHG emissions by increasing the share of EVs in their passenger car fleets.

The Total Cost of Ownership (TCO) is an important adoption factor for EVs. In literature and industry, there are conflicting results on the TCO of EVs compared to traditional ICE vehicles. For instance Burnham et al. (2021) estimates that the TCO sports utility vehicles in the United States are higher than the ones of comparable EVs. In contrast, Liu et al. (2021) acknowledge

[6] For simplicity, in this thesis, EVs refer to battery electric vehicles if not specified otherwise

that many recent studies come to a similar conclusion, but argue that this can be attributed to the restriction of those comparisons to a limited number of EV classes (e.g., compact vehicles with short-mid driving ranges). Furthermore, they find, that when comparing vehicles with similar weight and power characteristics, EVs are cost-competitive with ICE vehicles. Similarly, Wu et al. (2015) highlight the dependence of the TCO comparison on vehicle classes and driving range. They find that conventional cars remain cost-efficient in short-distance cases, while EVs become cost-efficient in medium- and long-distance cases. Element Energy (2021) argue that the lifetime TCOs of EVs are already lower than those of ICE vehicles in the EU. Similarly McKinsey Center for Future Mobility (2021) estimates that EVs will become more economical than ICE vehicles globally by 2025 at the latest[7]. Important factors for the TCO of EVs are lower fuel and maintenance costs that can outweigh higher initial investment costs. However, despite a potential lifetime cost advantage, the high price of EVs remains a key adoption barrier for many customers (Liao et al., 2017). This price is mainly driven by the high manufacturing cost of batteries, which comprise roughly 30% of total EV production cost (BloombergNEF, 2017). In politics and industry, a battery cost level of 100 \$ $(\text{kWh})^{-1}$ is often presented as an important threshold after which cost-parity with ICE vehicles should be widely achieved, and adoption is expected to significantly increase (Bajolle et al., 2022). Despite strong cost declines of 79%, as depicted in Figure 1.4, BloombergNEF (2022) still estimates current market prices of battery packs considerably higher at 151 \$ $(\text{kWh})^{-1}$ in 2022.

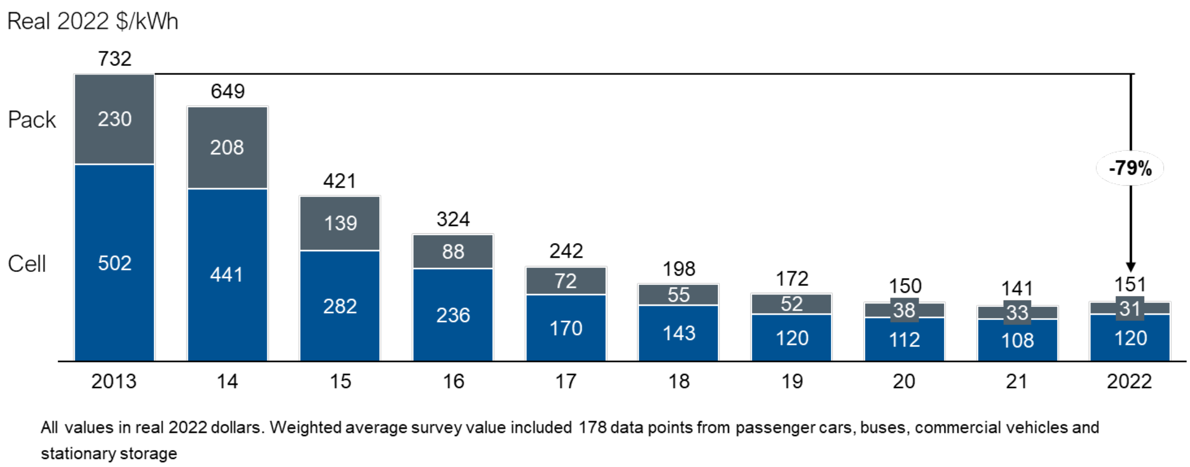

FIGURE 1.4: Volume-weighted average lithium-ion battery pack and cell price split, 2013-2022 (own representation after BloombergNEF, 2022)

[7] Liu et al. (2020), Element Energy (2021) and McKinsey Center for Future Mobility (2021) do not include subsidies in their TCO calculation.

In addition to their influence on EV cost, the battery's durability, energy density, and charging speed strongly influence important performance metrics of EVs, such as their lifetime and range. Therefore, OEMs and their suppliers are continuously working on developing new batteries and production processes to improve performance and costs.

1.2 Research objectives and methodology

This dissertation explores research questions at the intersection of accounting theory, the electrification of transport, and renewable electricity generation and storage. This overarching topic is addressed by three essays. The following chapter provides an overview of each essay's research objectives and methodology.

The first essay provides a literature review on the LC concept. LC reflect the average price an investor needs to realize to generate a zero Net Present Value (NPV) for an investment in a production facility and can be equated with the long-run marginal cost (Reichelstein and Rohlfing-Bastian, 2015). They are widely used in academia and practice in the energy sector, where the LCOE has become the predominant metric to compare the cost of generating electricity with different technologies (for example hard coal plants, solar PV or wind power, Tran and Smith, 2018).

Despite its widespread use in the energy sector, LC is not incorporated into most cost accounting textbooks such as Datar and Rajan (2018). Furthermore, there is potential to extend its application beyond the energy sector to more industries such as transportation or quantum- and high-performance computing. The objective of this essay is therefore threefold: (1) it provides an overview of the LC concept including its comparison to other frequently used cost measures such as FC and a discussion of its decision relevance including its advantages and limitations, (2) it provides an overview of the four most prevalent LC literature streams: LCOE, Levelized Cost of Energy Storage (LCOS), Levelized Cost of Hydrogen (LCOH), and Levelized Cost of Carbon (LCOC), and (3) it identifies potential future applications of the LC concept.

To provide an overview on the LC concept, the essay first explains the mathematical formulation of LC which is grounded in a verbal definition from Massachusetts Institute of Technology (2007), chapter 3: *LC is the constant dollar price that would be required over the life of the* *investment project to cover all operating costs, payment of debt and accrued interest on initial project expenses and the payment of an acceptable return to investors.*

It then relates LC to FC. The calculation of FC can vary and the relation to LC depends on assumptions, for example, on the nature of capacity degradation. Therefore, the results of multiple authors such as Rogerson (2008) or Reichelstein and Rohlfing-Bastian (2015) who have compared the two cost measures in different scenarios are structured and summarized. Furthermore, the essay analyzes the relation between LC and a FC measure that includes taxes and calculates capital cost based on linear depreciation and the assumption that on average, half of the initial capital investment is tied up. Finally, accounting theory papers from Mahlert (1976), Swoboda (1979), Küpper (1985), Joskow (2011), Hirth (2013) and others, on cost measures and their relation to the investment theoretic approach, are presented, and the advantages and limitations of the LC concept are assessed.

After the first recorded application of LCOE by Rosenthal et al. (1965) further literature streams in the energy sector on LCOS, LCOH, and LCOC have emerged. To provide an overview of all four literature streams, seminal and recent papers have been summarized. Within each literature stream, different sub-streams, for example on cost comparisons, policy implications, or methodological extensions of the LC concept have been identified and the literature is structured accordingly. The summary of each literature stream also includes a summary of its current and potential future relevance as well as potential future topics. Furthermore, a condensed overview of very small literature streams such as levelized cost of heating or water is given.

LC have become the predominant cost metric in many energy applications. It is plausible that other industries with similar characteristics could also benefit from the application of LC. To identify potential future use cases for LC, different industries are assessed based on their potential use of LC. In some cases, such as in mobility, a first LC measure has already been introduced (Comello et al., 2021) and could be used in more literature in the future. In others, such as patent licensing, nutrition, or cloud storage, the applicability of the LC concept is assessed based on the similarity of the applications to the energy sector.

The second essay presents a bottom-up cost model that enables the user to compare the cost competitiveness of different battery chemistries, cell designs, and manufacturing processes. Batteries make up about 30% of the production cost of EVs (BloombergNEF, 2017). Therefore, reducing battery production costs can help to reduce the production cost and the purchase price of EVs for end customers and facilitate their large-scale adoption.

Today, cost estimates for current and future battery prices from literature and industry vary significantly and do not provide a good reference for true production cost. Tesla, on one hand, announced on their first battery day in September 2020 that they plan to reduce the cost per kWh of a battery pack by about 56 % compared to the current state of art (Frazelle, 2021), resulting in battery cost between 48 and 53 $\$\,(\mathrm{kWh})^{-1}$. Assuming battery cell costs to account for 75 % of the battery pack costs, final cell costs would have to be between 36 and 40 $\$\,(\mathrm{kWh})^{-1}$. These cost assumptions have been met with scepticism from established OEMs because such a low cost level can only be achieved through significant and as-yet-unseen technical and material-based advancements. Literature, on the other hand, estimates prices much higher, and usually significantly above the 100 $\$\,(\mathrm{kWh})^{-1}$ level (see, e.g., Patry et al., 2015, Ciez and Whitacre, 2017, Philippot et al., 2019, Schneider, 1961, Nemeth et al., 2020, and others). As illustrated in Figure 1.5, due to the large variances in price estimates and a lack of convergence of cost over time, these estimates do not provide a clear answer to the level of battery prices.

In addition to a high variance in price estimates, most battery cost models also lack the ability for detailed and adjustable modeling of the production process including changes to individual production process steps, the sequence of production steps, and the battery design. For example, one of the most frequently used tools for battery cost estimation, the Argonne National Laboratories Battery Performance and Cost Model (BatPac), does not consider energy cost or individual scrap rates per process step and does not allow for changes of the sequence of production steps. However, all of these options for customization would be desirable, as energy and scrap can be significant cost factors, and the ability to model changes to the production process is important to be able to evaluate the cost potential of new production technologies and battery designs.

Finally, most of the presented cost models lack standardized and clearly defined cost measures. While most papers present a FC measure, its calculation is not clearly defined. For instance, capital costs are often not included and if they are, their calculation differs. Most models also do not include taxes. While this is understandable due to regional differences in corporate income taxes, it also means that an important cost factor is neglected. Therefore, most cost models do not calculate the true long-run marginal cost that would, for example, be reflected by LC (Reichelstein and Rohlfing-Bastian, 2015). Furthermore, it is possible that very low-cost

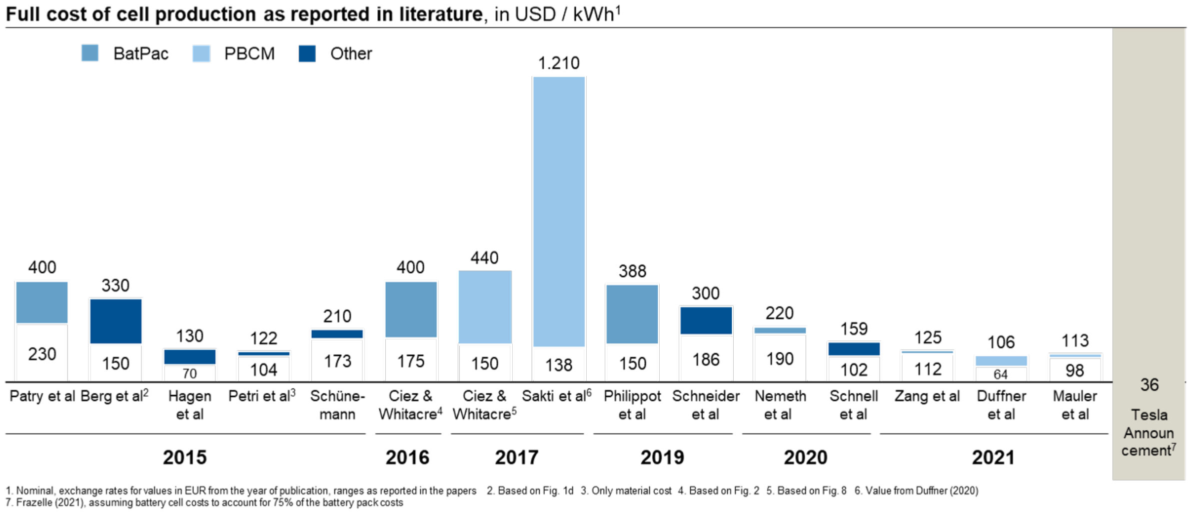

FIGURE 1.5: Battery cell production cost reported by literature and announced by Tesla.

estimates such as the announcement from Tesla refer to MC instead of FC . Since most authors do not present MC, this hypothesis can not be tested with existing literature.

To address the above-mentioned challenges, this essay presents a comprehensive extension to a model published by Schünemann (2015). It enables the user to calculate the FC, LC, and MC of different cell formats, cell chemistries, and production processes. The model consists of six stages: (1) The selection of the cell design including its format (for example, cylindrical or prismatic), its chemistry (for example, if silicon (Si) is used in the anode), and the annual production capacity of the factory producing the batteries. (2) The definition of the production process chain, i.e. the selection of the required manufacturing steps and their sequence. (3) The calculation of the required throughput of each manufacturing step to produce the defined annual capacity, considering the scrap rates of the machines used within the individual production steps. (4) The calculation of the number of required machines per production step, based on the required throughput from the previous step. (5) The calculation of the total manufacturing costs based on the required number of machines, personnel, material, factory size, energy, etc. (6) The calculation of FC , MC, and LC per kWh of the produced batteries.

To address the lack of reliable cost estimates and to assess how realistic Tesla's future cost claims are, the model is then applied to two state-of-the-art EV battery cells. The cylindrical 4680 (i.e., as used by Tesla) and for comparison the prismatic PHEV2 (i.e., as used by VW). For both cell formats, three different industry-relevant cell chemistries are evaluated: one with graphite and two with silicon-containing (3 and 5 wt. %) graphite as the active anode material. To provide realistic cost estimates, all parameters are collected and calibrated via literature and interviews with industry experts.

The third essay explores the influence of different battery chemistries on the fossil fuel reduction potential from residential rooftop solar PV and BES systems. In order to achieve their decarbonization goals, countries worldwide are transitioning to clean energy sources. In the energy sector, fossil fuels are burned to generate electricity, for example in natural gas or hard coal power plants. Replacing fossil fuels for electricity production could reduce global GHG emissions and increase countries' resilience during supply shocks such as the Russian invasion of Ukraine which has resulted in an increase in natural gas prices and spiking electricity prices in Europe (Arnold et al., 2022).

In the current literature, most authors focus on calculating the NPV-optimal solar PV-BES system size for a household. Depending on the authors, variations to models (e.g., stochastic vs. deterministic), markets (e.g., flat vs. time-of-use electricity tariffs), and countries are made (see, for example, Erdinc et al., 2015, Khalilpour and Vassallo, 2016, Khawaja et al., 2017, Cervantes and Choobineh, 2018, O'Shaughnessy et al., 2018, Javeed et al., 2021). None of the mentioned authors analyze the effects of different, state-of-the-art battery types on the optimal system size and NPV. However, the rise of electric mobility has triggered a rapid increase in global battery production, leading to declining battery costs due to learning and economies of scale (see e.g. Nykvist and Nilsson (2015), Matteson and Williams (2015), Nykvist et al. (2019)). Fluctuating raw material prices and technical advancements in energy density have lead to the development of new cathode chemistry combinations in Lithium-Ion Batteriess (LIBs). Historically, Sodium-Calcium Exchanger (NCX) batteries have been used predominantly in residential BES applications as well as in most EVs in the Western world. Lithium-Iron-Phosphate (LFP) batteries have rapidly gained market share in recent years, especially in China. While LFP batteries have a lower energy density than NCX batteries, they are cheaper, more thermally stable, and more durable (Li et al., 2020 and Preger et al., 2020). The volatility in lithium prices in recent years has also supported the development of lithium-free batteries. For example, Sodium-Ion Batterys (SIBs) that do not contain lithium are being developed and produced by two of the biggest LIB manufacturers: BYD (Batteries News, 2022) and CATL (Yingzhe, 2022). These changing market dynamics make it imperative to examine the effects on sizing and profitability of different battery types on residential solar PV and BES systems.

While some authors such as Weniger et al. (2013, 2016), Zhang et al. (2017), and Liu et al. (2020) include electricity independence, self-consumption and CO_2 emissions associated with solar PV and BES systems in their analysis, none of the reviewed literature assesses the fossil fuel reduction potential of a large-scale roll-out of such systems. In light of ambitious solar expansion targets and associated subsidies programs, for example, in Germany, it is important to be able to determine if such programs can support a significant reduction of fossil fuel consumption or if they would merely result in increased curtailment during times of peak generation and low or average consumption.

The fossil fuel reduction potential of a widespread roll-out of residential solar PV-BES systems is analyzed in a case study for Germany. The analysis consists of four steps: (1) In the first step, the NPV-optimal solar PV-BES system size for a private household is calculated. The results are generated for four battery types that reflect the historically most widespread battery types (NCX and LA) as well as recently developed battery types from e-mobility (LFP and SIB). (2) In the second step, the hourly electricity flows within the household[8] are simulated and the amount of electricity that could be used to substitute electricity generation from fossil fuels is calculated. In the following, this is referred to as the Net Additional Electricity (NAE) supply. (3) In the third step, the hourly data from one household is scaled towards a national level, represented by the market potential of residential rooftop solar PV in Germany from EUPD Research (2021). (4) In the fourth step, the national NAE supply is used to calculate the fossil fuel savings potential for each hour and the yearly average. To do so, it is assumed that in each hour, the electricity generation sources are substituted in descending order by their LCOE.

1.3 Findings and contribution

The **first essay** reviews the application of the LC concept in accounting and energy literature. It analyzes the decision relevance of LC, creates an overview of the LCOE, LCOS, LCOH, and LCOC literature, and identifies use cases where LC could be applied in the future.

LC is well suited for use in long-term capital allocation problems. Compared to traditional profitability measures such as the return on investment, NPV, or internal rate of return which require predictions about future revenues and costs, LC can rely solely on (current and future) cost data. This is an advantage because future revenues are often hard to predict due to uncertainties on

[8] I.e. how much electricity is generated, charged, discharged, fed into the grid, or used from the grid.

pricing power. Compared to traditional cost measures such as FC, LC is usually larger or equal because it also includes taxes and an appropriate allocation of depreciation and capital cost. Specifically, it is shown that LC is larger than FC if FC is calculated with two assumptions that are frequently used in industry: (1) Linear depreciation over an asset's lifetime and (2) capital cost based on the assumption that, on average, half of the initial capital is tied up.

LC can support capital allocation decisions through break-even calculations and cost comparisons, i.e., ranking and selecting different investment opportunities by their LC. A common example of this are investments in electricity generation capacity, where multiple production technologies such as wind, solar PV, or hard coal power plants are compared based on their LC. Using LC for cost comparisons, however, requires that all regarded technologies produce an identical homogenous good.

LC is suited for a single round of capacity investments with a finite horizon. Therefore, in settings with multiple overlapping capacity investments other or adapted models are necessary. Jorgenson (1963), Arrow (1964), Rogerson (2008), Rajan and Reichelstein (2009), Nezlobin (2012) and Nezlobin et al. (2012) present suitable models in these settings, both for finite and infinite horizon models. Furthermore, in such settings, the capacity investment and subsequently the LC can change over time. A prominent example of this is the reduction of solar PV prices in recent years. Here, LC does not provide guidance on how market participants should behave because it does not assess the option of postponing an investment.

An important limitation of LC is its disregard for variability in unit revenues. This is especially important for the application to RES where the generation of electricity is often correlated with lower market prices. Therefore, comparing LC to the average market price is not sufficient to assess the economic viability of an investment. Glenk and Reichelstein (2022b) propose a solution to tackle this limitation with the introduction of the levelized revenue of electricity and the levelized profit margin concept.

LC is widely used in both academia and practice, especially in the energy sector. Most notable are the literature streams on LCOE, LCOS, LCOH, and LCOC. The LCOE has been a commonly used performance measure to benchmark electricity generation technologies for more than 50 years (Tran and Smith, 2018, Aldersey-Williams and Rubert, 2019). Three distinct literature streams using the LCOE methodology have emerged. They (1) provide cost comparisons of electricity generation technologies, (2) evaluate policy implications and (3) develop more advanced cost measures based on the LCOE concept. The cost comparisons represent the origin of the LCOE, providing the largest and most mature stream, with multiple papers being published every year. This sub-stream will likely continue to offer more research avenues since new technologies emerge and the competitive landscape of electricity generation changes frequently. The second sub-stream of policy evaluations will provide further policy recommendations for a more cost-efficient clean energy transition since preventing climate change will likely remain a focus of many governments for the next decades. In the third stream, most papers extending the LCOE framework have been published in the last five years with many of them as recent as 2021. Hence, further academic projects in the next years are likely, e.g., on the LCOE of combined renewable and energy storage systems.

LCOS turned into a frequently used metric to assess the cost of energy storage. The literature stream emerges in the 2000*s* and has been highly active during the last 5-10 years. Two distinct literature streams are visible, which employ the LCOS for (1) cost comparisons of new storage technologies (e.g., Poonpun and Jewell (2008), Jülch (2016), Smallbone et al. (2017)) and (2) to further develop the methodology (e.g., Pawel (2014), Lai and McCulloch (2017), Comello and Reichelstein (2019)). Both streams appear to evolve simultaneously as new technologies emerge and are assessed in the cost comparison stream. At the same time, the methodological stream extends the LCOS framework, e.g., to consider capacity degradation of the storage technology (Rodby et al., 2020) or to evaluate combined storage and generation technologies (Lai and McCulloch, 2017). In both streams, many papers are published each year and this trend will likely continue, driven by the development of new storage technologies and the need for energy storage due to an increasing share of RES in the electricity mix. Potentially, a third stream may emerge on policy evaluation (similar to the LCOE stream) as the adoption of energy storage will be supported by legislation and subsidies.

LCOH is a novel and comparatively small research stream applying the LC framework. Most papers have been published in the last 5 years and the application of the LC measure is less dominant than in the LCOE or LCOS literature, as there are multiple papers that employ other (however similar) measures such as lifecycle costs (e.g., Guerra et al., 2019, Khzouz et al., 2020, Lee et al., 2009). Due to the increasing popularity of hydrogen, the LCOH literature stream will likely continue to grow and extend the application of LCOH not only to assessments of the economic viability of hydrogen but potentially to policy evaluations and more complex scenarios, similar to the LCOE and LCOS literature.

Similar to LCOH, the LCOC literature stream is much smaller than the LCOE or LCOS literatures. However, with the increasing relevance of carbon capture, it is expected to grow in the future as more policies and technologies arise.

Besides the existing literature streams, there is a significant potential for LC to be applied to other use cases, for example, in mobility where LC could calculate the cost per mile traveled, in nutrition where a levelized cost of calories measure could help identify cost-efficient food production technologies, or in cloud computing where a levelized cost of cloud storage measure could calculate the cost of storing a gigabyte over a certain amount of time.

This essay is the first review of LC known to the author and contributes to the existing literature in three ways: (1) It presents an extensive discussion on the advantages and disadvantages of LC and provides guidance on situations where LC can be a suitable cost measure. (2) It summarizes the literature of the four most widespread literature streams, introduces seminal papers, and gives an outlook on how these streams might develop in the future. (3) It identifies use cases where LC could be a useful cost measure and thus provides direction for further research.

The **second essay** shows that within the regarded scenarios both the cylindrical 4680 and the prismatic PHEV2 cell have similar production costs but that the distribution of costs differs. While material costs make up the largest share of the FC in both cases, the 4680 cell requires more machines and production personnel which in turn increases investment and depreciation costs and decreases the share of material costs.

The three cell chemistries differ by the used anode material. One variant uses graphite and two variants use Si-containing (3 and 5 wt. %) graphite as the active anode material. Adding Si increases the energy density of both cells due to its higher specific capacity. Because of the higher energy density, less material can be used on a per kWh basis which reduces the material and subsequently the FC slightly. However, a much larger effect is found when reusing scrap material which reduces cost by ca. 5%.

The results of 110-112 $\$\,(\mathrm{kWh})^{-1}$ for the PHEV2 cell and 112-113 $\$\,(\mathrm{kWh})^{-1}$ for the 4680 cell are in line with other literature-reported values of ca. 100-150 $\$\,(\mathrm{kWh})^{-1}$ but they are still higher then industry reports that often claim production cost of around or below 100 $\$\,(\mathrm{kWh})^{-1}$. This could be explained by multiple reasons: (1) Industry might report MC instead of FC or LC. The MC of the PHEV2 and 4680 cell are estimated between 103-104 $\$\,(\mathrm{kWh})^{-1}$ which is much closer to media-reported values and could explain part of the difference. However, this is still significantly above estimates of 48 to 53 $\$\,(\mathrm{kWh})^{-1}$. (2) Reports from the media are often based on rumors and unconfirmed sources inside the companies. This leaves the possibility that companies leak lower than actual values to boost their perceived competitiveness and put pressure on their competitors or suppliers. (3) Large companies could be able to achieve significantly lower material and production costs than the models in most papers assume. This could be due to economies of scale that are not reflected by most models' input parameters, including the one in this essay.

The essay shows that detailed cost models are useful for assessing the production cost of different battery designs and production processes. Results are calibrated with literature and industry, however, as industry reports are usually slightly lower than literature values it would be worthwhile to further explore the gap. It is also shown that the prismatic PHEV2 and the cylindrical 4680 cells have similar cost performance. Due to different cost structures driven by different shares of material and initial investment costs, the cells have a different exposure to changes in material costs. I.e., rising or falling material costs would have a stronger impact on the production cost of the PHEV2 cell. It is also shown, that clear and consistent cost measure definitions are important. The difference between cost measures can be up to 16% [9] and thus can mask other differences. For example, in the presented case, the differences between FC and LC are much larger than the differences between different cell chemistries within one cost measure.

This essay contributes to the existing literature by presenting a flexible bottom-up cost model for modern battery production which is calibrated with state-of-the-art battery designs and production processes based on current literature and expert interviews. The calculation logic of the model as well parameters will be made publicly available. This enables potential users to estimate the production cost of new battery chemistries and different production technologies and processes and to adapt the model if needed.

Furthermore, the essay provides a realistic production cost estimation and comparison of two battery cells: the PHEV2 and the 4680 cells. It contributes to the existing literature on battery production cost by adding a current cost estimate for two state-of-the-art battery cells and helps to ground skepticism on highly ambitious cost targets in facts, by showing that significant reductions across all cost dimensions including material costs would be necessary to achieve such cost reductions.

[9] For example 103.30 $\$\,(\mathrm{kWh})^{-1}$ MC vs 120.33 $\$\,(\mathrm{kWh})^{-1}$ LC for the 4680 cell without Si and scrap material recovery.

Finally, it contributes to the battery cost literature by highlighting inconsistencies in current cost calculation, providing a standardized and transparent cost measure framework, and introducing the levelized cost of battery production. Battery production requires large investments and the exclusion of taxes and improper accounting for capital cost can lead to the underestimation of actual production cost. In a time where significant investments into battery manufacturing are made, LC is a highly relevant cost measure because it can support capital allocation decisions through break-even calculations.

The **third essay** analyzes the optimal sizing of household solar PV and BES systems and their potential to reduce fossil fuel consumption on a national level. In a case study for Germany, the essay shows that residential solar PV-BES systems can reduce electricity consumption from fossil fuels in Germany by up to 35%. To achieve this, a net investment of 21-22 k€ per household would be required for a system with an LFP battery[10], generating an NPV of ca. 6 k€ per household.

The analysis highlights the importance of battery degradation and lifetime, as well as investment cost, as central factors for the usefulness of BES. It shows that the better durability of LFP batteries and SIBs makes installing larger PV and BES systems economical. Therefore, the achievable reduction of electricity from fossil fuels is ca. 9 percentage points higher when using LFP and SIB systems compared to systems with NCX or Lead Acid (LA) batteries while also increasing the household NPV by ca. 3.5 k€.

The results suggest that increasing the use of state-of-the-art LFP batteries and SIBs in household solar PV-BES systems could reduce fossil fuel consumption. Future research should focus on including further parameters such as ramp-up and ramp-down times of fossil power plants and more fine granular analysis on the potential for additional PV systems.

The essay contributes to the existing literature because it is, to the author's knowledge, the first comprehensive framework for analyzing the influence of different battery types on the system dimensions and economics of solar PV and BES systems. Therefore, it provides guidance for industry, consumers, and politicians on which battery types are most economically attractive in the context of a solar PV-BES system. Furthermore, to the author's knowledge, this is the first analysis of the fossil fuel reduction potential of a large-scale roll-out of residential solar PV and BES systems. This makes it highly relevant for governments that can use the model to

[10] While sodium batteries need lower investments and achieve a higher NPV, the more developed and available technology of LFP is discussed as a main result.

assess the cost and benefits of an increased roll-out of such systems and analyze the influence of subsidies and policies, such as different Feed-In Tariffs (FITs) or direct payments, to reduce initial capacity cost.

1.4 Structure of the Thesis

The remainder of this dissertation is structured as follows: chapter 2 presents the first essay on the decision relevance of the LC concept, its applications, and potential future use cases. Chapter 3 consists of the second essay, which introduces a bottom-up model for automotive battery production, and the levelized cost of battery production and conducts a case study on the production cost of two state-of-the-art batteries. Chapter 4 proceeds with the third essay on the fossil fuel reduction potential of residential solar PV-BES systems and the influence of different battery types on the system's performance. Finally, chapter 5 provides a summary and conclusion of the findings of the three essays, outlines implications for research, industry, and politics, and discusses potential avenues for future research. Supplementary information on input variables and mathematical proofs can be found in the appendix of this dissertation.

2 Applications of the levelized cost concept

Levelized cost is a life-cycle cost measure that aggregates investment expenditures and operating costs into a unit cost figure. So far, most applications of this concept have originated in relation to energy technologies. This paper describes the role of the levelized cost concept in cost accounting and synthesizes multiple research streams in connection with electricity, energy storage, hydrogen and carbon capture. Finally, we sketch multiple potential future applications of the levelized cost concept.

Keywords: Levelized cost, Full cost, Levelized cost of energy, Levelized cost of energy storage, Levelized cost of hydrogen, Levelized cost of carbon.

This paper has been published in the Journal of Business Economics, Vol. 93, pages 1125–1148, (2023) with my Co-Authors Gunther Friedl, Stefan Reichelstein, Amadeus Bach, and Maximilian Blaschke.

2.1 Introduction

The concept of levelized cost has a long history in the field of energy, frequently referred to as LCOE (Farrar and Woodruff, 1973). The main use of this concept has been to provide a unit cost measure, e.g., euro per kilowatt hour, to compare alternative energy sources in terms of their cost competitiveness. As a life-cycle cost measure, LCOE aggregates a share of the capital expenditures required for the initial capacity investment with operating expenditures required for the periodic energy generation. Thus, the unit cost of capacity is not a cash outflow, but an allocated cost. For many energy sources, e.g., nuclear, solar, and wind power, this cost component is in fact the dominant part of the overall LCOE.

A commonly accepted verbal definition of the LCOE dates back to a study by MIT on the future of coal (Massachusetts Institute of Technology, 2007, Chapter 3). In their study, LCOE is calibrated as the break-even value that must be achieved on average by the energy sold in order to adequately compensate a project's suppliers, employees and investors for their contributions. This article adopts the formal and generic LC concept in Reichelstein and Rohlfing-Bastian (2015). Accordingly, LC is calibrated as the average unit revenue that allows an investment project to break even (achieve a net present value of zero) over its entire life cycle.

Earlier studies have shown that the LC exceeds the measure of full cost, as usually defined in the cost accounting literature. The reason is that the standard definition of full cost does not include charges for interest, nor those that arise from corporate income taxes. In contrast, these types of expenditures are included in the LC metric in order to make the cost metric compatible with the net present value criterion. Here, we show that even if interest charges are accounted for in an approximate manner, as advocated in some cost accounting textbooks (Friedl et al., 2022), the resulting full cost metric will again be consistently below the levelized product cost.

Conceptualized as a life-cycle cost measure, LC is generally not the relevant cost for short run decisions, such as pricing or production volume decisions. Once an investment decision has been made, the LC metric carries significant sunk cost components. Under certain conditions, however, LC emerges as the relevant unit cost measure for long run decisions such as irreversible capacity investments. In the context of electricity generation, LCOE does allow for an "apples-to-apples" cost comparison of any two similar generation technologies, e.g., nuclear versus coal-fired power plants. In order to assess the competitiveness of electricity obtained from renewable energy sources versus that obtained from fossil fuel sources, however, the LCOE metric is by itself not sufficient. Instead, it must be supplemented with other metrics that effectively summarize the pattern of power generation and power pricing in real time.

Moving beyond electricity, we review multiple applications and variants of the levelized cost concept. In particular, this article covers unit cost measures that have been used to assess improvements in the economic viability of emerging technologies such as energy storage, hydrogen, and carbon capture and sequestration.

The remainder of the paper is organized as follows. Section 2.2 presents a formal LC framework and relates this metric to the incumbent cost accounting literature. Section 2.3 reviews specific applications of the levelized product cost concept in connection with different energy related technologies. Section 2.4 describes potential future applications. We conclude in section 2.5.

2.2 Levelized Cost Concept

2.2.1 Model Framework

The levelized cost of a product is a unit cost measure that aggregates the expenditures resulting from an upfront capacity investment and subsequent periodic operating expenditures. A commonly known verbal definition has been provided in a 2007 study by MIT on the future of coal. The MIT study defines LC as *the constant dollar price that would be required over the life of the investment project to cover all operating costs, payment of debt and accrued interest on initial project expenses and the payment of an acceptable return to investors* (Massachusetts Institute of Technology, 2007, Chapter 3). According to this definition, LC is a break-even value insofar as it yields the minimum price per unit of output that an investor would need in order to break even over the life-cycle of an initial capacity investment. Importantly, the cost measure is to be aligned with present value considerations, as the cost measure requires an acceptable return to both equity and debt investors. While the above definition does not explicitly mention taxes, in particular corporate income taxes, these can be included in the category of operating costs.[11] Reichelstein and Rohlfing-Bastian (2015) provide a formalization of the MIT (2007) definition. They represent the levelized cost as the unit cost of a product associated with an

[11] Earlier studies have also adopted a simplified version of the levelized cost concept, for instance, by calculating LC as the annualized initial investment and the total annual cost divided by the total units of output. Clearly, this approach does not presume the payment of a return to investors (Tegen et al., 2012; Brown and Foley, 2015).

initial investment that allows k units of the product to be produced initially and $x_t \cdot k$ units to be produced in period t. Here, $x_t \leq 1$ is a degradation factor to reflect the possibility that the initial production capacity may diminish over time. Formally,

$$LC(k) = w + f(k) + c(k) \cdot \Delta. \tag{2.1}$$

In this definition of the levelized cost, the time-averaged unit variable cost is given by:

$$w \equiv \frac{k \cdot \sum_{t=1}^{T} w_t \cdot x_t \cdot (1+r)^{-t}}{L(k)}.$$

The numerator represents the total discounted future variable cost, assuming $x_t \cdot k$ units are produced in period t, with $1 \leq t \leq T$, w_t represents the unit variable cost in period t, and r denotes the applicable cost of capital. To obtain the time averaged unit variable cost, the numerator is divided by the *levelization factor* $L(k) \equiv L \cdot k \equiv \sum_{t=1}^{T} x_t \cdot (1+r)^{-t} \cdot k$. It measures the total discounted output that is attainable from the initial capacity investment over the entire planning horizon of T periods.

The second component of LC is the time-averaged unit fixed cost, given by:

$$f(k) \equiv \frac{\sum_{t=1}^{T} F_t(k) \cdot (1+r)^{-t}}{L(k)},$$

where $F_t(k)$ is the total fixed operating cost in period t that is required for a facility scaled to size of k units of production capacity. Finally, the unit cost of capacity is defined as:

$$c(k) \equiv \frac{\nu(k)}{L(k)},$$

with $\nu(k)$ denoting the initial capacity investment expenditure for a facility scaled to size of k units of production capacity. To reflect the payment of income taxes, the LC needs to include a tax factor that acts as a multiplier on the unit cost of capacity:

$$\Delta = \frac{1 - \alpha \cdot \sum_{t=0}^{T} \hat{d}_t \cdot (1+r)^{-t}}{1 - \alpha}.$$

Here, α represents the effective corporate income tax rate and $\hat{d}_t$ is the share of the initial investment that can be written off in period t as a depreciation expense for income tax purposes. The possibility of $\hat{d}_0 > 0$ reflects that the tax code may allow for partial initial expensing. Assuming the $\hat{d}_t$ sum up to one, the tax factor will exceed 1, unless the entire capacity investment can be fully depreciated in the initial year of acquisition. In general, a more accelerated depreciation schedule will increase the depreciation tax shield and lower the LC through a smaller tax factor Δ.

Suppose next that the firm produces $x_t \cdot k$ units of output in period t and furthermore sells each unit at the constant price p. This would result in after-tax cash flows of $CFL_0 = -\nu(k)[1-\alpha \cdot \hat{d}_0]$ and

$$CFL_t = (p - w_t) \cdot x_t \cdot k - F_t(k) - \alpha \cdot I_t.$$

Here, I_t denotes the firm's taxable income:

$$I_t = (p - w_t) \cdot x_t \cdot k - F_t(k) - \hat{d}_t \cdot \nu(k).$$

When discounted at the interest rate r, the present value of the stream of after-tax cash flows CFL_t from 0 to T becomes:

$$NPV(k) = -\nu(k)[1 - \alpha \cdot \hat{d}_0] + \sum_{t=1}^{T} ((p - w_t) \cdot x_t \cdot k - F_t(k) - \alpha \cdot I_t) \cdot (1 + r)^{-t}.$$

By definition, LC is the unit revenue (p) that yields $NPV(k) = 0$. Solving the above linear equation, one obtains $p = LC(k)$, thus establishing $LC(k)$ as the critical price at which the investor breaks even on an investment in k units of capacity that allows $x_t \cdot k$ units of output to be produced in subsequent time periods.

In concluding this section, we note that in the special case of a *constant returns to scale technology*, i.e., $\nu(k) = \nu \cdot k$ and $F_t(k) = F_t \cdot k$, the levelized cost measure, $LC(k)$, reduces to a constant unit cost, denoted by LC, as it is independent of the scale of the investment. A further simplification is obtained in a *stationary environment* where $F_t = F$, $w_t = w$ and $x_t = 1$. In that case, the above levelization factor, L, reduces to $A(r, T)$, where $A(r, T)$ is the annuity factor, which makes an investor (with cost of capital of r) indifferent between receiving 1 Euro in each of the next T years, or receiving $A(r, T)$ Euro today.

2.2.2 Relation to Full Cost

While the levelized product cost concept, as introduced above, is a comprehensive life-cycle cost measure that aggregates fixed and variable costs incurred over time, this cost measure can generally not be equated with the full cost of a product, as commonly defined in the cost accounting literature. To establish the relationship between these two cost concepts, consider a setting with constant returns to scale in a stationary environment. In such settings, cost accounting books (Datar and Rajan, 2018) typically define the unit full cost of a product, of which q_t have been produced in period t as:

$$FC_t(q_t \mid k) = w + \frac{f \cdot k}{q_t} + \frac{d_t \cdot \nu \cdot k}{q_t}.$$

Here q_t denotes the quantity of the product produced in period t and $\{d_t\}_{t=0}^{T}$ denotes a depreciation schedule that the firm uses for internal, and possibly also external, reporting purposes. Assuming full capacity utilization, i.e., $q_t = k$ in a stationary environment, we note that if the initial investment is depreciated according to the straight-line rule, that is $d_t = \frac{1}{T}$ for $1 \leq t \leq T$, then $LC > FC_t(k \mid k)$ for all t. This observation follows directly because the tax factor Δ exceeds 1, and further:

$$c \equiv \frac{\nu}{\sum_{t=1}^{T}(1+r)^{-t}} > \frac{\nu}{T}.$$

The preceding inequality essentially reflects that the above measure of full cost does not include interest expenses. To account for the time value of money, it is useful to consider the following extended full cost measure:

$$FC_t^1(q_t \mid k) = w + \frac{f \cdot k}{q_t} + \frac{\left[d_t + r \cdot \left(1 - \sum_{i=1}^{t-1} d_i\right)\right] \cdot \nu \cdot k}{q_t} \cdot \Delta.$$

Once the cost of capacity includes interest charges on the remaining book value of the capacity asset and the cost measure also includes the tax factor Δ, the extended cost measure $FC_t^1(q_t \mid k)$ becomes compatible with the levelized cost measure LC. Key to this compatibility is that the chosen depreciation schedule reflects the intertemporal degradation of the asset, i.e., the pattern of the parameters $\{x_t\}_{t=1}^{t=T}$ (Reichelstein and Rohlfing-Bastian, 2015). Specifically, given a stationary environment ($x_t = 1$) and the assumption of full capacity utilization ($q_t = k$), it follows that $LC = FC_t^1(k \mid k)$ for all t, provided the d_t are calculated according to the annuity method.[12] Furthermore, for any given pattern of degradation factors $\{x_t\}_{t=1}^{t=T}$, there always exists a corresponding depreciation factor such that $LC = FC_t^1(k \mid k)$ for all t (Rogerson, 2008).

Given an arbitrary degradation pattern $\{x_t\}_{t=1}^{t=T}$ and depreciation schedule $\{d_t\}_{t=1}^{t=T}$, it is still true that the stream of extended full costs $FC_t^1(k \mid k)$ will be equal to LC, on average. Specifically, it follows from the conservation property of residual income (Preinreich 1938 and Lücke 1955) that:

$$\sum_{t=1}^{T} FC_t^1(k \mid k) \cdot (1+r)^{-t} = LC.$$

Some cost accounting textbooks (Friedl et al., 2022) account for interest charges corresponding to the initial capacity investment by adopting straight-line depreciation and imputing an interest charge equal to half of the initial investment in each period. This approach results in an unambiguous relationship between LC and the full cost measure:

$$FC_t^2(q_t \mid k) = w + \frac{f \cdot k}{q_t} + \left(\frac{1}{T} + \frac{r}{2}\right) \cdot \frac{\nu \cdot k}{q_t} \cdot \Delta.$$

Proposition 2.1. *Suppose a stationary environment with constant returns to scale. Given full capacity utilization, i.e., $q_t = k$,*

$$LC > FC^2(k \mid k)$$

for all $1 \leq t \leq T$.

The preceding result shows that while it is true that with straight-line depreciation the asset's remaining book value is, on average, equal to half of the initial investment, the resulting approximation of the imputed interest charges creates a systematic bias such that the resulting full cost measure $FC^2(k \mid k)$ is less than the levelized product cost measure LC. The intuition for this result is that the underlying approximation understates the applicable book value for the first $\frac{T}{2}$ years, yet the interest charges in these years receive relatively large weights due to discounting.

[12] Under the annuity method, the d_t satisfy $d_{t+1} = d_t \cdot (1+r)$, and d_1 is determined by the balancing requirement that the sum of all d_t is equal to 1.

2.2.3 Decision Relevance

Managerial accounting textbooks emphasize that for different types of managerial decisions, pertaining, for instance, to investments, product pricing and production volume, different cost measures are relevant. For short-run decisions, for instance, managerial accounting textbooks recommend the use of incremental costs rather than full cost measures, due to the fact that full cost measures generally include sunk costs. For long-run decisions, most managerial accounting textbooks do not point to a single unit cost measure, but instead recommend a corporate finance approach that focuses on the discounted stream of future cash flows (Hotelling, 1925, Schneider, 1961, Mahlert, 1976, Swoboda, 1979, Luhmer, 1980, Kistner and Luhmer, 1981, Küpper, 1984, Schweitzer et al., 2015, Datar and Rajan, 2018). In contrast, Mahlert (1976) and Swoboda (1979) advocate for the use of unit cost measures that are consistent with a corporate finance approach seeking to maximize the net present value of the long-run decision under consideration. In that vein, Küpper (1985) develops guidelines for cost measures grounded in investment theory. A recent synthesis is provided in Ewert et al. (2023).

As a unit cost measure, LC has been shown to be the relevant cost for certain long-run decisions involving capacity investments. Consider, for example, a setting where a firm has to choose between two production technologies that differ in both their required initial capital expenditures as well as their periodic operating costs. The two technologies would result in the same capacity level, k and be subject to the same degradation pattern $\{x_t\}_{t=1}^{t=T}$. Suppose further that in each subsequent period, the sales revenue attainable for each unit of output exceeds the variable cost and therefore the firm will always exhaust the available production capacity, that is $q_t = x_t \cdot k$. In such specific settings, the LC measure then provides the relevant cost in the sense that the technology with lower the LC always generates the higher net present value. This claim also applies in environments where the decision maker faces uncertainty regarding the attainable future sales revenues. The argument here builds directly on the reasoning provided in Section 2.1 above, showing that the LC measure is the effective unit cost measure in a net-present value calculation.

Earlier literature has pointed out that LC is not the relevant cost metric for ranking the competitiveness of power generation technologies based on fossil fuels, such as coal or natural gas, in comparison to renewable energy sources, such as wind and solar photovoltaic (PV) installations

(Joskow (2011) and Hirth (2013)). While both technologies generate the same output (electricity), they differ substantially in their cost structure. Renewable electricity requires a relatively high upfront capital expenditure but, in contrast to fossil fuel based generation, entails almost no variable cost. Nonetheless, a simple comparison of the levelized cost would be misleading in evaluating the profitability and competitiveness of these technologies. Contrary to the arguments provided in the previous paragraph, the renewable power generation source is restricted in producing electricity and revenues during those hours of the year when the natural resource, i.e., the sun or the wind, is available. Electric power generated from fossil fuels, on the other hand, is essentially dispatchable allowing the plant to tailor its output to the revenues available at different hours of the year.

To obtain a relevant cost measure for comparing dispatchable and intermittent power sources, Reichelstein and Sahoo (2015) argue that the levelized cost metric should be adjusted by a co-variation coefficient. As the name suggests this coefficient captures the covariance between electricity generated and the market prices available for electricity at different points in time. The co-variation coefficient is always greater than zero and exceeds one only if there is a positive correlation between the hours of high output generation and above average market prices for electricity. Investment in a renewable power generation source is shown to be profitable, in the sense of a non-negative net present value, if the average price of electricity is at least as large as the LC divided by the co-variation coefficient.[13]

In the economics literature, marginal cost is arguably the most common measure of relevant cost, at least in connection with decisions concerning production volume and pricing. Under certain conditions, LC can be identified with the long-run marginal cost of a product. Reichelstein and Rohlfing-Bastian (2015) argue this point in a model setting of a competitive industry in which a large number of firms have access to the same stationary constant returns to scale technology. Demand in each period is subject to random shocks. Given initial capacity investments, firms act as price takers with the consequence that the product price in any given period is either equal to the short-run marginal (variable) cost in case there is excess capacity, or, if the industry's aggregate capacity is fully utilized, the equilibrium price is equal to consumers' willingness to pay at the aggregate capacity level. The main result then is that in equilibrium the initial aggregate capacity level will be chosen such that the expected market price is equal to the LC

[13] One implication of this result is that if electricity is sold at a constant price under a so-called Power Purchasing Agreement (PPA), then the technology that has the lower LC is more profitable, regardless of whether the generation technology is dispatchable or intermittent.

in each subsequent period. This finding identifies the LC as the long-run marginal cost to the extent that in a competitive equilibrium the (expected) market price “must" be equal to firms’ long-run marginal cost.

The LC concept presented here assumes one upfront capacity investment. In the earlier literature on capital accumulation, e.g., Jorgenson (1963) and Arrow (1964), firms make a sequence of overlapping capacity investments in an infinite horizon setting.[14] In these models the cost of *one unit of capacity made available for one period of time* can be identified unambiguously. It can be shown to be equal to:

$$c = \frac{\nu}{\sum_{t=1}^{T} x_t \cdot (1+r)^{-t}},$$

which aligns with the definition of the capacity cost component of the LC in Section 2.1 above. Some microeconomics textbooks, e.g., Carlton and Perloff (2005), define the long-run marginal cost of a product as:

$$LMC = w + \nu \cdot (r + \delta),$$

where δ is introduced as a parameter that reflects “economic depreciation". If economic depreciation is equated with capacity degradation, which furthermore is proportional to the remaining capacity in each period, then $\delta = 1 - x$ and $x_i = x^i$. Finally, if the planning horizon is set at $T = \infty$, then

$$c = \frac{\nu}{\sum_{t=1}^{\infty} x^t \cdot (1+r)^{-t}} = \nu \cdot (r + 1 - x) = \nu \cdot (r + \delta).$$

Thus, the microeconomic operationalization of LMC coincides with the levelized product cost, subject to suitable parametric specification and the absence of fixed operating costs and income tax effects.

LC can also be established as the relevant cost for a monopolist seeking to determine an optimal expansion of capacity. Suppose, for simplicity, the monopolist faces an identical demand curve in each of the next T periods, and furthermore has access to a stationary constant returns to scale technology. A central result in Reichelstein and Rohlfing-Bastian (2015) shows that the optimal capacity level is such that the marginal revenue at the production volume corresponding to full

[14] More recent studies on capital stock accumulation by firms have examined the impact of the choice of depreciation schedules on the relation between historical and long-run marginal cost (Rogerson, 2008, Rajan and Reichelstein, 2009, Nezlobin, 2012, Nezlobin et al., 2012).

capacity utilization in each period is equal to the LC for the product in question. Thus, this result extends the standard textbook prescription of a monopolist choosing the optimal output level such that marginal revenue is equal to marginal cost.

The preceding result can be extended to environments where demand in future periods is subject to random shocks and therefore the monopolist will not exhaust the entire capacity available unless the marginal revenue at the capacity limit exceeds the short-run variable (marginal) cost. In such settings with demand uncertainty it can be shown that the optimal capacity investment is such that the expected marginal revenue evaluated at the sequentially optimal output quantity (given the optimal investment) is equal to the LC. Uncertainty about future demand essentially entails a call option. This real option becomes more valuable with a higher level uncertainty, thus resulting in larger capacity investments.

2.3 Energy Related Applications

Dating back to Rosenthal et al. (1965), the concept of levelized product costs appears to have emerged from the literature on electricity generation. In the intervening years, the Levelized Cost of Electricity has become a standard metric approach for benchmarking the economics of different electricity generation technologies (Tran and Smith, 2018, Aldersey-Williams and Rubert, 2019). Variants of the original LCOE have been adapted and expanded in energy subfields other than electricity. For instance, the LCOS presents a life-cycle cost measure of electricity storage services provided by batteries, pumped-hydro, or mechanical storage devices. For hydrogen, the LCOH provides a cost metric that is increasingly used to assess the prospects for a hydrogen economy. Since hydrogen offers multiple applications beyond energy storage, we view it as a separate research stream in this section. Finally, we cover several recent studies that have calculated a LCOC in connection with facilities that can capture and sequester CO_2. Figure 2.1 provides a graphic overview of the history of these literature streams.

2.3.1 Levelized Cost of Electricity

The term "Levelized Cost of Electricity" goes back at least to the 1973 publication by Farrar and Woodruff (1973). Since then, the LCOE metric has been widely relied on to compare and rank the cost of producing electricity with alternative generation technologies (Short et al., 1995).

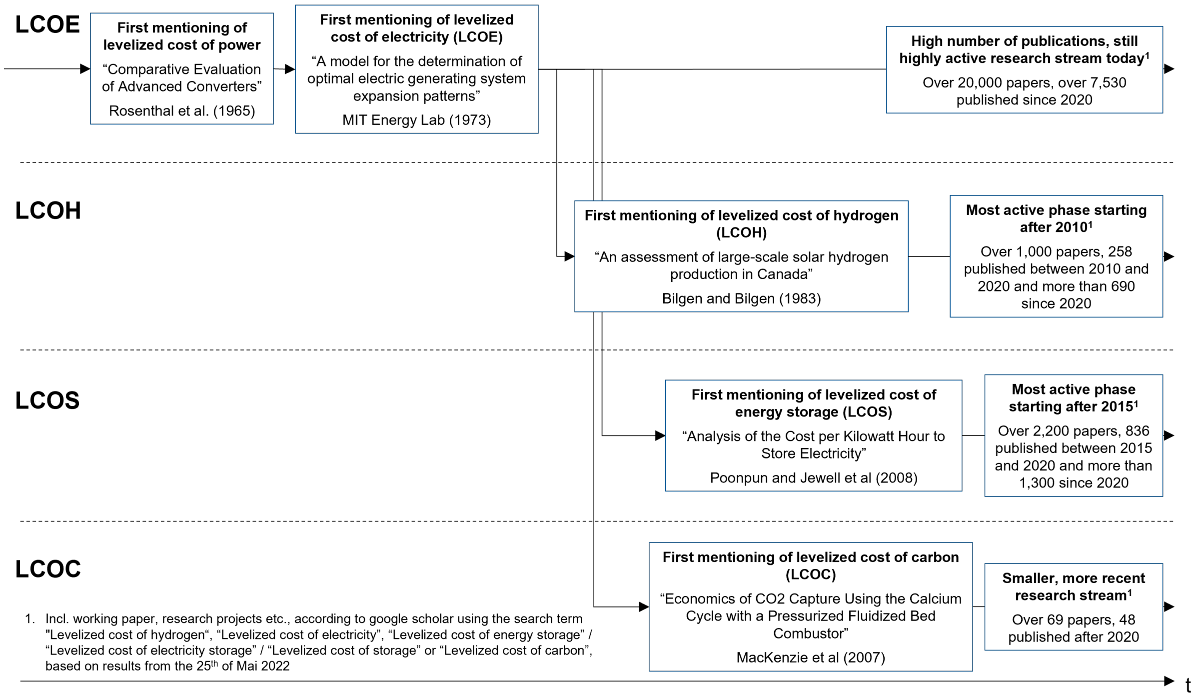

FIGURE 2.1: Emergence of the levelized cost metric for electricity, energy storage, hydrogen and carbon

Power generation provides a natural use case for a life-cycle cost concept that seeks to assess the unit economics of alternative generation technologies that differ substantially in terms of their fixed and variable cost structure; see, for instance, Reichelstein and Yorston, 2013, Hernández-Moro and Martínez-Duart, 2013, Branker et al., 2011, Massachusetts Institute of Technology, 2007.

As a unit cost measure, LCOE is usually expressed in terms of dollars (or Euro) per kWh. The expenditure required for the capacity investment in power generation is expressed in dollars per kilowatt. Of critical importance for the unit cost of capacity (the variable c in Section 2) is the levelization factor L, which in electricity related applications typically takes the form:

$$L = \sum_{t=1}^{T} x_t \cdot (1+r)^{-t} \cdot 8,760 \cdot CF_t.$$

Here, 8,760 refers to the number of hours in the year, while CF_t denotes the average capacity utilization factor in year t. For dispatchable power generation sources, CF_t could in principle be close to one, i.e., the power plant is a base-load generation facility capable of running at full capacity around the clock (except for select hours of scheduled maintenance). For renewable energy sources, such as solar PV and wind power, the capacity factor CF_t is exogenously determined by the availability of the underlying natural resource. For these technologies, the capacity factors are usually below 0.5, and sometimes as low as 0.15, thereby increasing the unit cost of the corresponding LCOE.

A fundamental drawback of wind and solar PV power is not only their relatively low capacity factors, but also their intermittency, that is, the plant's inability to deliver energy during certain hours of the year. For this reason, it would not be appropriate to conclude that a renewable energy source, which has a lower LCOE than its dispatchable counterpart running on fossil fuels, will also be more profitable in terms of a higher net present value (Joskow, 2011, Hirth, 2013). Recent studies seek to provide a unified economic assessment framework by introducing the concept of a levelized profit margin that takes into account the correlations between hourly electricity prices and capacity factors (Reichelstein and Sahoo, 2015, Glenk and Reichelstein, 2022b). The study by Glenk and Reichelstein (2022b) concludes that in both California and Texas the levelized profit margin of natural gas power plants has remained roughly constant despite the tangible decline in the capacity utilization factor of these plants. Yet, this effect has effectively been compensated by higher sales revenues during hours of high electricity prices, typically when renewable energy sources do not feed electricity to the grid. In contrast, both wind and solar PV have seen improved levelized profit margins in large part due to falling life-cycle costs.

For individual power generation technologies, the LCOE metric has been used to gauge the magnitude of cost declines due to learning-by-doing. For example, Hernández-Moro and Martínez-Duart (2013) estimate the LCOE trajectory of solar PV and concentrated solar power using learning rates. They find that in comparison to concentrated solar power, solar photovoltaic power generation exhibited a stronger LCOE decline. In the context of wind power, Glenk et al. (2021) find that for the years 1990-2020, the LCOE of wind power has declined at a rate of approximately 23% with every doubling of cumulative deployments. While the capacity acquisition cost of wind turbines (the parameter ν in Section 2) has not declined nearly that quickly, the overall drop in the LCOE of wind power reflects a significant "denominator effect." Specifically, the capacity factor, CF, of wind turbines has improved substantially, owing to improved materials that entail lower frictions in the rotation of the turbines.

The LCOE metric has also been prominent in studies seeking to evaluate the effect of new regulations, including subsidies and charges for carbon emissions. These studies are important in the context of the global energy transition as governments around the world seek to accelerate the expansion of new low-emission power sources through targeted subsidies. For example, Reichelstein and Yorston (2013) found that in 2013 the LCOE of solar PV in the U.S. would have increased by approximately 70% in the absence of the Investment Tax Credit (ITC) and the availability of an accelerated tax depreciation schedule. Taken together, these two incentive provisions lowered the tax factor (the variable Δ in Section 2) from approximately 1.3 to 0.8.

Anticipating the reduction in the ITC for solar PV in the US from 30% to 10%, as specified in the regulations at the time, Comello and Reichelstein (2016) calculated a gradual step-down in the ITC that would leave the LCOE unchanged, provided the investment cost in solar PV systems would continue on its historical decline path. Similarly, Ouyang and Lin (2014) estimate the LCOE for solar PV, wind and biomass in China in order to project the subsidies required to support further expansion of renewables. Simsek et al. (2018) conduct a related study in the context of concentrated solar projects in Chile. Finally, Comello et al. (2018) examine solar PV's competitive position in the U.S. and its potential evolution through technological advances and supportive public policies, including federal ITCs.

In concluding this subsection, we mention several papers that have sought to embed the LCOE metric in a broader context. Xu et al. (2021) adopts a modified LCOE approach in evaluating policies for additional offshore wind production in six Chinese provinces. Darling et al. (2011) focus on highlighting sensitivity and uncertainty in LCOE calculations by proposing a new method for solar PV that relies on parameter distributions of instead of point estimates. Bruck et al. (2018) introduce an expanded LCOE framework, which considers penalty payments for violating contractual minimum or maximum purchase limits.

2.3.2 Levelized Cost of Energy Storage

The intermittency of renewable electricity generation has created a growing need for energy storage, in particular the storage of electric power. The LCOS is a generic unit cost measure that allows for a comparison of alternative energy storage services that can be provided, for instance, by a battery, a closed loop pumped hydro system or a mechanical storage device. In terms of the system acquisition, every energy storage system requires both a power and an energy storage component. The power component relates to the amount of energy that can be charged or discharged at any given point in time. Its capacity is typically measured in kW. The size of the energy storage component, in contrast, is measured in kWh. It indicates the total amount of energy that can be charged and discharged in one cycle. Combining these two system components, Comello and Reichelstein (2019) decompose the overall levelized cost of energy storage as follows:[15]

$$LCOS = LCOEC + \frac{1}{D} \cdot LCOPC.$$

Here, LCOEC represents the levelized cost of the energy storage component and LCOPC the levelized cost of the power component. The power component is multiplied by the inverse of the duration, D, which indicates the time required to fully charge or discharge the storage device, assuming the charge or discharge function is performed at maximum capacity. Formally, the duration of the storage device is given by:

$$D = \frac{k_p}{k_e}$$

where k_p and k_e represents the size of the power and energy component, respectively. To illustrate the duration concept, batteries that are sold off-the shelf for residential applications frequently have a duration of either two, four or six hours.

The LCOS metric is calibrated as the minimum service fee per unit of energy discharged that an investor will need to receive in order to break even on the initial acquisition of the storage system. This calculation is critically dependent on the number of charge and discharge cycles per year and the round-trip efficiency of the storage device. The round-trip efficiency factor (denoted by η, with $0 \leq \eta \leq 1$) gives the percentage of the energy that can ultimately be discharged. Conversely, $1 - \eta$ is the percentage of the energy lost in the charge and discharge process. If the service fee per kWh discharged is p^o, the overall net present value of the investment becomes:

$$NPV(k_p, k_e) = \sum_{t=1}^{T} N \cdot p^o \cdot \eta \cdot x_t \cdot k_e \cdot (1+r)^{-t} - \nu_p \cdot k_p - \nu_e \cdot k_e.$$

Here, the variables x_t and T are as introduced in Section 2, N is the number of annual charge and discharge cycles, while ν_e and ν_p represent the unit acquisition costs for the energy storage and power component, respectively. Setting the above equation for the $NPV(k_p, k_e)$ equal to zero, Comello and Reichelstein (2019) show that $p^o = LCOS$ is the break-even service fee per

[15] Comello and Reichelstein (2019) abbreviate the levelized cost of energy storage as LCOES.

kWh for a storage device that initially can store at most k_e kWh of energy in N cycles per year, subject to the device (dis)charging at most k_p kW of power at any given point in time.

The above definition of LCOS as the break-even service fee per unit of energy discharged is consistent with existing studies (Jülch et al., 2015, Pawel, 2014, Smallbone et al., 2017, Rodby et al., 2020). In addition to LCOS, several papers discuss related metrics (Belderbos et al., 2017). Lai and McCulloch (2017) proposes a metric labelled *levelized cost of delivery* for a combined solar PV and energy storage system. In connection with battery storage, Rodby et al. (2020) construct a model that allows for storage capacity degradation with the possibility of rebalancing. They find that investors can reduce the overall resulting LCOS by oversizing the battery in the first place. In connection with behind-the-meter battery installations, Comello and Reichelstein (2019) examine the optimal size of a battery system for households with a solar PV rooftop system. Storing the electricity generated by the rooftop system allows the household to economize on grid electricity purchases. An optimally sized battery must balance the benefits of reduced electricity purchases against the LCOS of the battery system.

As a generic unit cost measure, LCOS allows for a comparison of competing storage technologies that can be deployed for alternative use cases. While multiple factors ultimately shape this cost comparison, recent studies have focused on roundtrip efficiency, discharge cycles per period and recycling costs (Mostafa et al., 2020, Rahman et al., 2020, Schmidt et al., 2019). In terms of alternative storage technologies, recent studies have compared li-ion batteries, lead-acid batteries, vanadium redox flow batteries, flywheels, supercapacitors, pumped hydro-storage, pumped heat, power-to-gas (hydrogen), liquid air and compressed air (Jülch et al., 2015, Poonpun and Jewell, 2008, Schmidt et al., 2019, Steckel et al., 2021, Smallbone et al., 2017, Xie et al., 2019).

2.3.3 Levelized Cost of Hydrogen

In the transition towards a decarbonized energy economy, hydrogen is increasingly viewed as a potentially valuable energy carrier. The list of potential use cases for hydrogen comprises fuel for transport (Jones, 2012, Van Renssen, 2013, Goodall, 2017), energy storage for industrial heat and power (Jacobson, 2016, Zakeri and Syri, 2015, Evans et al., 2012, Nat Energy, 2016), or a feedstock for chemicals processing (Schulze et al., 2017). At the same time, some observers question the economic viability of hydrogen on account of its considerable primary energy requirements and its high production cost.

Recent discussions about the emergence of a hydrogen-based energy economy have focused on electrolytic hydrogen, where the H_2 molecule is obtained by infusing electric current into water. In contrast, traditional "gray" hydrogen is obtained from natural gas (methane) through a steam methane reforming process. If the CO_2 emissions that arise in connection with steam methane reforming (amounting to about 2% of global emissions) are captured and sequestered, the resulting hydrogen is usually labeled "blue". In subsidizing the production of "green" hydrogen, the European Union mandates that the required electricity come from renewable power sources. Regardless of the applicable color scheme, the levelized cost of hydrogen is usually defined as the break-even value per kilogram of H_2 that an investor would need to obtain in the marketplace in order to recover the expenditures associated with the initial capacity investment as well as all subsequent operating costs.[16]

Parkinson et al. (2019) calculate the LCOH of twelve different hydrogen production technologies. Their research indicates that while fossil-fuel-based hydrogen production remains the most affordable option, it only provides a modest level of carbon reduction. Grimm et al. (2020) use the LCOH to compare the production costs of two solar-assisted hydrogen production technologies. Minutillo et al. (2021) investigate the costs of different water electrolysis plant sizes and electricity configurations to re-fuel hydrogen with smaller on-site production units. Franco et al. (2021) rely on the LCOH metric to assess the costs of different offloading pathways for hydrogen production with offshore wind farms. Glenk and Reichelstein (2019) demonstrate that the economics of green hydrogen improves considerably if the initial investment is structured as a hybrid system that combines electrolyzer capacity with a renewable energy source. With electricity prices fluctuating increasingly across the hours of the year, electric power obtained from the renewable power source can then be dispatched to the grid during hours of relatively high prices, or alternatively converted to hydrogen through electrolysis during off-peak hours for electricity prices. The key to favorable LCOH values is that the size of the electrolyzer is chosen optimally in relation to the size of the power generation facility. Such hybrid energy systems will be eligible for significant subsidies under both the Inflation Reduction Act in the U.S. and the green hydrogen initiative of the EU.

Electrolyzer technologies have also experienced significant learning effects in recent years. These gains have resulted in both substantial savings on the system prices for electrolyzers and higher

[16] Some studies have considered closely related life-cycle cost measures; see, for instance, Guerra et al., 2019, Khzouz et al., 2020, Lee et al., 2009.

conversion efficiencies for electrolytic processes. So-called reversible fuel cells have seen particularly steep learning effects (Glenk and Reichelstein, 2022a). A significant advantage of reversible fuel cells is that they can run bi-directionally, that is, they can either convert water and electricity to hydrogen, or, in the opposite direction, hydrogen and oxygen can be converted back to water and electricity. As a consequence, these types of electrolyzers can achieve particularly high capacity factors resulting in lower LCOH values. A recent study by (Glenk et al., 2023b) projects that, assuming continued learning effects for electrolyzer technologies, the variable cost of electricity will account for almost 80% of the overall LCOH of electrolytic hydrogen by the year 2030.

2.3.4 Levelized Cost of Carbon

There is widespread agreement that in order to slow, and ultimately stop, climate change, economies around the world will not only need to reduce their CO_2 emissions but also need to deploy negative emission technologies by means of CO_2 removals from the atmosphere. CCS technologies enable the capture of CO_2 from point sources, e.g., power plants and manufacturing facilities, or alternatively from the ambient air, e.g., direct air capture and photosynthesis by trees. The levelized cost concept has been applied to comparing alternative CCS technologies in terms of a *Levelized Cost of Carbon* metric that yields the minimal price per ton of CO_2 that would be required in order for a particular capture technology to deliver an acceptable return to investors.

For CO_2 capture from point sources, Psarras et al. (2017) break the overall levelized cost of capture into three components corresponding to flue gas separation, compression and transport to the ultimate carbon sink, e.g., a geological storage site. As one would expect, higher concentrations of CO_2 in an industrial flue gas is known to decrease the cost of separation. This concentration tends to be relatively high in manufacturing processes such as ethanol, fossil fuel power generation or Portland cement (Rubin and Zhai, 2012, Psarras et al., 2017). Several alternative point source capture technologies are principally known and understood today, including Calcium Looping, Oxyfuel, and Amine Scrubbing (İşlegen and Reichelstein, 2011, MacKenzie et al., 2007, Friedmann et al., 2020, Glenk et al., 2023a). However, because relatively few large-scale CCS systems have been deployed to date, there is no consensus on which one of these technologies achieves the lowest levelized cost per ton captured.[17]

In the context of the cement industry, Glenk et al. (2023a) conclude that a future CO_2 emission charge of around €100 per ton would be required in order for cement producers to have incentives to install the so-called LEILAC capture technology. LEILAC, which stands for Low Emissions Lime and Cement, refers only to the capture of the process emissions that arise when calcium carbonate is converted to clinker, the main ingredient in Portland cement. In order for cement manufacturers to have incentives for comprehensive decarbonization through other CCS technologies, such as calcium looping, the prevailing CO_2 price would have to be at least in the range of €160 per ton of CO_2.

Direct Air Capture (DAC) is one prominent negative emissions technology. It has the obvious disadvantage that the concentration of CO_2 in the atmosphere is (still!) relatively low in comparison to that of industrial flue gases. At the same time, DAC facilities are entirely flexible in terms of their location, allowing them to economize on both energy costs and CO_2 transportation costs. While early studies put the corresponding LCOC in excess of \$300 per ton (Simon et al., 2011), more recent projections by European and North American companies suggest that a unit cost in the range of \$ 95-240 per ton might be attainable once additional DAC plants experience the anticipated effects of learning-by-doing (Keith et al., 2018). Finally, the emissions that result from decomposing biomass can be avoided (and therefore yield negative emissions) if the biomass is combusted and the corresponding emissions are captured and sequestered (Lehtveer and Emanuelsson, 2021, Cheng et al., 2021). Alternatively, the biomass is directly sequestered before it decomposes and emits CO_2. With carbon removal of biomass still at an early stage, the levelized cost of these processing technologies appears to be still relatively high Clifford (2023). Nonetheless, corporate buyers are willing to pay for these removals in order to acquire carbon offsets in the voluntary carbon markets.

2.3.5 Other Environmental Applications

In addition to the research highlighted above, the LC concept has been applied in other environmental contexts. For instance, LC has been employed to assess the unit cost for heating (usually measured by thermal energy output) in order to compare the cost competitiveness of different technologies. Gabbrielli et al. (2014) compare the levelized cost of heat from solar collectors

[17] McCoy and Rubin (2009) analyze the variability and impact of storage costs on the LCOC. They find that the type of storage reservoirs has considerable impact on the required capital investment and the resulting LCOC.

with heat from natural gas, Welsch et al. (2018) and Tian et al. (2018) analyze and optimize district heating systems, Kim et al. (2019) conduct an economic and environmental assessment of a hybrid renewable energy system. Finally, Yang et al. (2021) calculate the levelized cost of heat that is stored as thermal energy.

Similarly, as air conditioning or cooling become more widespread, a developing research stream investigates and utilizes the levelized cost of cooling. Most papers in this field conduct economic analysis of different cooling technologies. For example, Bellos and Tzivanidis (2017), Li et al. (2017) and Altun and Kilic (2020) conduct economic analysis of solar cooling systems and Sadi et al. (2021) calculate the LC of a biomass-based cooling system for buildings.

With globally decreasing freshwater resources, a new research stream investigating the levelized cost of water emerged. For example, Loutatidou and Arafat (2015) and Behnam et al. (2018) calculate the levelized cost of water in combined power, heating and desalination systems. Chong et al. (2019) assess the economic feasibility of specific desalination technologies. It should be noted that all these authors focus on desalination. However, the levelized cost of water can also be applied in other contexts, such as water purification.

In the context of mobility and transport, Comello et al. (2021) have introduced the Levelized Cost per X-mile (LCXM) concept. This cost metric is closely related to the TCO model, which has been widely used in transportation studies (Lebeau et al., 2015 and Lajunen and Lipman, 2016). The “X" in LCXM refers to alternative cost objects, for instance, ton- or passenger miles. In contrast to the TCO metric, LCXM is a unit cost measure aimed at the cost of transporting one ton of cargo or one passenger for one mile on a particular route. Comello et al. (2021) apply the LCXM metric to optimize the composition of a fleet of transit buses that can either be equipped with Diesel or battery electric transit buses.

2.4 Potential Future Applications

In addition to energy-related applications, the LC concept may gain traction in several other contexts. In this section, we sketch potential future LC applications in settings with competing generation technologies or managerial options that may differ in both their required initial capital expenditures as well as their periodic operating costs.

Agricultural commodities: Climate change, supply shocks, and technological advances affect the global agricultural sector. The LC concept can support decisions concerning competing agricultural food commodities by conducting a comparison of the per-unit nutritional value. In addition, LC can support managerial decisions regarding different production technologies for one agricultural product, for example, by comparing traditional food production methods, such as genetically modified crops, vertical farming, or investments in automated farming vehicles and artificial intelligence solutions.

Network industries: Friedl and Küpper (2011) show that adequate cost measures based on the annuity method for calculating depreciation and capital costs can improve the efficiency of investments in regulated markets such as network markets. The LC of network usage could help companies to determine the long-term unit prices in network industries with different production technologies, for example, by comparing the LC of internet access in different regions between a physical fiber network, cell phone towers, and satellite-based solution. In addition, in cases of monopolistic power, LC calculations can determine optimal capacity and output levels.

Cloud storage and computing: Tech companies such as Amazon, Alibaba, Alphabet, Microsoft, SAP, and Tencent generate increasing revenues from cloud storage and computing solutions. In this competitive field, companies need to choose between in-house sourcing or purchasing storage and power. LC can support this decision between a high-upfront investment in in-house capacity or purchasing storage and power on a predominantly variable cost-based structure.

Patent licensing: Intellectual property for patents is associated with ongoing R&D costs or high upfront investments to purchase patent portfolios externally. However, the usage and licensing of intellectual property itself do not require any significant variable costs. From the perspective of an investor deciding between buying or developing a portfolio of patents to use and license, the LC provide a metric to assess which option yields lower life-cycle costs. Historically, licensing fees for patents have often been calculated based on revenues from the associated products (Friedl and Ann, 2018). However, there is an ongoing discussion about whether cost-based valuation approaches for intellectual property rights could be a valid alternative (Parr, 2018 and Gamarra and Friedl, 2023). LC could be a suitable metric to implement as a cost-based approach.

Other potential applications: In addition to the aforementioned potential applications of LC. there is a wide range of other fields where LC could be used, e.g., E-Commerce, FinTechs, or DNA sequencing. For E-Commerce companies, LC can be used to evaluate the size and geographical spread of investments in new facilities. In the case of FinTechs, LC can support technological investment or in-sourcing decisions. Lastly, for DNA sequencing, different production technologies determining the order of nucleotides in a DNA can be compared based on their LC.

2.5 Conclusion

Levelized cost is a generic life-cycle cost product metric that aggregates capacity related investment expenditures and ongoing operating costs into a unit cost figure. Essential to the economic interpretation of this concept is that the allocation of upfront fixed costs to individual product units is consistent with the net present value criterion. Provided this allocation is made judiciously, the LC can be interpreted as the long-run marginal cost of a product, or alternatively, as a break-even product price at which the required investment becomes marginally profitable. This calibration makes the LC the unit cost measure metric relevant for long-run decisions.

As of today, most applications of the levelized product concept have originated in relation to energy technologies. This essay has synthesized multiple research streams relying on levelized cost measures in connection with electricity, energy storage, hydrogen and carbon capture. The widespread use of the LC metric in energy related fields suggests multiple other future applications. In general, we envision future potential for this cost concept whenever decision makers seek to capture the unit economics of projects with a long planning horizon.

3 Production cost modelling of Lithium-Ion batteries

Battery production cost models play a central role in evaluating and optimising the cost competitiveness of different battery cells and production technologies. They are essential to reduce the cost of EVs to increase their adoption. This essay presents a detailed bottom-up cost model that enables users to calculate the production cost of different cell formats, chemistries, and production processes. The flexible and modular nature of the model makes it easy to analyse the production cost implications of changes to the cell or the production process. The production cost is presented as FC, MC and LC to compare the results with literature and industry and properly reflect capital and imputed interest costs. The model is validated with two case studies: the production of a cylindrical 4680 cell and a prismatic PHEV2 hardcase cell. For both cell formats, three different chemistries are evaluated. NMC811 cathodes are combined with graphite and silicon anodes with 0 wt. %, 3 wt. % and 5 wt. % Si. The parameters for both cells and production processes are compiled from literature and expert interviews.

Keywords: Lithium-Ion Battery, Battery Production, Battery Cost, Levelized Cost, Electric Vehicles.

A different version of this essay has been accepted for publishing in Nature Communications Engineering, with my co-authors Maximilian Lechner, Anna Kollenda, Konrad Bendzuck, Julian Burmeister, Kashfia Mahin, Josef Keilhofer, Maximilian Blaschke, Gunther Friedl, Ruediger Daub, and Arno Kwade.

3.1 Introduction

To tackle climate change, countries worldwide take measures to foster the electrification of mobility. A key barrier to this endeavour is the cost markup of EVs compared to ICE vehicles. This markup is predominantly caused by the high production cost of EV batteries which make up roughly 30% of EV production cost (BloombergNEF, 2017). Therefore, it is essential to reduce battery production costs to enable a substantial increase in EV adoption.

Battery cost models such as the BatPac can help to reduce battery costs by enabling researchers and engineers to analyse and subsequently optimise the cost implications of different battery cell formats, chemistries, and production processes. In the past, a wide variety of models from authors such as Gallagher et al. (2014), Sakti et al. (2014), Schünemann (2015), Philippot et al. (2019), Wentker et al. (2019), Nelson et al. (2019), and Duffner et al. (2021) has emerged. However, these models lack either the flexibility to model different battery designs and production processes or omit important cost factors such as energy cost or individual scrap rates. Furthermore, most models lack standardised and clearly defined cost measures. While most models present FC, they often lack a clear definition of its calculation, for example, if capital costs are included and how they are calculated. Finally, the results of the cost models vary significantly.

Besides the large variability of cost estimates in the literature, there are also significant discrepancies between literature-reported values and some industry reports. For example, Tesla announced on their first battery day in September 2020 that they plan to reduce the cost per kWh of a battery pack by about 56 % compared to the current state of art (Frazelle, 2021), resulting in battery cost between 48 and 53 $\$\,(\text{kWh})^{-1}$. Assuming battery cell costs to account for 75 % of the battery pack costs, final cell costs would have to be between 36 and 40 $\$\,(\text{kWh})^{-1}$. Established OEMs have met these cost assumptions with scepticism because such a low-cost level can only be achieved through significant and as-yet-unseen technical and material-based advancements. Such ambitious cost targets raise the question if they are realistic and can be supported by cost models. Furthermore, they raise the question if such low targets can be due to differences in cost accounting methods, for example, if they only reflect MC.

This essay presents an extension to a battery cost model published by Schünemann (2015) and Schünemann et al. (2016). The model enables the user to calculate the FC, LC, and MC of different battery designs and to adjust the sequence of production steps and the parameters of each step. This allows for comparing different cell designs and production methods and understanding how each design decision can impact the cost of cell production.

The application of the model is demonstrated on two state-of-the-art battery designs: a cylindrical 4680 cell (as used, for example, by Tesla) and a prismatic PHEV2 hardcase cell (as used, for example, by VW). For both cell formats, NMC811 cathodes are combined with graphite and silicon anodes with 0 wt. %, 3 wt. % and 5 wt. % Si. Furthermore, two cases with and without the recovery of scrap material are compared.

The remainder of this assay is structured as follows: section 3.2 provides a brief introduction into the typical production process for modern EV batteries, an overview of existing battery cost models and their limitations, the typical cost structure of battery cells, and introduces FC, MC as well as the LCBP that is used in the cost modelling. Section 3.3 describes the developed cost model, the two cell designs, and the corresponding production processes. Finally, section 3.4 presents and discusses the calculated production costs for the 4680 and PHEV2 cells, and section 3.5 provides a conclusion.

3.2 Production costs of lithium-ion batteries

The production of battery cells requires a sequence of complex production steps, often conducted in a controlled environment such as a dry room. It requires high investments into machines and production facilities and is energy intensive. Combined with high raw material cost, e.g., for lithium, it makes battery cells the most cost-intensive component of EVs. Therefore, accurately calculating their cost is of significant importance to OEMs. Bottom-up cost models calculate production cost based on calculations of the required material, machines, labour, etc., for producing a specified factory output. With the help of these cost models, companies can evaluate and optimise their battery cell design and production processes and allow for benchmark studies to compare with competitors.

3.2.1 Modern battery production processes

The specific battery production process depends on multiple parameters such as the battery cell design, its chemistry, and the used production processes, which are often part of the proprietary knowledge of the producers (Schünemann, 2015). Therefore, there is not universally applicable or standardized production process, but rather many different ones with slight variations. In the following, the key steps of the process depicted in Figure 3.4, which is used in the model presented in this essay, are explained. The process has been chosen based on literature examples (e.g., Schünemann, 2015) and in consultation with industry experts.

In the first steps of the battery production process, the electrodes are produced. This is an important part of the overall cell production because the electrodes are responsible for a large share of the cell cost (Schünemann, 2015). The electrode production consists of the component handling, mixing, coating and drying, calendering, and post-drying.

Component handling describes the initial handling of the required raw materials such as lithium.

In the **mixing** step, the powdered raw materials are processed into a slurry. Today's industrial mixing processes mainly use batch processes, e.g., in planetary mixers that take up to six hours to complete with a capacity of up to 2000 L per pass (CHARGED Electric Vehicles Magazine). More recent developments are moving towards continuous processes, where a throughput of up to $2500\,\mathrm{L\,h^{-1}}$ could be possible (Bühler Group). A key challenge within the mixing step is to maintain a high slurry quality while increasing the required scale of production (Keppeler et al., 2021), but various studies have shown that continuous mixing processes can deliver a similar slurry quality compared to batch processes and that large scale production is possible (Schünemann et al., 2016, Dreger et al., 2015, Haarmann et al., 2021).

After mixing, during the **coating and drying**, the electrode slurries are coated onto their respective current collector foil. A key performance indicator for coating is the coating speed which is often around $80\,\mathrm{m\,min^{-1}}$, but successful production has also been reported at higher speeds of up to $100\,\mathrm{m\,min^{-1}}$ (Keppeler et al., 2021). The subsequent removal of the solvent from the wet film (i.e., the drying) has a significant impact on the resulting electrode quality (Westphal and Kwade, 2018) and is the process step with the highest energy consumption (Thomitzek et al., 2019). Process parameters must be selected in such a way that no segregation occurs in the particulate system, so that, for example, the mechanical properties of the coating are not negatively affected, since these also determine the further processability (Zhang et al., 2022, Westphal and Kwade, 2018).

During the **calendaring**, the dry electrode is compacted (often by a two-roll calender) to increase its energy density. Typically, the process speeds are similar to those of the coating step and are usually between 30 and 100 $\mathrm{m\,min^{-1}}$ (Kwade et al., 2018, Meyer et al., 2017).

Calendering also leads to a moisture uptake (Huttner et al., 2021), requiring a reduction of water content of the electrodes prior to the transfer into dry or inert atmosphere (Stich et al., 2017). This **post-drying** step is conducted, for example, by infrared belt dryers (Huttner et al., 2020).

After the post-drying, during the cell production phase, the electrodes and the other components of the cells (separator, casing, auxiliaries) are assembled (Kwade et al., 2018). Today, there are three main principles to assemble lithium-ion battery electrodes: winding, stacking and Z-folding (Kwade et al., 2018). Both cell designs presented in this essay use winding (see Figure 3.3). Therefore, the cell production described in the following consists of the steps slitting, winding, contacting, inserting and closing of the lid, electrolyte filling, and wetting. It is conducted in a so-called dry room with a defined, dry atmosphere. Commonly, the dry room has an ambient temperature of 20 °C and dew points between -40 and -60 °C. Creating these conditions represents a significant cost factor due to the high energy consumption of the used air conditioning systems (Yuan et al., 2017, Thomitzek et al., 2019, Vogt et al., 2021). The high cost of the dry room are necessary, however, because of the aforementioned sensitivity of cells to moisture.

In the first step of the cell assembly, the electrode coil is **slitted**, meaning it is cut into smaller webs (Pettinger, 2018). Common cutting systems using blades or lasers achieve speeds above 100 $\mathrm{m\,min^{-1}}$ and are usually not a limiting factor of the cell production throughput, but excellent cut edge quality is required to produce the high performance batteries required for EVs (Kriegler et al., 2021). In the case of stacking or Z-folding of electrodes, the electrodes must first be separated out of the web into individual sheets which can be done using different technologies such as punching dies or lasers (Pettinger, 2018, Kwade et al., 2018, Kriegler et al., 2021).

Afterwards, for the **winding** step, there are different processes for cylindrical cells (such as the modeled 4680 cell) and prismatic cells (such as the modeled PHEV2 cell). For cylindrical cells, the electrodes and the separator are wound around a nail-shaped winding mandrel, resulting in a round winding. For prismatic cells, the webs are wound around a flat winding mandrel resulting in a flat winding of similar dimensions to a cell of stacked electrodes (see Figure 3.3) (Pettinger, 2018). In both cases, the anode sheet is usually larger than the cathode sheet. In all stacking processes, the deposition accuracy of the electrodes with the separator is an important parameter. Even small deviations can lead to a significant reduction in cell performance or reproducibility (Leithoff et al., 2020).

The wound cell stack is then **inserted** into the cell housing, leaving an unsealed opening for the filling process (Knoche and Reinhart, 2015). The cell housing of LIBs can be made of flexible pouch foil or rigid materials such as steel or aluminium casings. Pouch cells usually consist of two pieces of aluminum composite foil, of which at least one, and often both, are thermoformed to accommodate the prismatically wound or stacked cell stack. A gas pouch is integrated into the setup to absorb excess electrolyte and gases produced during the electrochemical activation. Metal casings are usually deep-drawn from aluminum or stainless steel panels (Pettinger, 2018).

During the **filling** and **wetting** steps, the cell stack is soaked or wet with liquid through the unsealed opening. For industrially produced large-format battery cells, this process may involve multiple filling and wetting cycles and can lead to a duration of several hours to days (Wood et al., 2019). Options to improve the economic efficiency of the process (and thus reduce the cell production cost), are via the acceleration of wetting by means of vacuum application (Weydanz et al., 2018) or targeted structuring of the electrodes (Habedank et al., 2019).

After the filling and wetting, the **forming and degasing** of the cell is performed. Forming describes the first charging and discharging of the cell during which the electrolyte forms the so called Solid Electrolyte Interface (SEI). The SEI is composed of decomposition products of the electrolyte, lithium ions and the anode surface due to the resulting reaction in the anode potential operating window (An et al., 2016). Since the SEI-formation consumes lithium-ions, a capacity loss which amounts to roughly 10 % of capacity for graphite anodes occurs (An et al., 2017). Nevertheless, the SEI is essential for a long and stable operation of the cell as it prevents any further reactions with the electrolyte (Wood et al., 2019). Usually, the first charging and discharging cycle is carried out at a low current which is increased in the subsequent steps. Due to the many steps, the whole process can last up to several days (An et al., 2017). However, the exact formation protocols are typically undisclosed by the cell manufacturers (Wood et al., 2019). From a cost perspective, the formation step poses the second biggest cost factor after the cost of raw materials (Wood et al., 2015). This can be explained by the high number of required charging- and discharging cycles, which lead to a considerable production footprint and associated investment cost. Consequently, it is of great interest to lower the overall formation time in order to increase the throughput and, hence, reduce the production cost (Mao et al., 2018).

During the first charging of the battery material, a certain amount of gas is created (especially in larger cells), which needs to be removed from the cells before they can be closed. The degasing process depends on the cell type. For pouch cells, a separate gas bag which is vacuumized and cut off once the pouch bag is completely sealed, is used. For hardcase cells, a small opening on the top of the case is left so that the resulting gas can be removed before the cell is closed (Heimes et al., 2018, Pettinger, 2018).

When the cells are **closed**, the **aging** process, which is the most time-consuming production step, is conducted. The cells are stored in aging shelves and towers for two to three weeks to analyze their self-discharging performance (Heimes et al., 2018, Kwade et al., 2018). During the aging process, Open-Circuit-Voltage (OCV)-measurements are carried out at regular intervals to forecast the cell's lifetime (Michaelis et al.). Due to the long storage time, aging requires considerable equipment and space (Wood et al., 2019), and a change of the aging duration has direct cost-implications (Schünemann et al., 2016, Michaelis et al.).

Finally, the **End-of-Line testing**, which consists of two steps, takes place. First, the cells are removed from the aging shelves and put into the testing modules where tests like OCV-tests, pulse tests, or internal resistance measurements are conducted. Second, based on the test results, the cells are graded in different classes based on the customer requirements (Heimes et al., 2018, Pettinger, 2018).

3.2.2 Review of existing cost models and further relevant studies

Due to the increasing importance of EVs and battery cells, the literature on cost estimations of battery cells is growing rapidly. This section provides a brief overview of the most commonly used cost models. More detailed reviews of battery cost models can be found in Duffner et al. (2020) and Mauler et al. (2021).

One of the most frequently used tools for battery cost estimation is the BatPac. It was first released in 2011 by Nelson et al. (2019) and has since been updated several times. This work mostly focuses on version 5.0 from 2022, which is currently the newest version available. The Microsoft Excel-based bottom-up model enables users to calculate battery cell and pack costs for different chemistries under a specified production volume within a pre-defined factory layout and manufacturing process.

The model is frequently used, adapted or extended by various authors, such as Gallagher et al. (2014), Eroglu et al. (2015), Nelson et al. (2015), Patry et al. (2015), Ciez and Whitacre (2016), Ahmed et al. (2017), Safoutin et al. (2018), Philippot et al. (2019), Nemeth et al. (2020), Wang et al. (2020), Zang et al. (2021). Some of the model's limitations are, for example, the disregard of energy cost. In energy-intensive industries such as battery production, energy can become a major cost factor, especially in times of high electricity prices. Furthermore, the model does not account for individual manufacturing steps (e.g. calendering, drying, etc.) but only provides scrap rates on a high level (mixing, coating, electrode sitting, cell stacking, and electrode filling). However, more granular scrap rates would be necessary to measure the overall impact of improving the productivity of individual manufacturing processes. Besides, the model does neither allow to adjust the sequence of production steps in the manufacturing process nor to tailor the individual steps towards different cell designs (e.g. pouch, prismatic or cylindrical cells). These limitations reduce the tool's applicability when comparing and optimising different cell designs and production processes.

A frequently used modelling technique is Process-Based-Cost-Modelling (PBCM). PBCM is a widely accepted approach using technical parameters to calculate manufacturing cost in a bottom-up cost model (Field et al., 2007). PBCMs translate product characteristics (e.g., battery capacity) into technical parameters (e.g., required materials) which are then translated into operational parameters (e.g., required machines) and finally translated into manufacturing cost (e.g., material costs, machine investments, etc.) (Field et al., 2007). They are frequently used in battery literature, e.g. by Sakti et al. (2014), Berckmans et al. (2017), Ciez and Whitacre (2017), Sakti et al. (2017), Duffner et al. (2021) and Mauler et al. (2021). Most of these approaches are similar to the BatPac in using a bottom-up model to calculate manufacturing costs. However, they usually model manufacturing costs more accurately than the BatPac by including installation costs, machine downtimes, lead times and individual scrap rates for each manufacturing step. Most authors tailor their models to answer specific research questions (e.g., Ciez and Whitacre, 2017 compare cylindrical and prismatic cells) and resign from making their models available to the public. Therefore, it is difficult to use many of these PBCM models as generic tools for the cost estimation of different battery cells and manufacturing processes.

Finally, some authors use models without reference to PBCM, such as Kalhammer et al. (2007), Hagen et al. (2015), Petri et al. (2015), Schünemann (2015), Berg et al. (2015), Wood et al. (2015), Schmuch et al. (2018), Schnell et al. (2019), Wentker et al. (2019), Schneider et al. (2019) and

Schnell et al. (2020). For example, Amirault et al. (2009) developed a Battery-Weight-Model that estimates the weight of the battery based on the weight of the car it is used in. The model then estimates the battery production costs based on the battery's weight using assumptions on the relationship between battery weight and production costs. Like the mentioned PBCM models, these models are often neither publicly available nor designed to model cost for specific cell designs or manufacturing processes. Therefore, they are not meant to be used as generic tools for cost estimation of battery cells and manufacturing processes.

When analysing cost estimations made in previous literature, the high spread of the results between different authors is remarkable, especially in the earlier works between 2015 and 2019. For example, Petri et al. (2015) report cell costs between 104 to 122 $\$\,(\mathrm{kWh})^{-1}$, whereas Sakti et al. (2017) report a range of 138 to 1.210 $\$\,(\mathrm{kWh})^{-1}$. This can partially be attributed to the technological advances in battery manufacturing and cost differences associated with different cell designs. However, it also shows that there is not sufficient convergence in models and technologies towards an achievable price for a best-in-class design so far.

Notably, most cost estimations within academic literature state significantly higher costs than what can be assumed from companies like Tesla who report 110 to 120 $\$\,(\mathrm{kWh})^{-1}$ in 2020 and 48 to 53 $\$\,(\mathrm{kWh})^{-1}$ in 2025 for battery packs (Nextmove, 2020 and Frazelle, 2021), which would imply cell cost of as low as 36 to 40 $\$\,(\mathrm{kWh})^{-1}$ in 2025.

When summarising previous literature, it becomes apparent that current cost models are not precise enough. They frequently state significant variances in price estimations and deviate from industry-reported numbers. They often lack critical cost factors (e.g. electricity costs or scrap) and do not enable the user to quickly model different technologies for individual production steps. Therefore, further research should establish detailed and flexible bottom-up cost models calibrated with industry-reported costs. These models would allow OEMs and other researchers to estimate costs for different cell designs and manufacturing processes accurately.

3.2.3 Cost structure of battery cell production

The major share of battery cell cost is due to materials accounting for 58 to 77 % of total cost (Berckmans et al., 2017, Kwade et al., 2018, Philippot et al., 2019, Duffner et al., 2021). Depreciation and labor costs usually account for 6 to 16 % and 2 to 12 % respectively (Schünemann, 2015, Kwade et al., 2018, Philippot et al., 2019, Duffner et al., 2021).

Capital costs on the required investments, energy costs and other costs such as maintenance make up smaller shares of the total cost (ca. 3 % according to Kwade et al., 2018). Figure 3.1 illustrates the share of cost factors according to Kwade et al. (2018).

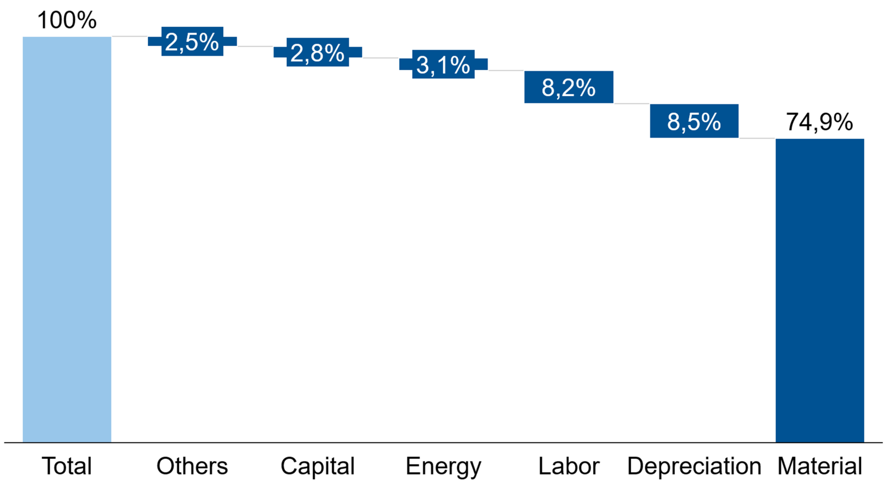

FIGURE 3.1: Battery production cost breakdown (own representation after Kwade et al., 2018)

.

Due to the significant shares of material, depreciation and labour costs, modelling approaches should consider individual scrap rates, machine performance, capital investments, labour requirements etc., per manufacturing step to enable more accurate cost estimations. This would also allow users to estimate the cost-effectiveness of new manufacturing processes for individual manufacturing steps.

3.3 Cost Model Approach

The presented model comprises six distinct stages (cf. Figure 3.2): (1) and (2) establish the cell design, properties, and process chain, along with the overall production volume. (3) calculates the required material throughput for each selected process based on individual scrap rates. (4) determines the resource requirements. (5) calculates the individual process costs followed by the calculation of full, marginal, and levelized cost in (6).

We adapt the model structure from Schünemann (2015) and Schünemann et al. (2016) and extend it with a more detailed cost calculation, two state-of-the-art battery cell formats and updated process parameters collected via literature review and expert interviews. In the following, we provide a brief explanation of the cell designs and the production processes.

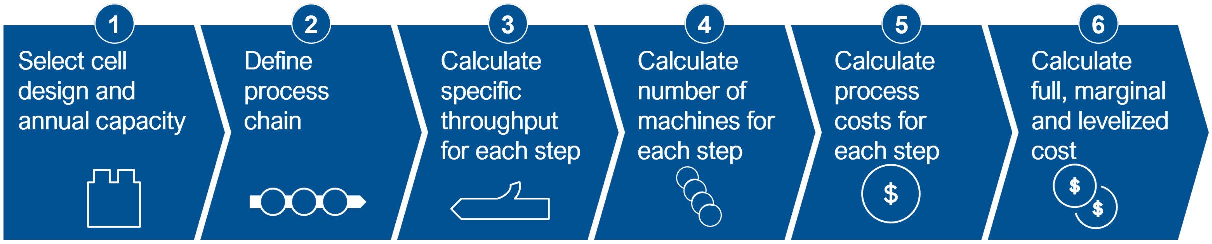

Figure 3.2: Calculation procedure of the battery cost model used in this essay

3.3.1 Cell design

Two cell formats are investigated based on their relevance within the automotive sector: A cylindrical cell with modern dimensions (4680, as used by Tesla) and a standard prismatic hard case cell (PHEV2) with flat cell winding. Both cells are depicted in Figure 3.3.

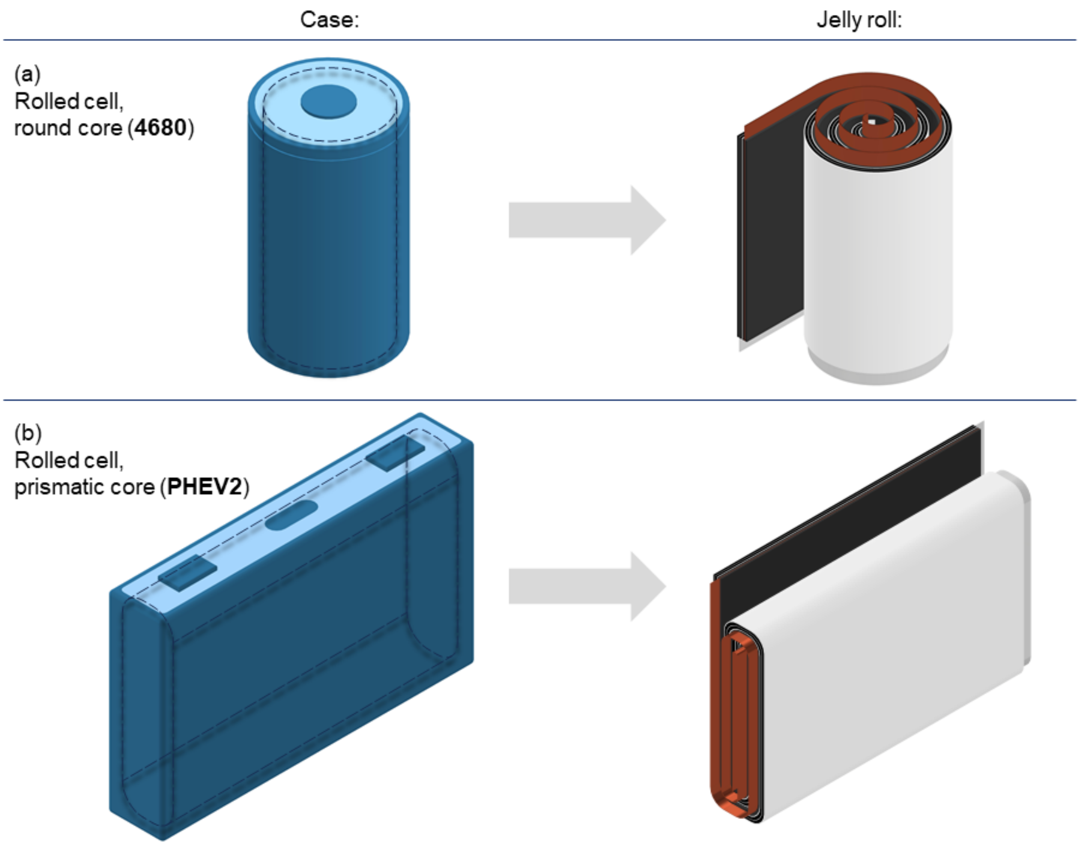

Figure 3.3: Illustration of the two modelled state-of-the-art battery cells including the type of jelly roll

For each format, three industry-relevant cell chemistries are compared. Each of the three cell configurations uses NMC811 cathode active material. For the anode, one variant with Graphite (G) and two variants with silicon-containing (3 and 5 wt. %) graphite as the active anode material are chosen. We assume common materials for inactive electrode components, such as the binder, conductive additive, and solvent, and for the inactive cell components, such as the electrolyte and separator (Kwade et al., 2018). Table 3.1 provides a summary of the electrode property inputs and Table 3.2 lists the corresponding performance parameters of the cells. For the material costs of the individual cell components, we gathered price estimations from a material price study by Pillot (2020) and combined them with the values from other cost models such as Schnell et al. (2020) and Knehr et al. (2022).

Table 3.1: Key parameters for the electrode design

	Cathode (NMC811)	Graphite	G + 3 wt. % Si	G + 5 wt. % Si
Specific capacity, in $mAh\,g^{-1}$	200[a]	360[b]	475**	522**
Areal capacity, in $mAh\,cm^{-2}$	5.00[c]	6.00	6.00	6.00
Solvent	NMP	Water	Water	Water
Slurry solid content, in wt. %	70	55	55	55
Current collector, in µm	Al / 12	Cu / 8	Cu / 8	Cu / 8
Porosity, in %	22.0[c]	22.0[c]	28.2***	32.3***
SEI loss*, in %	-	7.29[d]	8.50[d]	9.51[d]

* Capacity loss at cathode due to solid electrolyte interphase (SEI) formation at the anode
** Calculated based on the specific capacity of Si, G, and respective mass fractions
*** Calculated based on Si expansion
[a, b, c, d] Heck et al. (2020), Andre et al. (2017), Günter and Wassiliadis (2022), and Moyassari et al. (2022) respectively

Table 3.2: Resulting performance parameters for each cell

Parameter	PHEV2			4680		
	Graphite	G + 3 wt. % Si	G + 5 wt. % Si	Graphite	G + 3 wt. % Si	G + 5 wt. % Si
Capacity* / Ah	53.05	56.29	58.00	26.71	28.34	29.21
Nominal voltage / V	3.7	3.6	3.6	3.7	3.6	3.6
Energy content* / Wh	196.29	202.64	208.80	98.83	102.02	105.16
Cell weight / g	892.40	898.97	903.34	400.25	403.48	405.64
Energy density* / $Wh\,kg^{-1}$	219.96	225.40	231.14	246.95	252.88	259.19

* After cell formation (including losses due to SEI formation); no losses at the anode assumed

3.3.2 Production processes

We assume a yearly production volume of 10 GWh. The factory is located in Germany and operates 360 days a year, with a 3 shift operation lasting 8 hours each (including a 1-hour break). The modelled plant incorporates an excess capacity of 25 % (Nelson et al., 2019), providing a buffer against potential production interruptions. Table 3.3 presents the overarching production parameters used in the case study.

TABLE 3.3: General factory parameters for the production scenarios

Parameter	Value	Unit	Comment
Location	Germany	-	Influences labour, construction, and energy costs
Yearly production capacity	10	GWh	
Operating days	360	d/y	
Employee working days	208	d/y	
Working hours per shift	8	h/shift	Including 1 hour break
Shifts per day	3	shifts/d	
Excess capacity	25	%	Additional capacity to reduce downtime

The process chain used in this case study was chosen based on literature sources such as (Schünemann, 2015) and industry experts. It is shown schematically in Figure 3.4. The figure illustrates the flow of materials and by-products in the light blue path. The dark blue path illustrates the sequence in which the required throughput and subsequently the required amount of material, number of machines, personnel, etc., are calculated. This is the so-called anterograde calculation which starts from the last step of the production process and then moves backwards to account for the individual scrap rates within each production step[18].

It consists of a batch mixing process, continuous coating and drying, and subsequent calendering. The electrode coils are post-dried before they are transferred to the dry room. These process steps (up to slitting) can be modelled identically for both cell types, except for minor differences such as the coating width. The electrode slitting process varies due to differences in electrode and cell dimensions. The winding process differs significantly between the two cell formats, as the PHEV2 cell utilises a flat wound jelly roll instead of the round winding of the 4680.

The main difference in the process sequences of the cell designs lies in the contacting step. For the PHEV2, the current collectors are contacted before case inserting and lid closing. Meanwhile,

[18] I.e., the occurrence of scrap in a production process forces the previous production step to have a higher output to meet the final required output of the factory.

for the 4680, this step happens after inserting. The rest of the process chain is the same for both cell types. After electrolyte filling through an opening at the top of the case and a wetting step, the cells are charged and discharged during the formation process, which builds the SEI on the anode surface. Simultaneously, the cells are degassed through the filling hole. Once the formation and degassing are completed, the cells are closed and rested in the ageing step to track the self-discharge behaviour. Afterwards, the end-of-line test serves as quality assurance before packaging and shipping the cells.

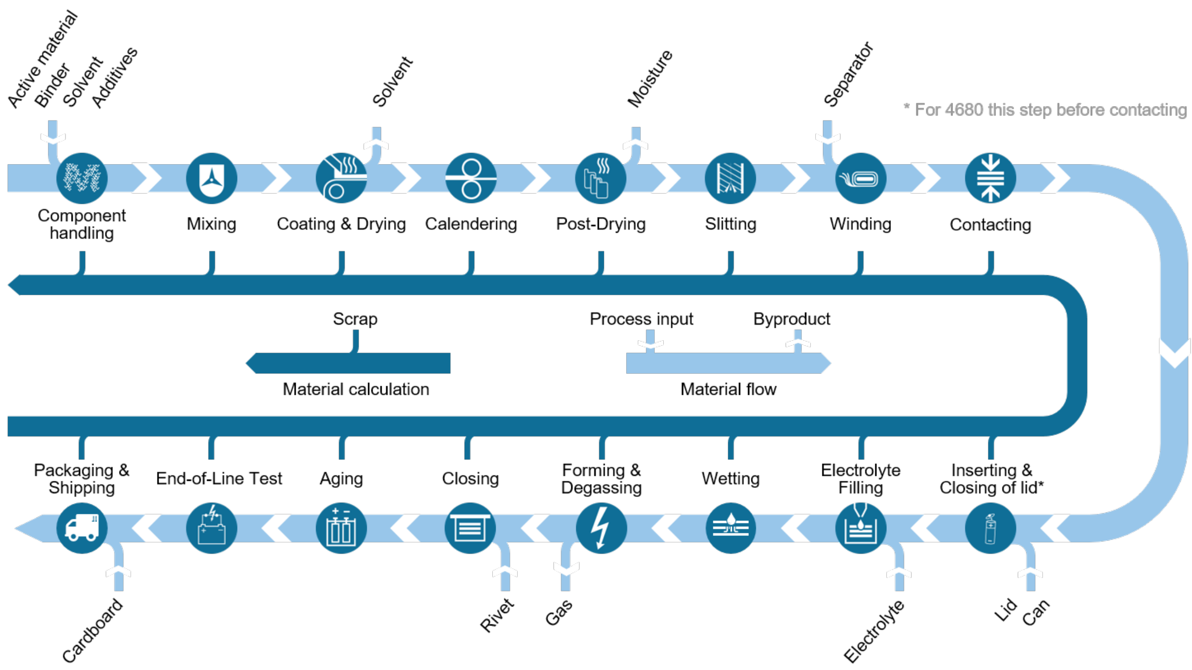

FIGURE 3.4: Production processes for the modelled PHEV2 and 4680 cells

3.3.3 Factory size and cost calculation

Before the full, marginal, and levelized cost can be calculated, it is necessary to calculate the overall factory dimensions and the resulting investment, fixed, and variable cost (i.e., steps $3-5$ from Figure 3.2).

First, the number of cells that need to be produced is calculated by dividing the specified factory output ($o_t = 10\,\text{GWh}$ in the case study) by the energy content of the cells.

Next, in step 3, the required throughput per process step is calculated in the anterograde material flow calculation, using the individual scrap rates per process scrap. This enables us to account for a compounding effect of losses from scrap over the entire production process. For example, if a production process consisting of three production steps with scrap rates of 10%, 5%, and 7% should produce 100 units of output, then the required input into the last step is $100 \cdot (1 - 7\%)^{-1} \approx 108$, the required input for the second to last step is $108 \cdot (1 - 5\%)^{-1} \approx 114$, and the required input for the first step is $114 \cdot (1 - 10\%)^{-1} \approx 127$. Conversely, the amount of scrap per process step is calculated by multiplying the input with the individual scrap rate. With the throughput and scrap per process step we can also calculate the required material input per process step as well as the material waste that can be avoided with scrap reduction.

Afterwards, in step 4, the calculation of the required number of machines $N_{\text{Units,j}}$ per process step j is conducted based on the throughput per process step, the throughput per machine, and the defined overcapacity which accounts for machine downtimes. It is then used to calculate the shopfloor space, energy consumption, and personnel per process step.

Finally, in step 5, the total production cost are calculated[19]. In this model, we take the following eight cost factors into account: Direct material, direct personnel, personnel overhead, direct energy, energy overhead, investment, maintenance, and ramp-up cost.

The **direct material** cost, $C_{\text{Mat}} = \sum_{m \in M} m_M \cdot C_M$, are calculated based on the required amount of material m_M and material cost per kg C_M. We differentiate the material cost by the following cell components: Anode solvent, Cathode solvent, Anode coating, Cathode coating, Anode current collector, Cathode current collector, Separator, Electrolyte, and Casing (i.e. $M = \{\text{Anode solvent, Cathode solvent, ..., Casing}\}$).

Direct personnel cost consists of skilled and assistant workers. The number of employed skilled and assistant workers

$$N_j = \frac{N_{\text{Shift,Day}} \cdot N_{\text{Workdays}}}{N_{\text{Workdays,Empl}}} \cdot \sum_k N_{\text{j,k}} \cdot N_{\text{Units,k}}$$

$$j \in \{\text{Skilled, Assistant}\},\ k \in \{\text{Process Steps}\}$$

consist of the number of required skilled/assistant worker per machine and process step $N_{j,k}$, the number of machines per process step $N_{\text{Units,k}}$, the number of shifts per day $N_{\text{Shift,Day}}$, the number of work days per employee $N_{\text{Workdays,Empl}}$, and the number of days the factory is running per year N_{Workdays}. The yearly direct personal cost is then calculated as $C_{\text{DP}} = \sum_j C_j \cdot N_j,\ j \in \{\text{Skilled, Assistant}\}$ with $C_j = N_{Workdays,Empl} \cdot N_{Shift,Hour} \cdot c_j$, the cost per employee.

[19] This step is also called the retrograde value flow calculation.

The number of **indirect personnel** is calculated by applying an overhead charge to the total number of direct personal. We differentiate between leadership overhead and cleaning staff and use differentiated overhead factors, x_j, and cost factors, C_j, for both to calculate the overall indirect personnel cost $C_{\mathrm{IP}} = \sum_j C_j \cdot x_j \cdot (N_{\mathrm{Skilled}} + N_{\mathrm{Assistant}})\,,\; j \in \{\mathrm{Leadership},\ \mathrm{Cleaning}\}$. The parameters for direct and indirect personnel cost can be found in appendix A.2.

Direct energy cost, $C_{\mathrm{DE}} = C_E \cdot \sum_k E_k \cdot N_{\mathrm{Units,k}},\; k \in \{\mathrm{Process\ Steps}\}$, are calculated by multiplying the electricity consumption per machine E_k[20] by the number of machines per process step and an electricity price C_E.

Indirect energy cost, $C_{\mathrm{IE}} = C_E \cdot \sum_j P_j \cdot A_j,\; j \in \{\mathrm{Basic},\ \mathrm{Dry\ room},\ \mathrm{Lab\ space}\}$, are calculated based on the size of the basic, dry, and laboratory areas in the factory, A_j, annual their electricity consumption per m^2, P_j, and the electricity price C_E.

Investment cost consist of two components: the cost of buying and replacing the production machines as well as the cost to build the factory including buying its property. The cost of buying machines, $C_{\mathrm{Mach}} = \sum_k C_{\mathrm{Mach,k}} \cdot N_{\mathrm{Units,k}},\; k \in \{\mathrm{Process\ Steps}\}$ are calculated based on the number of machines and the price per machine $C_{\mathrm{Mach,k}}$. The cost for building the factory $C_{\mathrm{F}} = \sum_j C_{\mathbf{F,j}} \cdot A_j,\; j \in \{\mathit{Basic},\ \mathit{Dry\ room},\ \mathit{Lab\ space},\ \mathit{Property}\}$ depend on the dimensions A_j of the different areas (basic, dry room, lab space), and the property, as well as a building / acquisition cost per m^2, $C_{\mathrm{F,j}}$. We calculate the required areas based on the number of machines and the size of the machines. Afterwards, we apply additional factors for machine operators, intermediate storage, and other administrative areas on the shopfloor. The resulting total production area[21] is further marked up by administrative, social, and shipping areas and the size of the property is calculated by multiplying the resulting factory size by a factor that describes the usual ratio of property to factory. For the periodic investments it follows $I_0 = C_{\mathrm{Mach}} + C_{\mathrm{F}}$ and $I_t = C_{\mathrm{Mach}}$ with t $\in \{10, 20, 30, 40\}$ for a 50 year factory lifetime and a 10 year replacement cycle for the machines (Knehr et al., 2022)

Maintenance cost $C_{\mathrm{Maint}} = 1.5\% \cdot I_0$ are calculated as 1.5% of the total investment costs (Schünemann, 2015).

Ramp-up cost are calculated as proposed by Knehr et al. (2022) as a 5% surcharge on the material cost and a 10% surcharge on direct personnel and overhead and personnel. With

[20] There is always one type of machine used per process step
[21] the sum of the basic, dry room, lab space and additional production areas

overhead consisting of indirect personnel, energy overhead and maintenance it follows $C_{\mathrm{RU}} = 5\% \cdot C_{\mathrm{Mat}} + 10\% \cdot (C_{\mathrm{DP}} + C_{\mathrm{IP}} + C_{\mathrm{IE}} + C_{\mathrm{Maint}})$.

Finally, we calculate the periodic variable cost $w_t = C_{\mathrm{Mat}} + C_{\mathrm{DP}} + C_{\mathrm{DE}}$, fixed cost $F_t = C_{\mathrm{IP}} + C_{\mathrm{IE}}$, and linear depreciation cost $d_t = C_{\mathrm{F}} \cdot T_{\mathrm{F}}^{-1} + C_{\mathrm{Mach}} \cdot T_{\mathrm{Mach}}^{-1}$ with the lifetime of the factory T_{F} and the lifetime of the machines T_{Mach}[22].

3.3.4 Cost calculation for battery cell production

Essential metrics for measuring battery production costs are full, levelized, and marginal costs.

FC is calculated by dividing the total yearly production cost by the total yearly production output in kWh (Datar and Rajan, 2018). Several studies (e.g. Gallagher et al., 2014, Hagen et al., 2015, Vaalma et al., 2018 and Wentker et al., 2019) have analysed the FC of battery production, offering benchmarks for researchers and the industry. However, as the components of FC are not clearly defined, they also provide room for misinterpretation.

One example of this is capital cost, where authors often use different calculation methodologies. Some, like Duffner et al. (2021), use the annuity method, which calculates capital cost based on the tied-up capital in each period, while others, like Schünemann (2015) use a simplified approach based on the assumption that on average half of the initial investment is tied-up capital. The BatPac model presumably includes capital cost in a yearly cost measure called "profit" as a fixed percentage on the total initial investment and working capital (Knehr et al., 2022). This is, however, oversimplified as it neglects the depreciation reducing the amount of tied-up capital and also neglects interaction effects between depreciation and taxes. Since depreciation payments can change over time (depending on the depreciation schedule), the taxes that must be paid can also change. Finally, a large share of authors in our literature review does not mention capital cost in their work at all (i.e., Hagen et al., 2015, Berg et al., 2015, Petri et al., 2015, Ciez and Whitacre, 2016, 2017, Zang et al., 2021 and Mauler et al., 2021). For comparability with these authors and since there is no consistent calculation method used by the other authors, this essay omits capital cost in the FC calculation.

Furthermore, in many cases, full cost neglect taxes and their interaction with depreciation (depreciation reduces the taxable profits). Only the BatPac model considers taxes in their General,

[22] In this work we assume stationarity, i.e. $w_t = w$, ... However, since the following cost measures also work in non-stationary settings we keep a notation with a year t

Sales and Administration cost component which is calculated as 25% of direct labour and variable overhead plus 25% of depreciation cost (Knehr et al., 2022). Since this is a simplified calculation and no other authors mention taxes in their work, we also do not include taxes in the full cost calculation and use the following formula:

$$FC = \frac{I_0 + \sum_{t=1}^{T_F} (I_t + w_t + F_t + d_t)}{\sum_{t=1}^{T_F} o_t}.$$

LC is a more complete and more clearly defined metric. It describes the average price an investor needs to realise from selling a product to achieve a zero NPV. This includes covering all operating expenses, payment of debt and imputed capital cost on the initial project expenses, and an acceptable return to the investor (Massachusetts Institute of Technology, 2007, Chapter 3 and Friedl et al., 2022). This essay follows the formal definition of LC from Reichelstein and Rohlfing-Bastian (2015), but adapts the calculation logic to include recurring investments, e.g., into machines that must be replaced before the end of the factory lifetime. To receive the levelized cost, the formula to calculate the NPV of an investment in a battery factory is set to zero and solved for the price. The NPV is defined as

$$\begin{aligned} NPV = &- \sum_{t=0}^{T_F} I_t \cdot \gamma^t \textit{ (Discounted yearly investments)} \\ &+ \sum_{t=1}^{T_F} p \cdot o_t \cdot \gamma^t \textit{ (Discounted revenues)} \\ &- \sum_{t=1}^{T_F} w_t \cdot o_t \cdot \gamma^t \textit{ (Discounted yearly variable cash flows)} \\ &- \sum_{t=1}^{T_F} F_t \cdot \gamma^t \textit{ (Discounted yearly fixed cash flows)} \\ &- \sum_{t=1}^{T_F} \alpha \cdot (p \cdot o_t - w_t \cdot o_t - F_t - d_t)\, \gamma^t \textit{ (Discounted yearly tax payments)} \end{aligned} \tag{3.1}$$

with $\gamma \equiv (1+r)^{-1}$ a discount factor where the cost of capital is defined by r, p the price realised from selling one unit of output, and α the effective corporate income tax rate.

Setting formula 3.1 to zero and solving for p yields the LCBP

$$LCBP = p = \frac{\sum_{t=1}^{T_F} w_t \cdot o_t \cdot \gamma^t}{\sum_{t=1}^{T_F} o_t \cdot \gamma^t} + \frac{\sum_{t=1}^{T_F} F_t \cdot \gamma^t}{\sum_{t=1}^{T_F} o_t \cdot \gamma^t} + \frac{\sum_{t=0}^{T_F} I_t \cdot \gamma^t - \alpha \sum_{t=1}^{T_F} d_t \cdot \gamma^t}{(1-\alpha) \sum_{t=1}^{T_F} o_t \cdot \gamma^t}. \tag{3.2}$$

The relation between FC and LC depends on the definition of FC. If FC Reichelstein and Rohlfing-Bastian (2015), including taxes and the annuity method for depreciation and capital cost, then FC and LC are equal. However, as indicated above, most papers do not use the annuity method for calculating capital costs and do not include taxes. Therefore, as shown in proposition 2.1, FC is lower than LC.

Another important cost measure is the MC. MC reflect the costs to produce another unit of output. Hence, they are an important measure for short-term production decisions. I.e., the battery production should be stopped if the selling price of a battery cell drops below its MC (Datar and Rajan, 2018). In the case of battery cells, MC includes all material, variable energy, and direct labour necessary to produce another kWh of battery capacity[23] but neglects fixed costs like investments in the production facility. From a company's point of view, MC can be a useful cost measure after an investment decision has been made when the investment can be considered a sunk cost. It is possible that reports of very low battery production costs, such as Nextmove (2020) refer to MC instead of FC. Therefore, we also report marginal cost to test this hypothesis.

MC is calculated by dividing the yearly material, variable energy and variable personal costs by the yearly factory output (in kWh)[24]. For energy and personal costs, only electricity and personnel directly required to operate the machines on the shopfloor are considered (i.e. overhead such as managers or electricity for heating are not considered in the MC). To calculate the marginal cost we use the following formula:

$$MC = \frac{\sum_{t=1}^{T_F} w_t}{\sum_{t=1}^{T_F} o_t}.$$

Because MC do not include any fixed cost or depreciation, they are significantly lower than FC or LC.

A summary of the calculation and cost factors included in the full costs, levelized costs and marginal costs can be found in Table 3.4. When interpreting the results, it is important to note that all calculated cost measures purely reflect the production cost of different battery cell designs. They do not consider differences in the battery quality (which, for example, can

[23] Note that battery factories produce their output on a cell or pack basis and not based on individual kWh. However, for comparability, this essay relates costs to kWh instead of individual battery cells or packs

[24] As all these costs are linearly increasing with the production output, these average yearly variable costs are equal to the MC

influence its lifetime) or their end-of-life value (for example, from second-life usage or recycling) which can affect the lifecycle cost of producing, using, and disposing of a battery.

Table 3.4: Cost factors included in marginal cost, full cost, and levelized cost.

Cost measure	Included cost factors
Full cost	**Variable cost**: Direct material, personal and energy **Fixed cost**: Personal overhead, energy overhead and maintenance **Depreciation**: On factory and machine investments
Levelized cost (LCBP)	**Variable cost**: See above **Fixed costs**: See above **Depreciation**: See above **Capital cost**: On factory and machine investments **Taxes**: On yearly profits after depreciation
Marginal cost	**Variable cost**: See above

3.4 Results

The case study covers twelve cases: two cell formats (4680 and PHEV2), three cell chemistries, and the option to recover scrap material. Figure 3.5 presents the FC, LC, and MC for each configuration. The calculations are based on the production processes shown in Figure 3.4, assuming a factory output of 10 GWh per year.

When analysing the FC and cost shares, several effects become apparent:

(1) The costs of the cylindrical 4680 and the prismatic PHEV2 cell format barely differ. The small differences (around 1% between formats) cannot be interpreted as one cell design being superior because of the model's sensitivity to changes in input parameters.

(2) Reducing material costs has a high potential for reducing overall costs, as the material cost accounts for over 80 % of the overall cell costs. Similarly, it becomes apparent that reaching a material cost reduction through efficient scrap recovery can significantly impact the total costs. This underlines the need for the scale-up of efficient recycling processes.

(3) The addition of Si to the cell chemistry increases the energy density of both the PHEV2 and the 4680 cell, as Si has a higher specific capacity (cf. Table 3.2). This is because adding Si to the anode active material increases the energy density of the anode. Therefore, if the energy capacity (in kWh) of the cell is kept constant, less anode active material is required

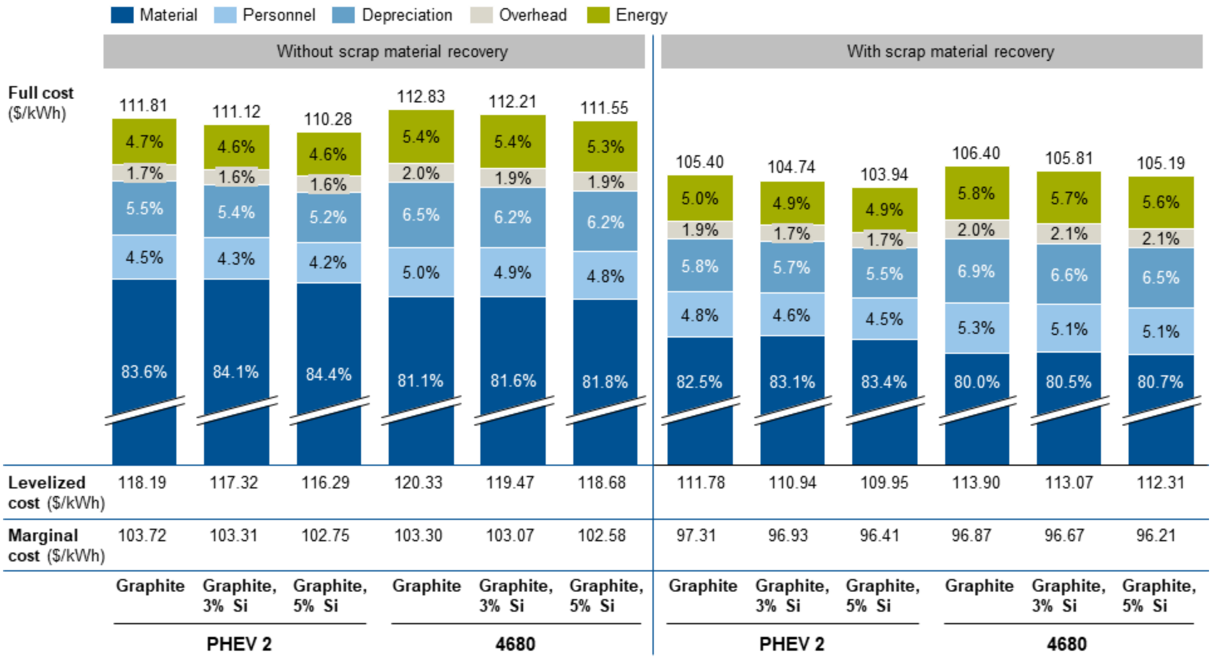

FIGURE 3.5: FC, LC, and MC cost breakdown of the PHEV2 and the 4680 cells with and without the recovery of scrap material

which reduces the material cost. Furthermore, less material for passive components is required because a thicker application of active material to the passive components is possible, further reducing the material costs. These effects are slightly counteracted by the increased SEI loss associated with adding Si which slightly increases the amount of required cathode active material[25] which increases material costs. In total, the cost reductions from reducing anode active material and passive material slightly outweigh the cost increases from increasing cathode active material.

(4) The material expansion during cycling causes an accelerated cycle life ageing of silicon-containing anodes (Kalaga et al., 2018). Even though this does not influence the production costs, the effect should be considered since it increases the life cycle cost of silicon-containing cells. Regarding the current EV mileage requirements of 200,000 km, a lifetime of around 1,000 cycles would be necessary for a single range of 200 km, which reduces with increasing energy densities (Thielmann et al., 2020). Therefore, in particular, for a second-life scenario, the impact of cycle life on life cycle cell costs becomes crucial.

[25] To put it simply, SEI loss "traps" lithium from the cathode at the anode and thus requires more lithium-containing cathode active material.

(5) LC are $5 - 7\%$ higher than FC. While it is no surprise that LC are higher than FC, it is important to recognize the extent of the difference and its implications. I.e., a firm that would set their prices to FC would not be able to recover their capital cost and tax payments. In contrast, LC, can be identified as the long-run marginal cost under certain conditions and include the payment to all involved parties (suppliers and employees, the state via taxes, investors via an acceptable return to their investment, etc.). Therefore, it is natural that the LC are also closer to the reported market values by BloombergNEF (2022) and we argue that LC should be included in future cost models.

Capital and space requirements

Figure 3.6 highlights a notable difference in the investment and space requirements of factories producing 10 GWh of the investigated cells. The overall investment cost and the factory size for the 4680 cell is 16-19% higher compared to the PHEV2 cell. This is because a higher throughput of 4680 cells is required to achieve an annual output of 10 GWh. Since the machines for both cell formats are assumed to have the same throughput per cell, more machines are necessary for the 4680 cell. Even though the machines for the PHEV2 cell production are more expensive, this results in higher investments and space requirements for the 4680 factory. Despite those higher investments, the FC (in $\$\,(\mathrm{kWh})^{-1}$) of both cells are similar because the higher energy density of the 4680 cell reduces its required material and material costs. In total, both effects even each other out.

Figure 3.6 also illustrates that machines make up about 67% of the overall investment costs for both cell formats, highlighting the importance of developing more efficient or less expensive manufacturing technologies. The remaining 33% of investment consists of the acquisition of property, construction of the factory, and ramp-up costs. Of these, ramp-up costs and the construction of lab space and dry rooms are the most significant cost factors. They underline the necessity for further optimisation to achieve smoother and cheaper ramp-ups with less waste and to reduce the required lab space and dry rooms. For the latter, the model presented in this essay provides a fine-granular overview of the factory's space requirements (cf. Figure 3.7) that can help identify process steps responsible for large portions of the dry room and lab space and analyse the effectiveness of measure to reduce those spaces (e.g., by using smaller machines).

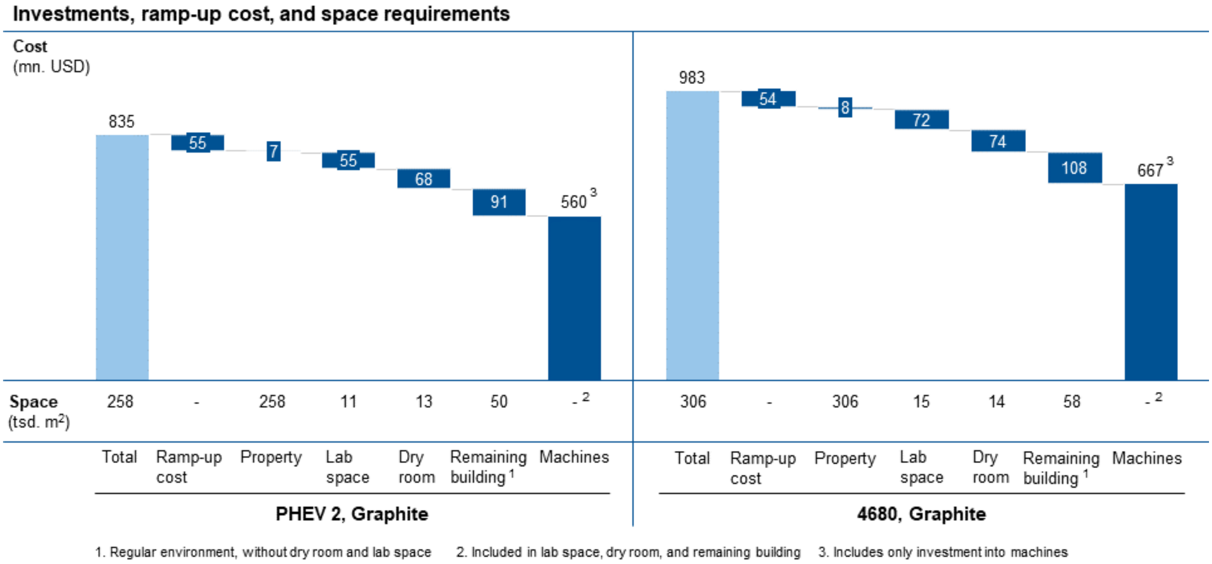

FIGURE 3.6: Investment, ramp-up cost, and space requirements of the graphite-based PHEV2 and 4680 cells

Discrepancy of research and industry reported values

Figure 3.8 shows that the results of the 4680 and PHEV2 cells are comparable to previously reported values from the literature. Authors like Schnell et al. (2020), Zang et al. (2021), Duffner et al. (2021) and Mauler et al. (2021), estimate cell production costs around 100-150 $\$\,(kWh)^{-1}$. Notably, the material cost share in this study is higher than in older publications (e.g., Schünemann, 2015). A reason for this could be that production processes have been optimized (especially with regard to process speeds) and made more cost-efficient in the past (Duffner et al., 2021). In contrast, no considerable changes to material costs have occurred[26], resulting in a higher material cost share of the total cost. Another effect could be the weak USD-to-Euro-exchange rate (1.054 USD per Euro from Exchange Rates UK, 2022). As the prices for several machines were gathered in Euro, a weak exchange rate reduces the converted USD prices. This can reduce the depreciation cost and increase the share of material cost of the FC.

[26] Lithium prices have actually increased in recent years (Statista GmbH, 2022b).

Outdoor | Production | Remaining building

Area	Space, in tsd. m² Normal	Dry room	Lab	Total	Machines
Property[1]	181.5	-	-		-
Ancillary, functional and social areas	18.2	-	-		-
Warehouse and shipping	16.3	-	-		-
Administration	8.2	-	-		-
Mixing	0.4	-	-		Machine (Anonde / Cahtode): Mixer (8/5), Doser (4/2)
Coating & drying	2.8	3.4	-		4
Calendering	0.3	0.3	-		1 Anode, 1 Cathode
Post-drying	0.2	0.6	-		3 Anode, 4 Cathode
Slitting	-	0.8	-		2 Anode, 2 Cathode
Winding	-	1.2	-		29
Contacting	-	0.7	-		7
Inserting & closing of lid	-	0.3	-		3
Electrolyte filling	-	2.0	-		8
Wetting	-	0.8	-		47
Forming & degassing	-	0.9	-		68
Closing	-	1.6	-		6
Aging	-	-	8.3		485
End-of-line test	-	-	0.2		17
Packaging & shipping	2.5	-	2.5		-
Total	230.3	12.7	11.1		

1. The property is usually 2.5 times larger than the factory (Expert interviews)

(A) Prismatic PHEV2 cell

Outdoor | Production | Remaining building

Area	Space, in tsd. m² Normal	Dry room	Lab	Total	Machines
Property[1]	215.5	-	-		-
Ancillary, functional and social areas	21.6	-	-		-
Warehouse and shipping	19.4	-	-		-
Administration	9.7	-	-		-
Mixing	0.3	-	-		Machine (Anonde / Cahtode): Mixer (8/5), Doser (4/2)
Coating & drying	2.8	3.4	-		4
Calendering	0.5	0.5	-		2 Anode, 2 Cathode
Post-drying	0.2	0.6	-		3 Anode, 4 Cathode
Slitting	-	0.8	-		2 Anode, 2 Cathode
Inserting & closing of lid	-	0.4	-		7
Winding	-	0.3	-		23
Contacting	-	0.9	-		13
Electrolyte filling	-	2.5	-		15
Wetting	-	1.1	-		96
Forming & degassing	-	1.5	-		133
Closing	-	2.0	-		12
Aging	-	-	11.2		988
End-of-line test	-	-	0.4		35
Packaging & shipping	3.3	-	3.3		-
Total	273.2	14.1	14.9		

1. The property is usually 2.5 times larger than the factory (Expert interviews)

(B) Cylindrical 4680 cell

FIGURE 3.7: Required areas and number of machines for a 10 GWh factory for the prismatic PHEV2 and the cylindrical 4680 cells with graphite anodes

When looking at the calculated cell production FC of 110-113 \$ $(\mathrm{kWh})^{-1}$, it becomes apparent that these values are still higher than the lowest industry-reported values of around 100 \$ $(\mathrm{kWh})^{-1}$ from Kane (2019) and Nextmove (2020). We find three potential explanations for this:

(1) The industry reports marginal instead of full or levelized cost because they consider the initial factory investments as sunk cost. The MC calculated in this essay of 103-104 \$ $(\mathrm{kWh})^{-1}$ are only slightly higher than the values reported in the media and could explain a significant part of the difference.

(2) The values reported in the media are often based on rumours or unconfirmed sources inside the companies. This leaves the chance that companies circulate lower than actual values to increase their perceived competitiveness and put pressure on their competitors or suppliers.

(3) Large companies can achieve significantly lower material and production costs than the models in most papers assume. This could be due to economies of scale that are not reflected by the input parameters of most models.

OEMs like Tesla, e.g., try to build up in-house component manufacturing for the cathode active material, one of the cell's most expensive components. For this purpose, they aim to run their own lithium production near the production site so that the supply of low-priced materials is

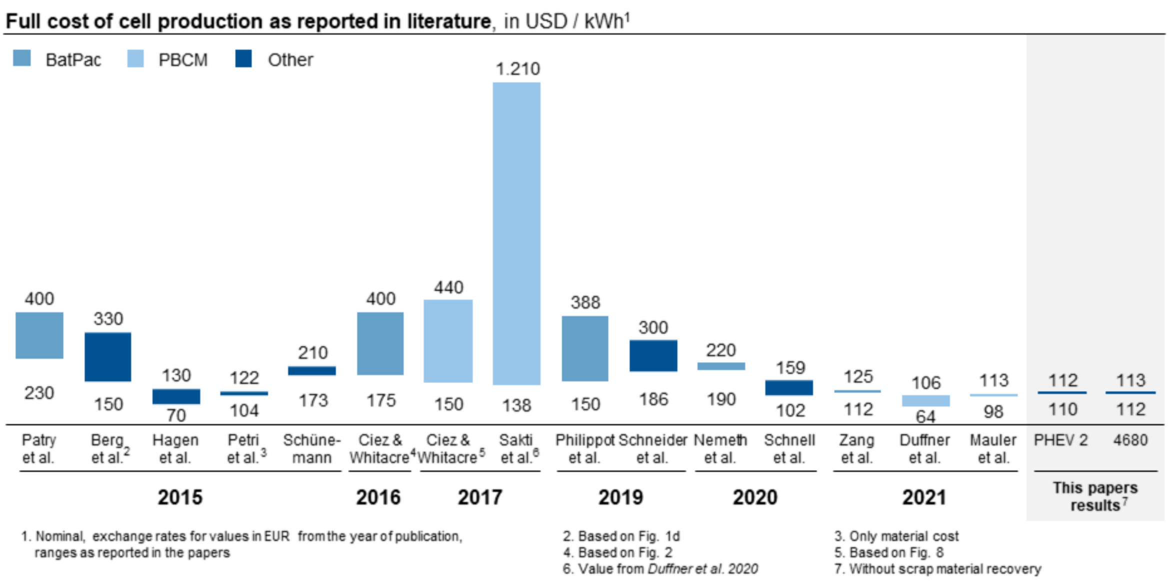

FIGURE 3.8: Comparison of results with literature reported values

ensured (Nextmove, 2020 and Stanek and Konersmann, 2020). Furthermore, the operation of recycling plants by the battery manufacturer could contribute to advantages on material prices and supply security (Scheller et al., 2020). In academic modelling, these aspects cannot be considered since their economic benefits are kept highly confidential by OEMs . The material prices in this essay were gathered from material price studies such as Pillot (2020) and other cost models such as Knehr et al. (2022) and Schnell et al. (2020). Potential economies of scale are therefore not considered.

Acquiring validated industry data (e.g., on machine specifications and material prices) and conducting sensitivity analyses on factors such as cell chemistries, production processes, and material prices could help test the existing hypotheses and identify further reasons for the gap between current literature and industry-reported values.

When comparing our results to overall market price data instead of cost claims from individual OEMs , however, our results appear very reasonable. For example, as depicted in figure 1.4, BloombergNEF (2022) reports average battery cell prices of ca 108-112 $\$\,(\mathrm{kWh})^{-1}$ in 2020 and 2021, and 120 $\$\,(\mathrm{kWh})^{-1}$ in 2019 and 2022. These values are much closer to our results and would, for instance, in the case of the 2022 data allow for a ca. 10 $ margin per kWh. Notably, these values are also very close to our LCBP of 118-120 $\$\,(\mathrm{kWh})^{-1}$ which supports the accuracy of our model as well as the usefulness of the LCBP metric for price setting.

Currently, the model assumes a fixed construction cost and energy consumption per m^2 for the dry room. However, these parameters depend on factors such as the location of the factory and the number of people in the dry room. Implementing an external dry room model could enable a more flexible investigation of different scenarios. The model structure could be modularised to include other peripheral models (e.g., for energy consumption) as well. This would enable an even more comprehensive and concise calculation of energy and cost.

3.5 Conclusion

This essay presents a battery cost calculation model that enables users to customize the battery format, chemistry and production processes, including both the parameters of individual production steps and the sequence of production steps itself. In a case study, the model is used to calculate the FC, MC and LC of a cylindrical 4680 cell and a prismatic PHEV2 hardcase cell with three different cell chemistries (with 0 wt. %, 3 wt. % and 5 wt. % Si). We highlight the differences between the three cost measures and the lack of standardised cost measures in the literature. The resulting FC of 110-112 $ $(\mathrm{kWh})^{-1}$ for the PHEV2 cell and 112-113 $ $(\mathrm{kWh})^{-1}$ for the 4680 cell are in line with literature-reported values and slightly above current reports from OEMs . We show that both cells have similar costs and that no significant cost reduction occurs when adding Si to the anode active material. As material costs are responsible for over 80% of FC our analysis also highlights, that production costs of 36-40 $ $(\mathrm{kWh})^{-1}$ can only be achieved with significant reductions in material costs.

4 | The impact of battery technology on residential solar PV and storage systems and their fossil fuel reduction potential

Decentralized electricity generation and storage systems are key to decarbonizing the electricity sector. In this essay, we compare the technical and economic attributes of different battery chemistries (LFP, SIB, NCX, and LA) and identify optimally-sized solar and storage combinations for individual households. Applying the model with current parameters to residential households in Germany, we find that LFP and SIB batteries can improve the system NPV by 4000 k€ while NCX and LA batteries are not economical. Installing such systems in all suitable one- and two-family households could reduce fossil fuel consumption in the electricity sector by up to 35% compared to 26% when installing systems with solar PV only. We find that 7% points of the difference can be attributed to the larger solar PV systems that become economical when installing a battery and 2% points can be attribute to the electricity supply shifting effect of batteries. However, the latter effect only becomes relevant when a sufficient amount of additional solar PV capacity is installed so that curtailment occurs.

Keywords: Solar PV, Fossil Fuel Reduction, Battery Electricity Storage.

I would like to thank Amadeus Bach for contributing data on the performance of different battery chemistries.

4.1 Introduction

Countries worldwide aim to reduce their electricity generation from fossil fuels to combat climate change and to increase their resilience to supply shocks such as the war in Ukraine. RES, such as residential solar PV, can substitute electricity generated from fossil fuels, but their intermittency poses challenges to grid stability. BES has the potential to solve these challenges by shifting electricity from times of oversupply, for example, during the day, to times of undersupply, for example, in the evening. However, historically high initial investment costs combined with low round-trip efficiencies[27] and short lifetimes remain a challenge to the extensive adoption of BES.

The advent of electrified mobility has led to the development of more durable battery chemistries that are also suited for BES. While extensive literature exists on the application of such battery systems in EVs and commercial grid-scale electricity storage (e.g., Schmidt et al., 2019, Guerra et al., 2021, Hunter et al., 2021, Sepulveda et al., 2021 and Darling, 2022), it is unclear which battery type is best suited for household electricity storage. Furthermore, it remains to be determined if private households' solar PV and BES systems can significantly contribute to reducing the share of electricity from fossil fuels on a national scale.

This essay provides a combined solar PV-BES optimisation framework to determine the NPV-optimal system sizes for different battery chemistries. Based on the individual households' system optimisation, we determine the potential to substitute electricity from fossil fuels for a national roll-out of such systems in an exemplary German setting. We disentangle the effects of additional solar PV generation capacity and additional flexibility from BES on fossil fuel replacement and contextualise the results within the current solar PV strategy of the German Federal Ministry for Economic Affairs and Climate Action. Our findings are particularly important for households, solar PV and BES providers, and policymakers when designing regulatory measures for the uptake of decentralised renewable generation and storage systems.

Closely related to our study are Comello and Reichelstein (2019) who calculate the optimal BES system size for an individual household in Germany and California with existing residential solar power. Similarly, Mulleriyawage and Shen (2020) show that adding BES to an Australian household increases the return on investment and reduces PV curtailment and greenhouse gas emission. In addition to both studies, an extensive literature body investigates different optimisation approaches for solar PV and BES system combinations (Erdinc et al., 2015, Khalilpour

[27] The electricity lost from charging and discharging the battery.

and Vassallo, 2016, Khawaja et al., 2017, Cervantes and Choobineh, 2018, O'Shaughnessy et al., 2018 and Javeed et al., 2021). We add to this literature stream by exploring emerging battery chemistries. Comparing different battery technologies is important, as the global battery market is shifting towards mass-produced electric batteries with multiple cathode chemistries. The rise of e-mobility has accelerated the global output of LIB, especially for high-nickel content batteries with high energy density. In recent years, cheaper and more durable nickel- and cobalt-free LIB gained rapid market share. Furthermore, a new generation of lithium-free batteries has been announced to be mass-produced in China (Yingzhe, 2022 and Batteries News, 2022). Hence, the battery landscape is rapidly changing, potentially impacting the EV and BES markets. Prior literature, however, largely neglects the differences in the economic potential of new battery chemistries despite significant cost and performance differences.

We further contribute to the literature by estimating the fossil fuel reduction potential from a large-scale roll-out of residential solar PV and BES systems. In its efforts to decarbonise its electricity system, Germany aims to build 22 GW of additional solar PV capacity annually until it reaches 215 GW in 2030 (Die Bundesregierung, 2023). Since half of the additional capacity should come from rooftop PV, it is important to analyse the potential contribution towards reducing the use of fossil fuels for electricity generation of such a build-out[28]. While some authors such as Weniger et al. (2013, 2016), Zhang et al. (2017), Liu et al. (2020), and Ren et al. (2021) include self-consumption, CO_2 reduction, and peak-load reduction in their analysis, none of them provide a granular analysis of the fossil fuel reduction potential of a large-scale roll-out of solar PV-BES systems. However, since solar PV systems mainly produce electricity during the day, when the share of renewables is often already high, it must be analysed if a significant addition of solar PV capacity can substantially replace electricity from fossil fuels or if it would instead increase the curtailment of RES. In this context, we also assess the role of residential BES capacity, which can shift renewable electricity to hours with high fossil fuel shares and thus increase the potential substitution.

In this essay, we consider four different battery types: Lithium-Iron-Phosphate, sodium-ion, Sodium-Calcium Exchanger, and Lead Acid batteries. LA batteries are the oldest and cheapest (on a $(\text{kWh})^{-1}$ basis) chemistry but they also have significantly lower round-trip efficiencies and lifetimes compared to LFP, NCX, and SIBs. NCX batteries are frequently used inEVs but are also the most expensive. Newer LFP batteries are 10-20% cheaper than NCX batteries and have

[28] The 22 GW include both residential and commercial solar rooftop PV. In this essay, we focus on the effects of residential PV.

significantly higher lifetimes[29]. SIBs are still in development but will most likely cost up to 30% less than LFP batteries while employing similar performance parameters (apart from a slightly lower RTE).

Our results show that state-of-the-art LFP and SIBs are economically superior to NCX or LA batteries when used with a solar PV system in a household setting. Currently, NCX and LA batteries have high market shares based on a long market presence. In contrast to current market volumes, we find that profit-maximising households will increase their NPV with LFP and SIBs. With those batteries, the optimal system size also increases. The NPV increase stems from lower degradation losses and, to some extent, smaller purchasing prices than NCX batteries.

If all 10.4mn suitable German one and two-family households (EUPD Research, 2021) would install an optimised solar PV and BES system, this would lead to an additional 56 - 96 GW of solar PV capacity and up to 82 GWh additional battery storage capacity. Notably, the potential additional solar PV capacity represents more than half of the required additional 148 GW to achieve Germanies goal of 215 GW by 2030 (Die Bundesregierung, 2023) and would require each household to invest 13,184-21,742 €. Such an investment scenario could lead to a 26-35% reduction in fossil fuel consumption for electricity generation in Germany.

This essay is structured as follows. Section 4.2 describes the optimisation model and our results and section 4.3 provides a discussion.

4.2 Model and results

4.2.1 Improvements in modern battery storage

The rise of e-mobility triggered a rapid increase in global battery production, leading to declining battery costs due to learning and economies of scale (see, e.g., Nykvist and Nilsson, 2015, Matteson and Williams, 2015 and Nykvist et al., 2019). These cost declines made many stationary BES applications both on a grid-level scale[30] and for private households[31] commercially feasible. Fluctuating raw material prices and technical advancements in energy density supported the development of new cathode chemistry combinations in LIBs. Historically, NCX batteries have

[29] A downside of LFP batteries compared to NCX is the lower energy density, however, while this is a relevant performance criterion for EVs, it is irrelevant for household BES.
[30] e.g., https://hornsdalepowerreserve.com.au/
[31] e.g., https://www.tesla.com/powerwall

been used predominantly in residential BES applications and in most EVs in the Western world. LFP batteries have rapidly gained market share in recent years, especially in China. While LFP batteries have a lower energy density than NCX batteries, they are cheaper, more thermally stable, and more durable (Li et al., 2020 and Preger et al., 2020). In early 2022, LFP cells were only used in 3% of EV batteries in the United States and Canada and only in 6% in the European Union. Still, they were utilised in 44% of new EVs in China (Jin and Lienert, 2022) and are expected to capture a large part of the global EV market in the future (IEA, 2022).

The volatility of lithium prices in recent years has also supported the development of lithium-free batteries. For example, sodium-based SIBs are being developed and will soon be mass-produced by two of the biggest LIB manufacturers: BYD (Batteries News, 2022) and CATL (Yingzhe, 2022). These changing market dynamics make it imperative to examine the economic viability of different battery chemistries for BES applications.

Besides the initial investment cost ν (including terminal recycling profits), round-trip efficiency η_b and capacity degradation x_i[32] are the main parameters for an economic evaluation of BES systems. These parameters determine how much electricity the battery may charge and discharge over the investment's lifetime. In practice, the available capacity of a battery decreases with usage and time due to degradation up to the point of rapid capacity decline (the so-called ageing knee), rendering the battery unusable. We model the battery capacity by defining a theoretical number of Equivalent Full Cycles (EFC) which we call EFC$'$ during which the battery degrades normally from charging and discharging until it hits a capacity threshold $\overline{x}$. At this point, the battery is assumed to have reached the ageing knee and its capacity drops to zero. The battery is typically charged and discharged 365 times a year for common household applications. The capacity (measured in percent of the initial battery capacity) in each year can be described as the ratio of remaining theoretical EFCs at the start of the year divided by the total number of theoretical EFCs.

To limit the degradation of the battery[33], we model the range of the Depth of Discharge (DOD) of NCX batteries to be between 90% to 10% and of LA batteries to be between 80% to 50% of their remaining capacities. LFP batteries have shown to be much less sensitive to a higher DOD (Viswanathan et al., 2022), and similar behaviour is assumed for SIBs. Therefore, no limit to the DOD is assumed for both chemistries. The resulting amplitude ζ of 80% (NCX), 30%

[32] The remaining capacity in year i as a percentage of the battery's initial capacity.
[33] Capacity degradation accelerates significantly by approaching the charging or discharging limit specifically for nickel-based LIBs and LA batteries.

(LA), or 100% (LFP and SIBs) is then considered in the calculation of EFCs in each year. If an NCX battery would be charged and discharged daily in the first year, the $EFC = \zeta \cdot 365 = 292$. With this information, the theoretical capacity of the battery in year i can be modelled as $x_i' = \left(1 - \frac{365 \cdot \zeta}{\mathrm{EFC}'}\right)^{i-1}$. The practical capacity, accounting for the ageing knee, is then

$$x_i = \begin{cases} x_i', & \text{if } x_i' > \overline{x} \\ 0, & \text{otherwise.} \end{cases} \tag{4.1}$$

Figure 4.1 depicts the different degradation profiles.

The resulting number of practical EFCs, EFC*, and the remaining performance and battery cost parameters used in this essay are summarised in Table 4.1. We note that the cost of the batteries power component, which determines the charging- and discharging speed of the battery, stay constant at $\nu_p = 220€\,(\mathrm{kW})^{-1}$ while the cost of the energy component ν_e differs based on the battery chemistry. We also note that a recycling profit of $\nu_R = 20€\,(\mathrm{kWh})^{-1}$ is only assumed for NCX batteries, mainly due to their Nickel, Cobalt, and Lithium content.[34] In contrast, the metals in LFP, SIBs, and LA batteries are likely less valuable than the corresponding recycling costs.

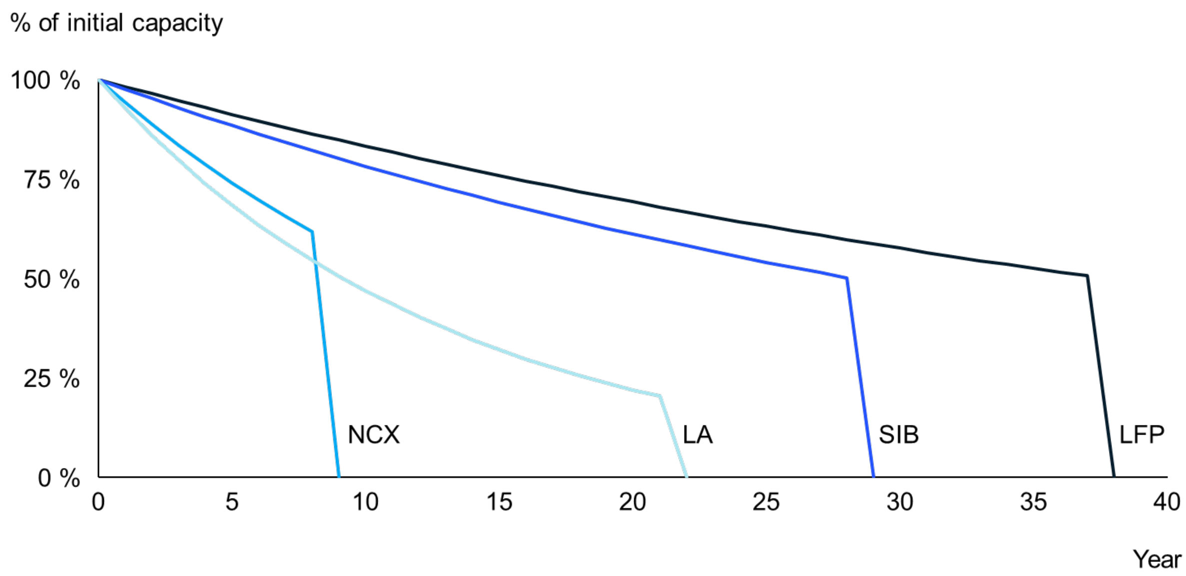

FIGURE 4.1: Capacity degradation of NCX, LA, sodium-ion, and LFP batteries.

[34] This estimate is based on comments from Redwood Materials and 2023 market prices for the metals. Changing market prices and economies of scale in the recycling industry can yield significant differences in recycling profits. For an overview of potential recycling profits, see Lander et al. (2021).

Table 4.1: Battery cost and performance parameters

Battery Type	ν_e, in €(kWh)$^{-1}$	η_b, in %	ζ, in %	$\overline{x}$, in %	**EFC**$'$, in EFCs	**EFC***, in EFCs
LFP	507	97	100	50	20,000	10,067
SIB	365	93.5	100	50	15,000	7,658
NCX	579	96	80	60	5,000	2,091
LA	315	82.5	30	20	1,500	1,217

4.2.2 Optimally sized solar PV and BES systems

Our optimisation framework follows the basic ideas of Comello and Reichelstein (2019) who consider a household with a (seasonally varying) load, generation, and storage profile as depicted in Figure 4.2.

They calculate the optimal energy and power component sizes of a battery supplementing a solar PV system based on the amount of electricity that can be used from the battery[35], derived from areas (1) - (3) in Figure 4.2. While we follow their approach for calculating the amount

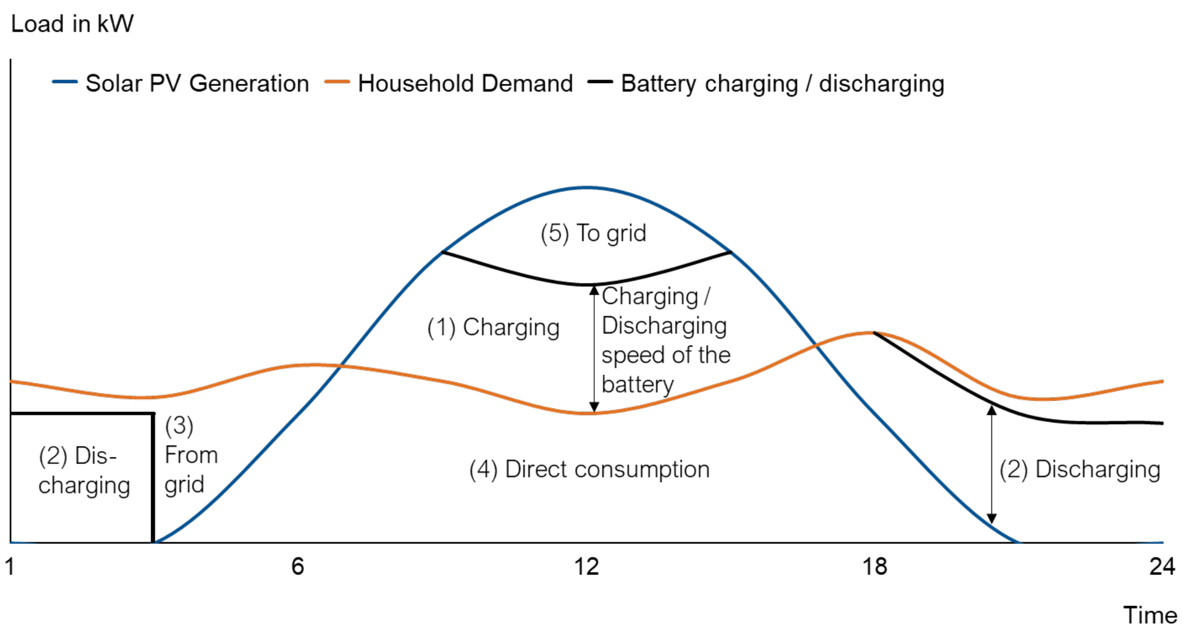

Figure 4.2: Pattern of daily electricity generation, consumption, charging, and discharging (own representation, after Comello and Reichelstein, 2019).

[35] The amount of electricity that can be used from the battery depends on both the power and energy component as the power component influences the speed at which electricity can be charged and discharged and the energy component determines the overall capacity of the battery.

of electricity charged and discharged, we extend the optimisation framework by conducting a combined optimisation of the dimensions of the battery capacity k_e, the batteries power component k_s, and the size of the solar PV panels k_{pv} of a solar PV and BES system. Furthermore, our analysis includes additional cost factors such as a terminal recycling value and a more fine granular battery degradation model.

We consider a rational household that will optimise the NPV of an investment in a solar PV and BES system. When the solar PV panels generate electricity, the household has three options: direct consumption, indirect consumption (via charging the battery and discharging it later), and feeding it into the grid[36]. Direct consumption is the economically preferable option in most countries as retail electricity prices are usually higher than the FIT. Furthermore, direct consumption avoids round-trip-efficiency losses from charging and discharging the battery.

Revenues are generated by direct consumption, which avoids buying electricity from the grid at a price p, by indirect consumption, which also yields p, but where the round-trip efficiency of the battery reduces the output of the battery, and by feeding electricity into the grid at a national FIT of $p^{FIT} < p$ which is paid for T_{FIT} years. In year i and season s, let $E_s^D(k_{pv}, i)$ be the electricity used for direct consumption (area 4), $E_s^I(k_e, k_p, k_{pv}, i)$ the electricity stored in the BES for indirect consumption (area 1, before RTE losses), and $E_s^G(k_e, k_p, k_{pv}, i)$ the electricity fed to the grid (area 5), all accounting for an annual degradation of η_{pv} per cent of the solar PV system. Then the revenue in year i and season s will be

$$\begin{aligned} Rev_s(k_e, k_p, k_{pv}, i) = p \cdot \big(&E_s^D(k_{pv}, i) + \eta_b \cdot E_s^I(k_e, k_p, k_{pv}, i)\big) \\ &+ p^{FIT} \cdot E_s^G(k_e, k_p, k_{pv}, i) \cdot 1_{i \leq T_{FIT}}. \end{aligned} \tag{4.2}$$

Formula 4.2 also shows that a kWh used directly (E_s^D), indirectly (E_s^I), and for feeding it into the grid (E_s^G) has a different value to the household due to differences in the associated prices (i.e., p for E_s^D and E_s^I and $p^{FIT} < p$ for E_s^G) and round-trip efficiency losses when using electricity indirectly (i.e. $\eta_b < 1$ in case of using the battery storage E_s^I). Therefore, the amount of electricity used within the three components E_s^D, E_s^I, and E_s^G of the revenue formula must be calculated individually.

[36] Depending on the country, there are different remuneration schemes for electricity that is not used by the generating household. In this essay, we assume a constant feed-in tariff.

The amount of electricity used directly from a solar PV system can be described by

$$E_s^D(k_{pv}, i) = \int_0^{24} \min\{k_{pv} \cdot \eta_{pv}^i \cdot G_s(t), L_s(t)\}dt \tag{4.3}$$

with η_{pv} the degradation factor of the solar PV panels, $G_s(t)$ the seasonal generation capacity factor, and $L_s(t)$ the seasonal demand curve. To calculate the amount of electricity used indirectly, we define

$$\begin{aligned} E_s^+(k_p, k_{pv}, i) = \int_0^{24} & [\min\{L_s(t) + k_p, k_{pv} \cdot \eta_{pv}^i \cdot G_s(t)\} \\ & - \min\{L_s(t), k_{pv} \cdot \eta_{pv}^i \cdot G_s(t)\}]dt \end{aligned}$$

as the amount of electricity that can be stored in the battery and

$$\begin{aligned} E_s^-(k_p, k_{pv}, i) = \int_0^{24} & [\max\{L_s(t), k_{pv} \cdot \eta_{pv}^i \cdot G_s(t)\} \\ & - \max\{L_s(t) - k_p, k_{pv} \cdot \eta_{pv}^i \cdot G_s(t)\}]dt \end{aligned}$$

as the maximum amount of electricity that the household could use from any given battery. In both cases, the actual quantity depends purely on the battery's power component, i.e., its ability to charge and discharge electricity.

$$E_s^I(k_e, k_p, k_{pv}, i) = \zeta \cdot x_i \cdot \min\{E_s^+(k_p, k_{pv}, i), E_s^-(k_p, k_{pv}, i), k_e\}dt \tag{4.4}$$

is then the electricity that can be used indirectly, accounting for DOD, the batteries capacity decline, and the limitation of the battery capacity k_e, which is not included in E^+ and E^-. Finally

$$E_s^G(k_e, k_p, k_{pv}, i) = k_{pv} \cdot \eta_{pv}^i \cdot \int_0^{24} G_s(t)dt - E_s^D(k_{pv}) - E_s^I(k_e, k_p, k_{pv}, i) \tag{4.5}$$

describes the amount of electricity fed into the grid, consisting of the total generation less the direct and indirect demand.

Substituting the formulas (4.3) to (4.5), as well as formula (4.2) into the NPV calculation yields

$$\begin{aligned} NPV(k_e, k_p, k_{pv}) = & \sum_{i=1}^{T} \sum_{s=1}^{12} \Delta_s \cdot (p \cdot \left(E_s^D(k_{pv}, i) + \eta_b \cdot E_s^I(k_e, k_p, k_{pv}, i)\right) \\ & \qquad + p^{FIT} \cdot E_s^G(k_e, k_p, k_{pv}, i) \cdot 1_{i \leq T_{FIT}}) \cdot \gamma^i \\ & - (\nu_e \cdot k_e + \nu_p \cdot k_p + F_b + \nu_{pv} \cdot k_{pv} \cdot (1 + V_{pv}) + F_{pv}) \\ & + \min\{k_e \cdot \nu_s, \overline{\nu_s}\} + k_e \cdot \nu_R \cdot \gamma^{T_R}. \end{aligned} \tag{4.6}$$

We constrain the size of the solar PV to $0 \leq k_{pv} \leq z$ where z is the maximum size of the solar PV that can be installed on the roof. To optimise the NPV in our case study, we implement the model in Python and use the L-BFGS-B algorithm for the constrained optimisation.

Furthermore, the household will be compensated in the form of **subsidies** for installing a battery and the recycling value at the end of the battery's useful life. Subsidies are often paid as a fixed purchase premium. In this essay, we assume a subsidy of ν_s € $(\text{kWh})^{-1}$ storage capacity with a limit of $\overline{\nu_s}$ € $(\text{kWh})^{-1}$ leading to a subsidy payment of $Sub(k_e) = \min\{k_e \cdot \nu_s, \overline{\nu_s}\}$.

The **recycling value** $Rec(k_e, T_R) = k_e \cdot \nu_R \cdot \gamma^{T_R}$ depends on the energy capacity of the battery, the recycling profit of the materials, the time T^R at which the battery capacity drops to zero and the battery is recycled, and the discount factor $\gamma = (1 + r)^{-1}$ with a discount rate r.

The **investment** cost of a solar PV and BES system depends on the purchase and installation cost of the battery and the solar PV system. The cost of BES systems scales linearly at a rate of ν_p€ $(\text{kWh})^{-1}$ and ν_e€ $(\text{kWh})^{-1}$ for the battery's power and energy components, plus a fixed installation cost of F_b€. The cost of the PV system also scales linearly at ν_{pv}€ $(\text{kWp})^{-1}$. However, the installation cost contains a fixed component F_{pv}€ as well as a variable component V_{pv} per cent that is applied on top of the cost of the panels. The total investment cost is modelled by

$$Invest(k_e, k_p, k_{pv}) = \nu_e \cdot k_e + \nu_p \cdot k_p + F_b + \nu_{pv} \cdot k_{pv} \cdot (1 + V_{pv}) + F_{pv}.$$

Following the definition of revenues, subsidies, recycling value, and investment cost, the NPV of the solar PV-BES system is

$$\begin{aligned} NPV(k_e, k_p, k_{pv}) = & \sum_{i=1}^{T} \sum_{s=1}^{12} \Delta_s \cdot Rev_s(k_e, k_p, k_{pv}, i) \cdot \gamma^i \\ & + Sub(k_e) \\ & + Rec(k_e, T_R) \\ & - Invest(k_e, k_p, k_{pv}) \end{aligned} \tag{4.7}$$

where Δ_s is a weighting factor for the season, and T denotes the lifetime of the solar PV system. The used parameters for an exemplary German setting can be found in Table 4.2.

To calculate the optimal system size for a representative household in Germany, we calculate the optimal system sizes for one household in each of Germany's 16 federal states and compute the weighted average based on the number of suitable one and two-family households per state from EUPD Research (2021). Figure 4.3a shows the optimal system dimensions of the representative households.

It shows that both LFPs and SIBs lead to similarly sized systems with about 9 kWp solar PV

TABLE 4.2: Model parameters for an exemplary German setting

Parameter	**Value**	**Unit**	**Description**
p	0.33	€ $(\text{kWh})^{-1}$	Average electricity market price
p^{FIT}	0.082	€ $(\text{kWh})^{-1}$	FIT*
T^{FIT}	20	years	Number of years for which the FIT is paid
ν_s	200	€ $(\text{kWh})^{-1}$	BES capacity subsidy
$\overline{\nu_s}$	45,000	€	Maximum subsidy
r	4.45	%	Cost of capital**
ν_{pv}	1.136	€ $(\text{kWp})^{-1}$	Solar PV purchase cost
F_{pv}	4.971	€ $(\text{kWp})^{-1}$	Fixed solar PV installation cost
V_{pv}	34	%	Variable solar PV installation cost
F_b	526	€	Fixed battery installation cost
T	30	years	Lifetime of the solar PV system
η_{pv}	0.5	%	Annual degradation of the solar PV system

* The FIT is reduced to 0.071 € $(\text{kWh})^{-1}$ for each kWp above 10 kWp. However, as most systems are below 10 kWp we assume a constant FIT of 0.082 € $(\text{kWh})^{-1}$
** The cost of capital r is based on a 100 per cent funding through a governmental lending program of the KfW: "KfW- Programm Erneuerbare Energien Standard"

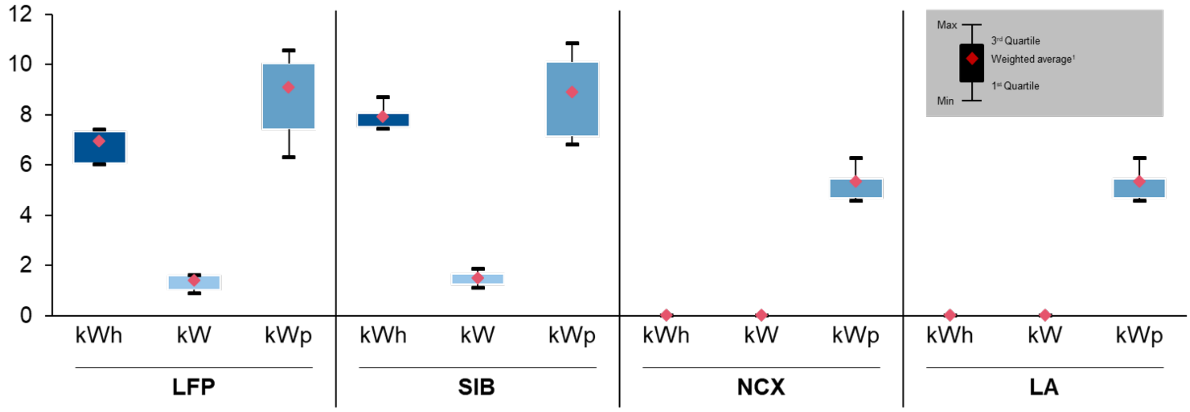

(A) Optimal battery capacity (kWh), power (kW), and solar PV (kWp) system size

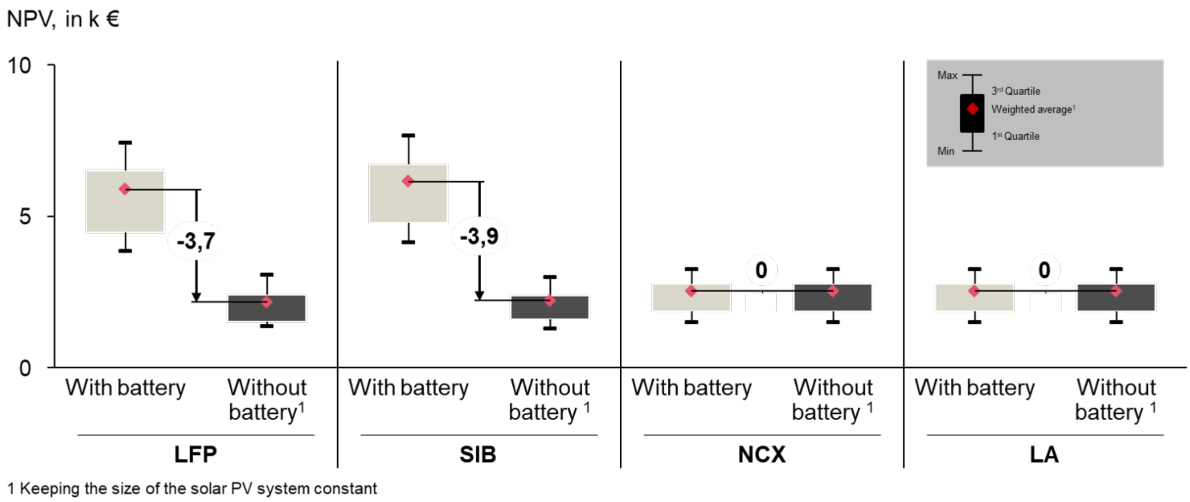

(B) NPV of the optimal system size compared to a system with the same solar PV capacity but no battery

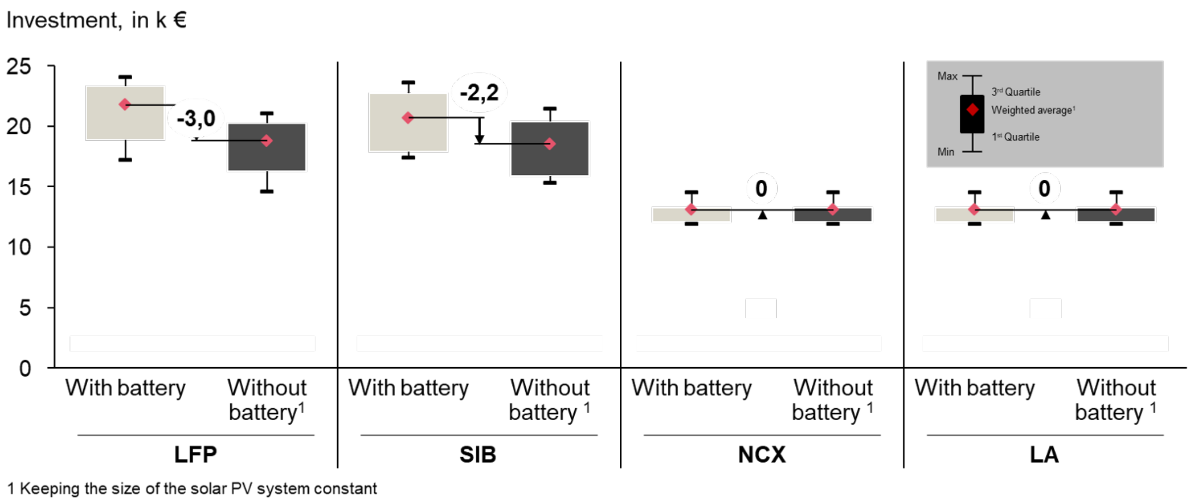

(C) Investment of the optimal system size compared to a system with the same solar PV capacity but no battery

FIGURE 4.3: Optimal system sizes

and 7 - 8 kWh BES at a duration[37] of ca. 5 hours. By contrast, NCX and LA batteries are not economical. In both cases, a smaller solar PV system of ca. 5 kWp is installed because less electricity can be used at the higher price p. These dynamics are also reflected by the economics depicted in Figures 4.3b and 4.3c. While the larger LFP and SIB systems also require a higher 21-22 k€ net investment[38] by the household, they lead to significantly higher NPVs of about 6 k€ compared to NPVs of about 2.5 k€ that can be achieved from the systems without batteries (NCX and LA) that require investments of ca. 13 k€.

Notably, the ca. 30% lower capacity cost of SIBs leads to a slightly larger installed capacity (8 vs 7 kWh compared to LFP) but does not significantly change the size of the power component, the solar PV system, and the system economics. This can partly be explained by the slightly lower durability and RTE of the SIB that reduce the economic value of the battery and partly by the decreasing marginal value of additional battery capacity, which increases the NPV of the system compared to the LFP system but does so only slightly.

Figure 4.3b also underlines the additional economic value of LFP and SIBs. When removing the battery from the systems but keeping the size of the solar PV system constant, the NPV decreases by nearly 4 k€.

The NPV of the solar PV-BES system is characterised by a high initial investment and recurrent returns over a comparably long lifetime of 30 years. Therefore, as depicted in Figure 4.4, the household's cost of capital has a significant influence on the optimal system size and its economics: (1) For values of r of up to 2%, the levelized cost (LC) of the solar PV system is below the FIT so that the maximum permittable size, which we set to 20 kWp, will be built. The battery is dimensioned at 9-10 kWh for LFP and SIB systems and 3-4 kWh for NCX and LA systems, respectively and independent of r, indicating the existence of an optimal ratio between solar PV and BES system sizes. (2) When r increases above 2%, the LC of the solar PV system increase above the FIT. Subsequently, both the solar PV and the BES system sizes decrease, but the initial decrease is significantly more substantial for the solar PV system. This is because after the solar PV system's size surpasses a threshold, an increasing share of the electricity generated by the marginal solar PV panel is sold to the grid. When the LC increase above the FIT, these panels become uneconomical, and the size of the solar PV system is quickly reduced. Opposed to this, the electricity stored in the battery will only be used for indirect consumption,

[37] The duration describes the ratio of the energy component and the power component, i.e., the time the battery can be charged/discharged at full capacity.
[38] The cost of purchasing and installing the solar PV-BES system less subsidies for the BES .

which has a much higher achievable profit. Therefore, the marginal value of the battery is still positive, and its size is reduced rather due to the smaller solar PV system[39] than due to a lack of economics of the battery. (3) When r increases above 6.5%, the solar PV system is not a viable investment when using NCX, LA, or no batteries. When using LFP or SIBs, this point is reached later when r rises above 8% because the batteries enable more electricity to be used to avoid buying electricity from the grid, thereby improving the system's LC compared to a solar PV-only system.

4.2.3 Fossil fuel reduction potential

Residential solar PV-BES systems can contribute to substituting electricity from fossil fuels in two ways. First, when the household consumes electricity from the solar PV system directly or indirectly, it can reduce the demand for electricity from the grid. Because electricity generated from fossil fuels usually has a higher LC than electricity generated from RES, this can reduce the amount of electricity produced from fossil fuels. Second, when the household produces more electricity than it can consume, it can feed the surplus into the grid, reducing the amount of electricity that needs to be produced from fossil fuels. We call the sum of these effects, i.e. the amount of electricity used directly, indirectly, or fed into the grid, the NAE supply.

To calculate the NAE supply and, subsequently, the fossil fuel reduction potential, we follow the four steps illustrated in Figure 4.5: (1) We calculate the optimal solar PV and BES system size for each battery type for one household in each federal state. (2) We simulate the hourly NAE supply from the solar PV-BES system of each household and battery type. (3) We multiply each household's hourly NAE supply by the number of potential new solar PV-BES systems in the respective federal state and sum the results up to a national total hourly NAE. (4) On a national level, we calculate the hourly amount of electricity from fossil fuels that could be substituted by the NAE and calculate the national average reduction potential of electricity from fossil fuels over the lifetime of the solar PV-BES systems.

Step (1) uses the model described in section 4.2.2. In contrast to the results of section 4.2.2, which show a national weighted average optimal system[40], the individual results of each federal state are kept for the calculation of the hourly NAE supply within each state.

[39] While the largest share of electricity from the latest added solar PV panels is fed into the grid, a smaller share can still be used for charging the battery.

[40] The dimensions and economics of the optimal systems of each federal state are weighted based on the number of potential new systems per state.

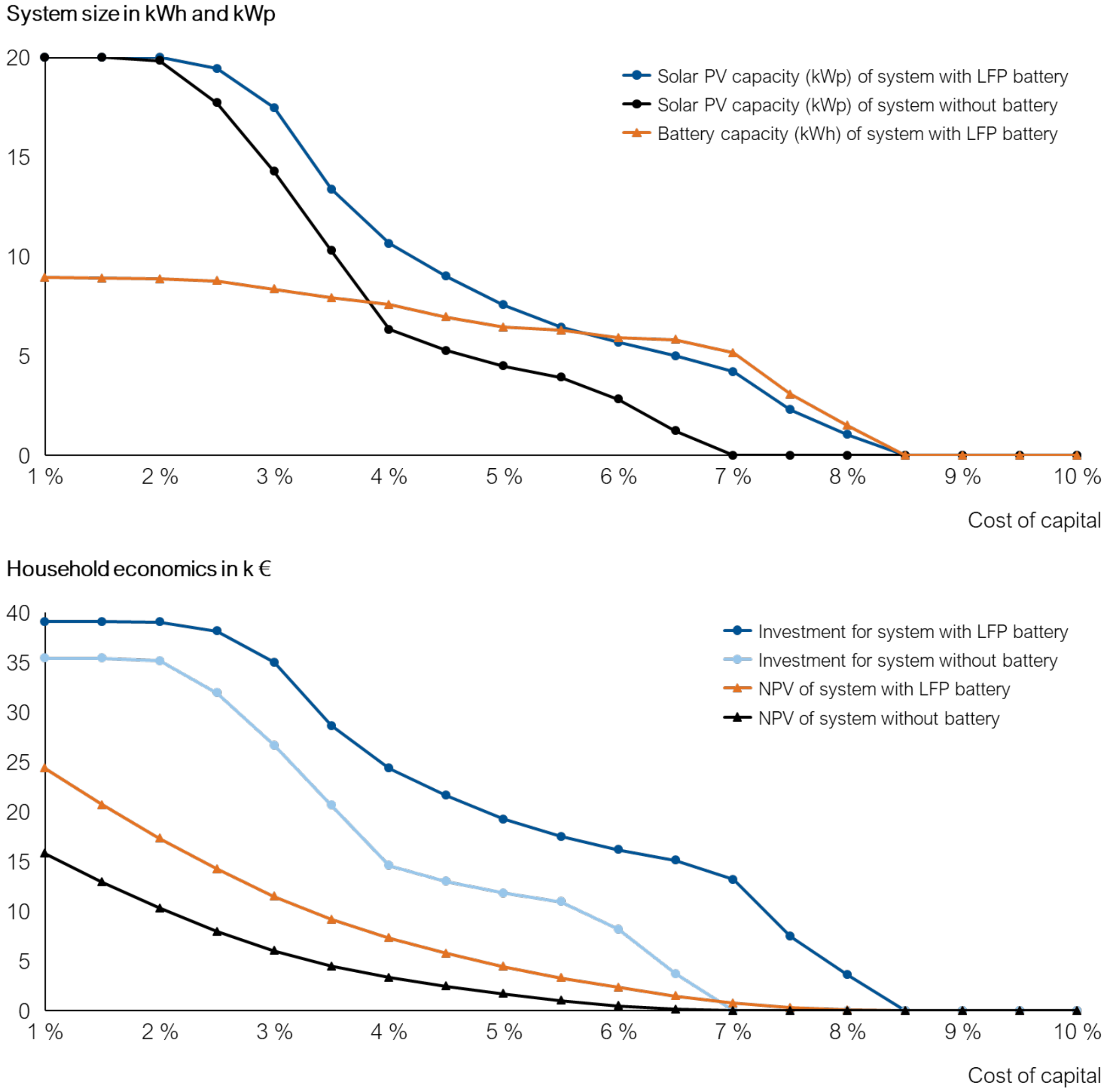

Figure 4.4: Sensitivity of system size and economics to the cost of capital, shown for a system with an LFP battery and a system without battery. Results for a system with a SIB are similar to a LFP battery; results for NCX and LA batteries are equal to a system without battery.

Because the electricity mix and, therefore, the amount of electricity from fossil fuels that can be substituted varies during the day, the fossil fuel reduction potential must be computed based on hourly data. Hence, in step (2), we simulate the hourly electricity flows of the households in each federal state across the solar PV systems lifetimes of 30 years. While we use the same solar radiation and electricity mix patterns each year, this enables us to account for battery and solar PV degradation. The electricity flows consist of the household's demand, generation, direct use, the State of Charge (SOC) from charging/discharging the battery, indirect use, and electricity

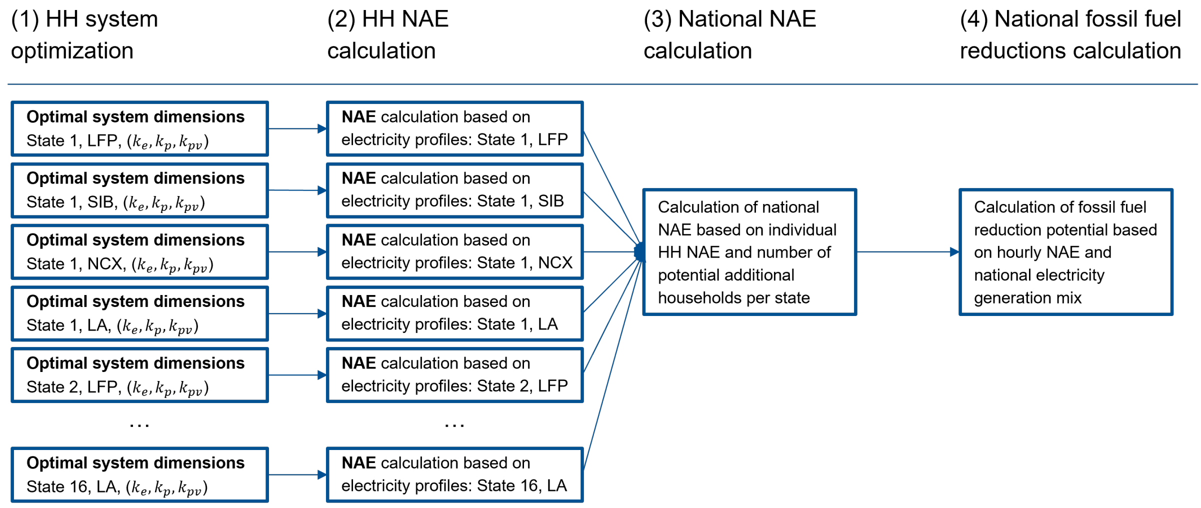

FIGURE 4.5: Model framework to calculate the fossil fuel reduction potential

fed into the grid. Based on these flows, we can calculate the NAE supply from the household in each hour as the sum of direct and indirect use as well as electricity fed into the grid.

To calculate the electricity flows, an iterative procedure is used. For each representative household, for each year and each month, a representative day is simulated. In case of a system without battery, the NAE is purely based on the additionally generated electricity from the solar PV system. In case of a system with a battery, the simulation first calculates the first point in time when generation of the solar PV system supersedes the households demand. This will be the starting point for the simulation which will then simulate a 24 hour cycle of the households electricity flows. It is important to start the simulation at this point in time (which, e.g., could be at 7am in the morning), because it enables the simulation to account for cases where the battery might be fully charged over the day and could be used for indirect use during the night, up until the next morning (e.g., 4am). If the simulation would start earlier, it would need to either assume that the battery is empty and might neglect the potential for indirect use of electricity, or make an assumption on the state of charge of the battery for which it would not have any basis.

If the simulation determines that supply does not supersede demand at any point during the day (e.g., in the winter), meaning that the battery is never charged, then the direct use is equal to the generation of the solar PV, the indirect use and the electricity fed into the grid are both set to zero, and the electricity consumed from the grid (which is calculated in the model for illustration purpose to show the entire electricity flows of the household) is calculated as the households' demand less its generation.

If the simulation determines that there are any hours where the battery can be charged, it proceeds with a 24-hour simulation starting at the first point in time where the battery is charged. For each hour the simulation then checks if generation supersedes demand[41].

If this is the case, then the direct use is equal to the households electricity demand. Furthermore, the amount of electricity that is used to charge the battery is calculated as

$$e_{Charge} = \min\{generation - demand, k_p^*, k_e^* \cdot \zeta - SOC\}$$

with *demand*, and *generation*, the households electricity demand and generation in the simulated hour, k_p^* the dimension of the power component of the battery in kW, k_e^* the energy component of the battery, and SOC the state of charge of the battery. The second and third component of the minimum operator model the limitations of charging the battery due to the size of the power component (i.e., in one hour the battery can not be charged with more than k_p^* kWh) and the energy component (i.e., the maximum amount of electricity that can be charged into the battery is based on its total capacity multiplied by the used amplitude ζ less the current state of charge). Naturally, the amount of electricity fed into the grid is then the remainder of electricity produced by the solar PV system that is neither used directly or indirectly, meaning

$$e_{ToGrid} = generation - demand - e_{Charge}.$$

If generation does not supersede demand, meaning that the household discharges the battery (or does not use it in the rare case of $generation = demand$) instead of charging it, then the calculation changes. The direct use is equal to the generation and there is no electricity flow to charge the battery. However, there is now indirect use of electricity that is discharged from the battery which is calculated by

$$e_{Indirect} = \min\{(demand - generation) \cdot \eta_b^{-1}, k_p, SOC\} \cdot \eta_b.$$

41 Naturally, this is always the case for the first hour of the simulation but can change afterwards

Here, the first component of the minimum shows the limitation of indirect use by the gap between the households demand and the generation from the solar PV system, implying that only the unfulfilled demand can be serviced from indirect use. The second and the third component of the minimum model the limitations of indirect use by the power component of the battery and the state of charge. These last two components are reduced by the round trip efficiency of the battery η_b which, in this model, is applied at the discharging of the battery. This means that, e.g., if the battery is charged at a certain SOC, then the electricity available for indirect use after discharging it from the battery is $SOC \cdot \eta_b$. After calculating the amount of electricity discharged from the battery, its new SOC is calculated by

$$SOC_{New} = SOC_{Old} - e_{Indirect} \cdot \eta_b^{-1}.$$

Here, the amount of electricity discharged from the battery for indirect use is divided by the round-trip efficiency to model that, in order to receive an amount of $e_{Indirect}$ kWh from the battery, a higher amount of $e_{Indirect} \cdot \eta_b^{-1}$ needs to be discharged from it.

An illustration of the resulting electricity flows from the simulation can be found in Table 4.3.

According to an analysis by EUPD Research (2021), 11.7mn one- and two-family households in Germany are suitable to install rooftop solar PV. 1.3mn of those had installed solar PV capacity by the end of 2020, leaving a potential of an additional 10.4mn households. In step (3), we calculate the total NAE supply by scaling the NAE supply of the individual solar PV-BES systems to these 10.4mn households. To account for differences in solar radiation across

TABLE 4.3: Exemplary electricity flows in kWh of a system with an LFP battery during a representative day in April.

Hour	**De-mand**	**Gene-ration**	**Direct Use**	**Indirect Use**	**Char-ging**	**SOC**	**To grid**	**NAE**
10	0.58	5.56	0.58	-	1.58	6.27	3.40	3.98
11	0.58	5.91	0.58	-	1.08	7.35	4.25	4.84
12	0.59	5.96	0.59	-	-	7.35	5.37	5.96
13	0.58	5.67	0.58	-	-	7.35	5.08	5.67
14	0.56	4.93	0.56	-	-	7.35	4.37	4.93
15	0.54	3.84	0.54	-	-	7.35	3.30	3.84
16	0.54	2.44	0.54	-	-	7.35	1.91	2.44
17	0.56	1.04	0.56	-	-	7.35	0.48	1.04
18	0.61	0.13	0.13	0.48	-	6.85	-	0.61
19	0.68	-	-	0.68	-	6.15	-	0.68

Germany, we calculate the national NAE supply as the sum of the 16 federal states' NAE supply based on the household NAE supply calculated in step (2) and the number of potential households for additional solar PV and BES systems in each state. While a scenario where all 10.4mn potential households install a solar PV-BES system can be considered unlikely, it is a worthwhile analysis as some German federal states are moving towards making rooftop solar PV mandatory (ENBW, 2022). To reflect the influence of the penetration of the mentioned 10.4mn households, we provide a sensitivity analysis on the fossil fuel reduction in Figure 4.7.

In step (4), the total hourly NAE supply is deducted from the electricity generation from fossil fuels to calculate the reduction potential of electricity from fossil fuels. When doing so, the merit order effect must be considered, which implies that different generation technologies are substituted in order of their descending cost. In the case of Germany, gas is the most expensive generation technology, followed by hard coal, lignite, other conventional sources (for example, biogas), etc. Figure 4.6 shows the generation from fossil fuels and the NAE supply on an exemplary day in April.

It illustrates that during the night when the NAE supply comes from electricity used indirectly from the battery, a substantial amount of electricity from gas could be substituted. Still, a significant share of fossil fuel generation from hard coal, lignite, and other conventional sources remains. During the day, however, the NAE supply supersedes the electricity generated from

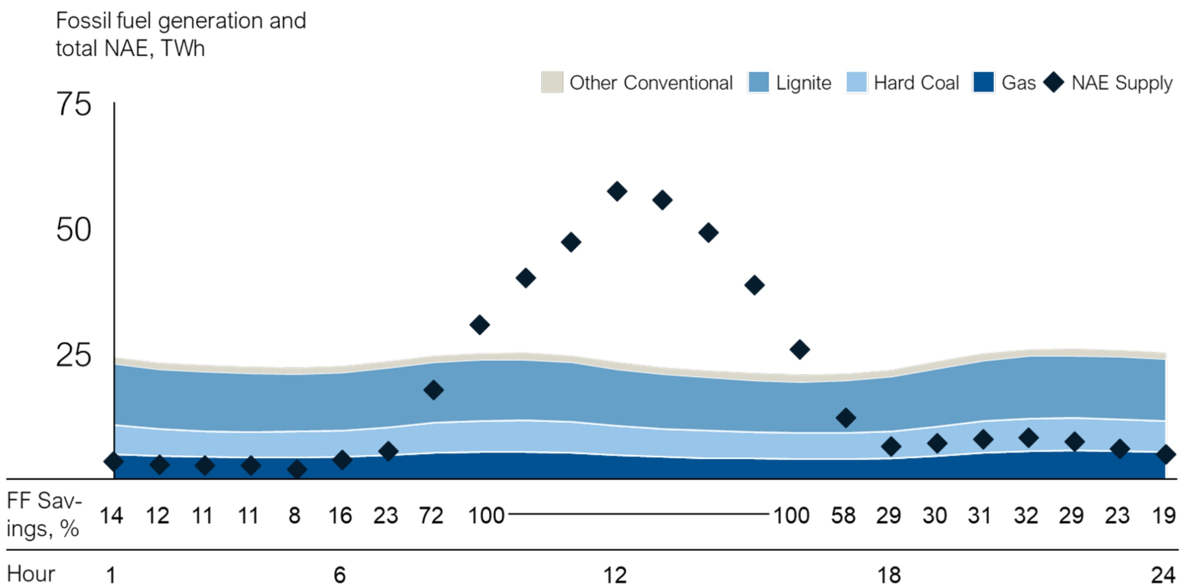

Figure 4.6: Fossil fuel generation and NAE supply from a system with LFP BES on a representative day in April

fossil fuels, implying that, theoretically, all generation from fossil fuels could be substituted. Averaging over a time horizon of 30 years, Figure 4.7 shows that a reduction of electricity from fossil fuels of up to 35% is possible.

Furthermore, the comparison of systems with LFP battery (referred to as case A), systems with equally sized solar PV panels but no battery (case B), and systems optimised for use without battery[42] (case C) enables us to entangle the effects of overall household penetration, the addition of BES, and the increase of the size of the solar PV system. With an increasing share of additional households, the fossil fuel reduction potential increases to up to 35%. While initially, the fossil fuel reduction potential increases linearly in the household penetration, it starts to flatten beyond penetrations of 60% in cases (A) and (B) and 90% in case (C). This is due to curtailment, which means that an increasing amount of the NAE supply occurs at times when 100% of fossil fuels are already substituted. The flattening occurs later in case (A) than in case (B) because the BES shifts NAE from peak times during the day into the night, which reduces curtailment. It occurs latest in case (C) because, due to the smaller solar PV systems, the NAE supply is not large enough to lead to significant curtailment. Overall, the results show that solar PV-BES systems have the potential to reduce electricity generated from fossil fuels significantly. While NCX and LA batteries are not economical from a household perspective,

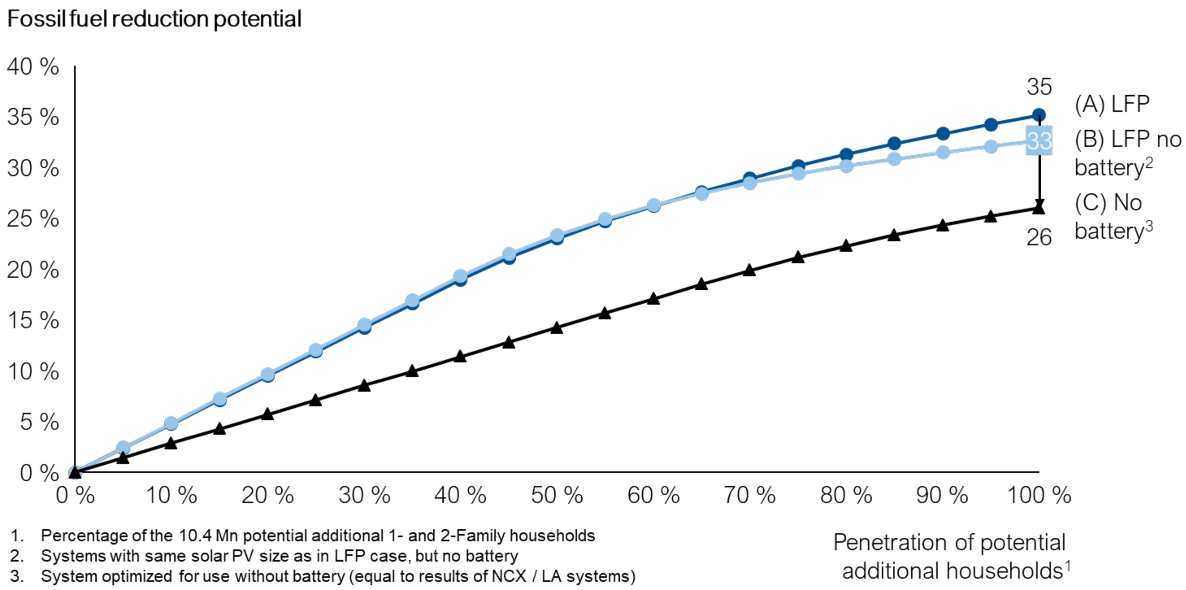

Figure 4.7: Fossil fuel reduction potential of a system with an LFP battery (results similar to an SIB system), a system with the same solar PV size but no battery, and a system optimised for use without battery (equal to NCX / LA systems where batteries are not economical).

[42] Resulting in smaller solar PV panels.

using BES with LFP batteries or SIBs is economical. It can increase the fossil fuel reduction potential by up to 9% points compared to systems optimised for use without BES. The difference can mainly be attributed to larger solar PV systems that become economical with the addition of BES, which contribute at least 7% points to the difference. However, when the penetration of potential additional households increases beyond 70%, the BES also contributes to the fossil fuel reduction potential by shifting NAE supply from peak times during the day, where curtailment can occur, to the night, when a larger share of generation from fossil fuels can be substituted.

In Germany, the roll-out of solar PV-BES systems sized according to section 4.2.2 with LFP or SIBs to all of the 10.4mn potential additional households would add a total of 93-94 GW of solar PV capacity. This represents over 60% of the additional 148 GW required to meet the target of 215 GW in 2030 (Die Bundesregierung, 2023). Notably, in the current PV strategy of the German government, residential and commercial rooftop PV is planned to make up about half of the 148 GW additional capacity, meaning that a roll-out to all potential households would over satisfy that goal and enable the addition of less capacity on commercial buildings or open land. While it is unrealistic to achieve such a capacity addition in a few years, a build-out until 2030 would require the addition of ca. 13 GW annually, which is closer to the current government's targets of 11 GW from 2026 onwards (Bundesministerium für Wirtschaft und Klimaschutz (BMWK), 2023). Based on a share of 45% of electricity from fossil fuels in 2021 and a reduction of 35%, this would reduce the share of fossil fuels to 29% and therefore significantly contribute to the target of 80% renewable electricity generation while providing a positive NPV to the investing households. In reality, however, multiple limitations to this analysis exist and will be discussed in the following section.

4.3 Discussion

Reducing carbon emissions in the electricity sector is essential to achieve decarbonisation goals and improving electricity systems' resilience. This essay shows that residential solar PV and BES systems equipped with state-of-the-art LFP and SIBs can significantly contribute to this endeavour.

We develop a model to determine the NPV-optimal dimensions of a residential solar PV and BES system. We show that LFP and SIBs are equally attractive and provide a ca. 4 k€ improvement of the NPV compared to systems without batteries because they enable the household to use a higher share of the generated electricity for self-consumption. In contrast, NCX and LA batteries do not improve the system economics compared to a system without BES. This is most likely due to their higher degradation, which increases the cost per kWh of stored electricity.

We find that the cost of capital, r, significantly influences the results of the optimisation, in particular, the size of the solar PV system. At $r \leq 2\%$, the LC of the solar PV system falls below the FIT, and the largest possible system will be installed. With increasing r, the dimension of the solar PV system decreases quickly until a large share of the generated electricity is used for self-consumption, after which the rate of decline slows until r surpasses 8.5% and the systems become uneconomical. In contrast, the battery capacity is much less sensitive to the cost of capital. It stays nearly constant until the cost of capital starts making the entire system unprofitable. At this point, the battery capacity decreases with a similar trajectory as the solar PV panels.

On a national level, we find that the installation of NPV-optimally sized solar PV and BES systems in all 10.4mn suitable one- and two-family households could reduce fossil fuel consumption by up to 35% when using systems with LFP or SIBs compared to 26% when using systems without batteries. We disentangle the effect into two components: 7% points of the difference can be attributed to the larger solar PV system size that becomes economical when using a battery. 2% points of the difference are due to the battery's supply-shifting effect, which enables the households to substitute more electricity during the night when a larger share of electricity is produced from fossil fuels. The latter effect becomes only relevant when a sufficient number of households have installed such systems leading to curtailment during peak solar PV generation hours.

While the results are encouraging, some limitations need to be considered. For instance, we assume a constant electricity price over the 30-year lifetime of the investment. However, in reality, electricity prices change constantly, and a significant addition of renewable electricity from residential solar PV-BES systems might even reduce the electricity price and, therefore, the NPV of the systems. However, it is unclear in which direction customer electricity prices would change due to competing factors: Lower energy generation costs of renewable power should decrease electricity prices. Contrary, higher grid costs due to the intermittency of renewable energy sources could increase electricity prices. Furthermore, trends like the electrification of transport could increase the overall electricity demand, and counter price decreases from more generation capacity.

Furthermore, in the calculation of the fossil fuel reduction potential, we use the 2021 hourly electricity mix for the entire 30-year time horizon. However, the electricity mix will most likely change, for example, by adding more RES capacity. This could increase the importance of the supply-shifting ability of batteries for fossil fuel reduction.

Finally, we assume that the NAE can always substitute produced electricity from fossil fuels. However, while some power plants, such as gas-fired, can be ramped up and down quickly, others, for example, using lignite, are usually not designed to be ramped up and down that quickly. Therefore, it is possible that, in some cases, NAE can not be used to substitute fossil fuels because the powerplants can not be ramped down quickly enough. Future research should address these limitations by including more factors such as a changing electricity mix and prices and a continuous build-out of residential solar PV capacity over time into the fossil fuel reduction analysis.

Our results provide valuable insights for households, policymakers, and solar PV-BES system providers. We determine the economics and dimensions of an NPV-optimal solar PV-BES system and highlight the influence of different battery chemistries on both. Furthermore, we show the fossil fuel reduction potential of a national scale-up of such systems.

5 Conclusion

Climate change is one of the fundamental challenges of our time. In order to limit its effects, countries worldwide need to collectively reduce GHG emissions. This dissertation has scrutinized the energy and transport sector, representing two of the most relevant sectors for reducing carbon emissions in order to achieve the goals of the Paris Agreement and limit global warming to 2 °C, or ideally to 1.5 °C.

Both sectors are responsible for a significant amount of global GHG emissions and both can be largely decarbonized with existing technologies. In the case of the energy sector, RES and electricity storage such as batteries or hydrogen as well as fossil-fuel based electricity generation combined with carbon capture technologies can be used to reduce carbon emissions. In the case of the transportation sector, EVs can be used to substitute ICE vehicles which could also lead to a reduction of carbon emissions, depending on the carbon intensity of the electricity used for fueling the EV and the carbon emissions associated for producing both types of vehicles. In both cases, transitioning to low carbon technologies would require significant additional investment and could be associated with increasing costs of energy and mobility. For example in electricity generation, the development cost of renewable energy such as wind farms and the cost for adding sufficient flexibility, for example via electricity storage, to the grid is often higher than the investments required to build new gas-fired power plants which typically have lower investment cost but higher operating costs from buying gas to fuel the plant. Furthermore, most renewable electricity has a volatile generation pattern that is often uncorrelated with typical demand patterns and can lead to price spikes and higher average electricity prices. Similarly, EVs are often more expensive than ICE vehicles and can also increase (at least the investment) cost of mobility. Therefore, the development of cost-competitive technologies is crucial to facilitate an economical transition to decarbonized industries.

Against this background, all three essays address the costs of decarbonizing the energy and transportation sector. The first essay discusses the levelized cost concept, a life-cycle cost measure that aggregates investment expenditures and operating costs to units of output. After providing a verbal and formal definition that follows Massachusetts Institute of Technology (2007, Chapter 3) and Reichelstein and Rohlfing-Bastian (2015), LC is compared to FC and its relevance for managerial decision making is discussed, including an outline of important limitation of the LC. Afterwards, the essay provides an overview of some of the most prominent literature streams of LC, the LCOE, LCOS, LCOH, and LCOC, as well as a short summary of other environmental applications such as heating, cooling, or water. Finally, it highlights potential future applications of LC such as patent licensing, cloud and quantum computing, or within network industries.

The essay highlights that the LC allocate fixed costs to individual units of a product in a way that is consistent with the NPV criterion and can be interpreted as the long-run marginal costs. Accordingly, the LC can also be seen as the break-even price at which a product becomes marginally profitable and is thus the unit cost measure relevant for long-run decisions. Important limitations of LC are its focus on a single round of capacity investments and its incapacity to capture the effects of the correlation between electricity prices and generation patterns of RES. When comparing LC to FC, the essay shows that LC is larger or equal than FC. This is because in practice and literature, FC are often calculated using the assumption that the applicable book value for the calculation of imputed interest charges is, on average, half of the initial investment. This approximation underestimates the book value in the first half of the depreciation period but these years receive relatively large weighting in the LC and NPV calculation. Finally, the essay shows that LC is a frequently and often predominantly used cost measure in the literature on electricity generation, energy storage, hydrogen, carbon capture, and other environmental applications where it is often used to compare the cost competitiveness of different technologies (for example for electricity generation or energy storage) and the influence on policy-decisions such as tax credits on the life-cycle cost of producing electricity, hydrogen, etc. Based on these applications of LC, the essay also sketches out potential future applications, for example in network industries, where LC could be used to determine the long-run unit prices of different technology networks such as fiber networks, cell phone towers, or satellite-based solutions.

In the transportation sector, EVs could contribute to the reduction of carbon-emissions but high vehicle purchase prices driven by high battery production costs are an important adoption-barrier for many potential customers. In order to reduce production cost, cost models can be used to identify cost efficient battery designs and to analyze the effects of changes to the production process. Therefore, the second essay presents a bottom-up cost model for state-of-the-art batteries for EVs. It addresses shortcomings of existing cost models by enabling the user to freely adjust the sequence of production steps, the individual parameters of each production step such as scrap rates, and by including frequently neglected cost factors such as energy cost. To enable accurate comparisons of the cost competitiveness of different battery designs, three cost measures are defined. FC, MC and the levelized cost of battery production. In a case study, the FC, MC and LCBP of two industry-relevant battery cell formats (4680 and PHEV2) and three cell chemistries (with 0 wt. %, 3 wt. % and 5 wt. % Si) in scenarios with and without the recovery of scrap material are calculated and compared to existing literature and industry reports.

The results of the analysis show that the difference in production costs of both cell formats is ca. 1% and thus insignificant. Furthermore, adding Si to the cell chemistries reduces the production cost slightly (ca. 1-2%) but introducing the recovery of scrap material has a more significant influence and can reduce production cost by ca. 6%. This is because material costs are responsible for over 80% of the cell costs. The FC of both batteries of 110-113 $\$\,(\mathrm{kWh})^{-1}$ are in line with results from the literature. LC are ca. $5-7\%$ larger than FC because they also include capital cost and taxes, making them a more complete cost measure. This is also supported by the fact that they are significantly closer to reported market prices, e.g., by BloombergNEF (2022). However, both FC and LC are significantly higher than reports by VW and Tesla of 100 $\$\,(\mathrm{kWh})^{-1}$. One explanation could be that both OEMs report MC.

Apart from differences in production processes and costs, different battery chemistries also posses different performance characteristics, e.g., with respect to their capacity degradation or round-trip efficiency. Therefore, the third essay presents a model that calculates the optimal system dimensions for a solar PV and BES system. It highlights the performance differences of LFP, SIB, NCX, and LA batteries with respect to capacity cost, durability, and round-trip efficiency and analyses their influence on the system dimensions and household economics. Furthermore, for the case of Germany, it estimates the electricity savings potential on a national scale. This enables an estimation of the effectiveness of a large-scale roll-out of residential solar PV and BES systems to all suitable one- and two-family houses. To account for uncertainty, sensitivity analyses are conducted on the cost of capital, the electricity price, and the share of suitable houses that install new systems.

The results show that modern battery chemistries such as LFP and SIBs can significantly improve the household economics of solar PV and BES systems. They improve the household NPV by ca. 4 k€ compared to systems without BES. In contrast, NCX and LA systems are not economical meaning that solar PV systems without BES yield a larger NPV than systems with NCX and LA batteries. Furthermore, a large-scale roll-out of such systems on all 10.4mn suitable one- and two-family households could reduce fossil fuel consumption by up to 35% compared to 26% when using systems without BES. The difference in the potential can be attributed to two factors: (1) that the addition of BES makes it economical for households to install larger solar PV systems because they can use a larger share of electricity directly or indirectly which yields higher returns than feeding the electricity into the grid, and (2) a demand shifting effect that moves the consumption of electricity generated from the solar PV systems into the night when more electricity from fossil fuels can be substituted. The latter effect, however, only appears when a large enough number of households install solar PV systems, leading to curtailment during hours with peak generation. Then, the BES systems can help reduce the amount of curtailment during the day by shifting the electricity supply to the night.

The essays highlight the importance of economic analysis and the use of suitable cost measures to facilitate a cost competitive decarbonization of industry. In particular, the first and the second essay discuss the levelized cost concept as a suitable cost measure not only for electricity generation but also in other use cases such as battery production. They show that classical cost measures such as full cost often do not reflect the true long run marginal cost of products. This is highly relevant in the context of decarbonization technology that often requires high upfront investments (for example, for building a battery manufacturing plant) and in times of high capital cost because the full cost measures used in practice often underestimate the imputed interest charges. Furthermore, essays two and three highlight the influence of different technologies on the cost of decarbonization and show that accurate cost models can help select the most cost efficient technologies. Especially in the context of batteries, they show that different battery designs and chemistries can lead to large differences in production costs and the economics of solar PV and battery storage systems. The recommendation for a cost measure that enables a comprehensive comparison of different technologies can be linked back to essay one which discusses the suitability of levelized cost as such a cost measure.

The findings of this dissertations raise important implications for industry and politics. For industry, especially in contexts with large upfront capital expenditures, companies should consider using levelized cost for unit costing. As discussed in the first essay, LC can be the relevant cost measure for capacity investments. Furthermore, it is shown that LC are larger or equal to the standard full cost measures used in industry. This means that pricing decisions based on such FC measures could lead to companies not recovering their true production costs. Essay three suggests that battery electricity storage for residential solar PV systems should adopt modern battery chemistries such as LFP or SIB which are much more economical than established NCX or LA chemistries and could be a unique selling point and justify higher product prices. Following this line of argumentation, essay three highlights the potential of residential solar PV and BES systems to reduce the usage of fossil fuels for electricity generation. It shows that a large-scale roll-out of such systems could substantially (up to 35% in the case of Germany) reduce electricity from fossil fuels such as gas, lignite, or hard coal. While the systems are often economical for the investing households, the cost of capital has a major influence on the profitability and also the optimal sizing of such systems. Therefore, to facilitate significant private investments, politics could consider providing loans with low and stable interest rates, as, for example, done by the KfW, to reduce the cost and risk for households and to incentivize private investment.

While these results are encouraging, there are also important limitations to consider. In battery production, material costs are the largest cost factor and often constitute over 80% of the full production cost. Since commodity prices, for example, lithium, have proven volatile and hard to predict, overall battery prices can also change regardless of technological advancements. This is illustrated by BloombergNEF (2022) which shows an increase in battery pack prices in 2022 after years of decreasing prices, likely driven by increasing lithium prices. Furthermore, large companies could be able to buy large amounts of lithium at lower-than-average market prices due to economies of scale. Since most large battery producers do not disclose their material purchase prices, these cost reductions can also not be captured by the model presented in the second essay. Finally, detailed bottom-up models inherently require a variety of parameters which should frequently be updated, as, for example, new and more cost-efficient production technologies are developed.

Future research could address these assumptions by trying to generate empirical data on material prices paid by large companies, for example by conducting anonymous interviews with the purchase departments from large OEMs to create a benchmark database for material prices paid for battery production. While there might be barriers for companies to disclose such data, it is possible that they would agree if in turn for providing their own data, they would also get access to the data from the other interviewed companies which could help them negotiate lower prices with their suppliers. Furthermore, additional battery chemistries such as LFP or SIB could be integrated into the model to enable the estimation of the production cost of these new battery chemistries that are gaining more traction in the EV market. As shown in essay three, these chemistries often show lower purchase prices compared to the chemistries from essay two. Therefore, it would be interesting to confirm these price differences based on the differences in production cost and to understand their drivers. If, for example, the differences would be driven mainly by material prices, it would be interesting to analyze how they might develop (and if they would persist) based on individual material price forecasts. Finally, as part of a periodic update of the used parameters to reflect changes in material cost, wages, productivity, etc., further sensitivity analysis and the integration of a separate / more detailed dry room model could further test and increase the robustness of the results. Currently, the model assumes fixed construction cost and energy consumption parameters for the dry room, regardless of the location of the factory and the number of people in the dry room. Since these factors can have a significant influence on aforementioned parameters, a separate / more detailed dry room model could enable the investigation and comparison of more scenarios (e.g., the production in different countries) and further increase the accuracy of the results.

Electricity grids and markets are highly complex systems that involve a large number of producers and consumers. Therefore, the analysis in the third essay of the effects of additional residential solar PV and BES systems on the generation mix should be considered a reasonable estimate of the overall impact, rather than a highly precise forecast. This is because a top-down calculation, as used in the essay, cannot account for the individual influence of grid capacity or the ramp-up and -down times of individual power plants. Furthermore, the essay uses the current average electricity price and the 2022 electricity mix as a prediction for the future. This is a pragmatic assumption but electricity prices have proven highly volatile in the past and could both fall (e.g., due to an increasing share of renewables with lower LCOE in the electricity mix) or increase (e.g., due to increasing demand for electricity from the electrification of industry) in the future. Similarly, changes to the electricity mix are likely. I.e., an increasing share of renewables in the mix is expected, however the exact trajectory is influenced by the development of the LCOE of different technologies which is, among others, driven by fossil fuel prices, material prices, political decisions, e.g. subsidy prices, etc.

Based on these limitations, future research should aim at analyzing the fossil fuel reduction potential using a fundamental electricity market model to incorporate changes of the electricity price and generation mix to increase the precision of the estimated fossil fuel reduction potential. I.e., this could be done using an agent-based simulation of the German electricity market, simulating the stochastic electricity demand during each hour and day and the volatile generation pattern of renewable electricity sources, and calculating the resulting behavior of the market participants (e.g., the decision of power plant operators to ramp their plants up and -down) and the realizing market prices. Such models are generally considered more accurate than top-down estimations as presented in the third essay and could also account for the influence of a significant addition of solar power and battery electricity storage on the realizing market price which could have an effect on the profitability and thus the optimal dimensioning of such systems. Furthermore, it should estimate the deviation of cost calculated with the current approach form the results calculated with a fundamental electricity market model. A small deviation would validate the simpler approach used in the essay in this dissertation and could be used as a justification to use the simpler top-down approach to more quickly test further scenarios, for example, the cost-competitiveness of new solid state batteries or the implications of different subsidies on the optimal BES dimensions. The latter could be intersting to politics to design incentive schemes that maximise private investment into BES systems and could help stabilize the German electricity grid. Finally, it would be interesting to establish a levelized cost metric for the residential solar PV and BES system and to decompose it to understand the cost of electricity used directly and indirectly and the individual contributions of the solar PV and the BES system. Especially understanding the additional cost of the BES system could help to make the economics of residential battery storage more transparent and develop simpler analytical models to calculate the optimal system size (vs. the algorithmic optimization approach used in essay three).

Appendix

A.1 Proof on the relation of LC and FC

Proof of Proposition 2.1. Given the assumptions of constant returns to scale, stationarity and full capacity utilization, we have

$$LC - FC_t^2(k \mid k) = \nu \cdot \Delta \cdot \left(\frac{1}{\sum_{t=1}^{T} (1+r)^{-t}} - \frac{1}{T} - \frac{r}{2} \right).$$

Hence, it remains to be shown that $\frac{1}{\sum_{t=1}^{T}(1+r)^{-t}} - \frac{1}{T} - \frac{r}{2} > 0$. Using the formula for the sum of the geometric series, we can rewrite

$$\frac{1}{\sum_{t=1}^{T} (1+r)^{-t}} = \frac{r \cdot (1+r)^T}{(1+r)^T - 1}$$

and

$$\frac{1}{\sum_{t=1}^{T} (1+r)^{-t}} - \frac{1}{T} - \frac{r}{2} = \frac{(1+r)^T \cdot (r \cdot T - 2) + 2 + r \cdot T}{2 \cdot T \cdot \left[(1+r)^T - 1 \right]}. \tag{A.1}$$

Since $2 \cdot T \cdot \left[(1+r)^T - 1\right] > 0$, the right-hand side of equation (A.1) is positive if the numerator is positive. We define $g(T) \coloneqq (1+r)^T \cdot (r \cdot T - 2) + 2 + r \cdot T$ and $h(r,T) \coloneqq -1 - r \cdot T + (1+r)^{T+1}$. We note $h(r,T) \geq 0$ because $h(0,T) = 0$ and $\frac{\partial}{\partial r} h(r,T) = (1+r)^T + T \cdot \left[(1+r)^T - 1\right] > 0$. For $T+1$, it follows that

$$\begin{aligned} g(T+1) &= (1+r)^{T+1} \cdot (r \cdot (T+1) - 2) + 2 + r \cdot (T+1) \\ &= g(T) + r \cdot \left[g(T) + h(r,T) \right]. \end{aligned}$$

Thus $g(2) > g(1) = r^2$, and more generally $g(T+1) > g(T) > 0$, yielding the claim that $LC(k) > FC_t^2(k)$. ■

A.2 General parameters of the battery cost model

Table A.1: Employee and logistics cost parameters

Parameter	Description	Value	Unit	Reference
N_{Workdays}	Operating days	360	Days/Year	Schünemann (2015)
$N_{\text{Workdays,Empl}}$	Employee working days	280	Days/Year	Braun and Walch (2017)
$N_{\text{Shift,Hour}}$	Working hours per shift	7	Hours/Shift	Schünemann (2015)
$N_{\text{Shift,Day}}$	Shifts per day	3	Shifts/Day	Schünemann (2015)
$x_{\text{Leadership}}$	Lead span	10	1/x	Schünemann (2015)
x_{Cleaning}	Span cleaning staff	10	1/x	Expert estimate
$c_{\text{Assistant}}$	Hourly rate supporting staff	37.628	USD*/h	IG Metall (2018)
c_{Skilled}	Hourly rate specialists	47.398	USD*/h	IG Metall (2018)
$c_{\text{Leadership}}$	Hourly rate indirect staff	61.385	USD*/h	IG Metall (2018)
c_{Cleaning}	Hourly rate cleaning staff	26.35	USD*/h	Expert estimate

*Average annual exchange rate Euro to US Dollar in 2022 of 1.054 Exchange Rates UK (2022)

Bibliography

Bundes-Klimaschutzgesetz (KSG). BGBl. I S. 3905, 2021. Germany.

ADAC. Pkw-Bestand in Deutschland: Erstmals mehr als eine Million E-Autos, 2023. URL `https://www.adac.de/news/pkw-bestand-deutschland/`. Accessed on April 26, 2023.

S. Ahmed, P. A. Nelson, K. G. Gallagher, N. Susarla, and D. W. Dees. Cost and energy demand of producing nickel manganese cobalt cathode material for lithium ion batteries. *Journal of Power Sources*, 342:733–740, 2017. ISSN 03787753.

J. Aldersey-Williams and T. Rubert. Levelised cost of energy – a theoretical justification and critical assessment. *Energy Policy*, 124:169–179, 2019. ISSN 03014215.

A. F. Altun and M. Kilic. Economic feasibility analysis with the parametric dynamic simulation of a single effect solar absorption cooling system for various climatic regions in turkey. *Renewable Energy*, 152:75–93, 2020. ISSN 09601481.

J. Amirault, J. Chien, S. Garg, D. Gibbons, B. Ross, M. Tang, J. Xing, I. Sidhu, P. Kaminsky, and B. Tenderich. The electric vehicle battery landscape: opportunities and challenges. *Center for Entrepreneurship & Technology (CET) University of California at Berkeley, Technical Brief*, 1, 2009.

S. J. An, J. Li, C. Daniel, D. Mohanty, S. Nagpure, and D. L. Wood III. The state of understanding of the lithium-ion-battery graphite solid electrolyte interphase (SEI) and its relationship to formation cycling. *Carbon*, 105:52–76, 2016. ISSN 00086223.

S. J. An, J. Li, Z. Du, C. Daniel, and D. L. Wood. Fast formation cycling for lithium ion batteries. *Journal of Power Sources*, 342:846–852, 2017. ISSN 03787753.

D. Andre, H. Hain, P. Lamp, F. Maglia, and B. Stiaszny. Future high-energy density anode materials from an automotive application perspective. *Journal of Materials Chemistry A*, 5 (33):17174–17198, 2017. ISSN 2050-7488.

F. Arnold, J. Junkermann, and P. A. Kienscherf. Energy crisis 2022: Gas price drives electricity price to record levels, 2022. URL `https://www.ewi.uni-koeln.de/en/aktuelles/mo-tool-2022-update/`. Accessed on August 10, 2023.

K. J. Arrow. Optimal capital policy, the cost of capital, and myopic decision rules. *Annals of the Institute of Statistical Mathematics*, 16(1):21–30, 1964.

H. Bajolle, M. Lagadic, and N. Louvet. The future of lithium-ion batteries: Exploring expert conceptions, market trends, and price scenarios. *Energy Research & Social Science*, 93: 102850, 2022. ISSN 2214-6296. URL `https://www.sciencedirect.com/science/article/pii/S221462962200353X`.

Batteries News. BYD plans to mass-produce sodium-ion batteries in Q2 2023, report says. 2022. URL `https://batteriesnews.com/byd-plans-mass-produce-sodium-ion-batteries-q2-2023-report-says/`. Accessed on January 28, 2024.

P. Behnam, A. Arefi, and M. B. Shafii. Exergetic and thermoeconomic analysis of a trigeneration system producing electricity, hot water, and fresh water driven by low-temperature geothermal sources. *Energy Conversion and Management*, 157:266–276, 2018. ISSN 01968904.

A. Belderbos, E. Delarue, K. Kessels, and W. D'haeseleer. Levelized cost of storage — introducing novel metrics. *Energy Economics*, 67:287–299, 2017. ISSN 01409883.

E. Bellos and C. Tzivanidis. Energetic and financial analysis of solar cooling systems with single effect absorption chiller in various climates. *Applied Thermal Engineering*, 126:809–821, 2017. ISSN 13594311.

G. Berckmans, M. Messagie, J. Smekens, N. Omar, and L. Vanhaverbeke. Cost Projection of State of the Art Lithium-Ion Batteries for Electric Vehicles Up to 2030. *Energies*, 10(9):1314, 2017.

E. J. Berg, C. Villevieille, D. Streich, S. Trabesinger, and P. Novák. Rechargeable Batteries: Grasping for the Limits of Chemistry. *Journal of The Electrochemical Society*, 162(14):A2468–A2475, 2015. ISSN 1945-7111.

BloombergNEF. Projected battery costs as a share of medium battery electric vehicle costs from 2016 to 2030, 2017. URL https://www.statista.com/statistics/797614/battery-share-of-medium-electric-vehicle-cost/. Accessed on April 27, 2023.

BloombergNEF. Lithium-ion battery pack prices rise for first time to an average of $151/kwh, 2022. URL https://about.bnef.com/blog/lithium-ion-battery-pack-prices-rise-for-first-time-to-an-average-of-151-kwh/. Accessed on April 27, 2023.

K. Branker, M. Pathak, and J. M. Pearce. A review of solar photovoltaic levelized cost of electricity. *Renewable and Sustainable Energy Reviews*, 15(9):4470–4482, 2011. ISSN 13640321.

D. Braun and M. Walch. Prozesskostenrechnung — was bisher fehlte. *Controlling & Management Review*, 61(4):64–70, 2017. ISSN 2195-8262.

C. Brown and B. Foley. Achieving a cost-competitive offshore wind power industry: What is the most effective policy framework? 2015.

M. Bruck, P. Sandborn, and N. Goudarzi. A levelized cost of energy (LCOE) model for wind farms that include Power Purchase Agreements (PPAs). *Renewable Energy*, 122:131–139, 2018. ISSN 09601481.

Bühler Group. Efficient continuous electrode slurry production. URL https://www.buhlergroup.com/content/buhlergroup/global/en/industries/batteries/Continuous-electrode-slurry-production.html. Accessed on May 11, 2022.

Bundesministerium für Umwelt, Naturschutz, nukleare Sicherheit und Verbraucherschutz. Förderung der Elektromobilität. URL https://www.bmuv.de/themen/luft-laerm-mobilitaet/verkehr/elektromobilitaet/foerderung. Accessed on April 26, 2023.

Bundesministerium für Wirtschaft und Klimaschutz (BMWK). Photovoltaik-Strategie: Handlungsfelder und Maßnahmen für einen beschleunigten Ausbau der Photovoltaik, 2023. URL https://www.bmwk.de/Redaktion/DE/Publikationen/Energie/photovoltaik-stategie-2023.pdf?__blob=publicationFile&v=4. Accessed May 21, 2023.

Bundesverfassungsgericht. Verfassungsbeschwerden gegen das Klimaschutzgesetz teilweise erfolgreich, 2021. URL https://www.bundesverfassungsgericht.de/SharedDocs/Pressemitteilungen/DE/2021/bvg21-031.html. Accessed on May 24, 2023.

A. Burnham, D. Gohlke, L. Rush, T. Stephens, Y. Zhou, M. A. Delucchi, A. Birky, C. Hunter, Z. Lin, S. Ou, et al. Comprehensive total cost of ownership quantification for vehicles with different size classes and powertrains. 2021.

D. W. Carlton and J. M. Perloff. *Modern Industrial Organization.* Pearson Addison Wesley, New York, 2005.

J. Cervantes and F. Choobineh. Optimal sizing of a nonutility-scale solar power system and its battery storage. *Applied Energy*, 216:105–115, 2018. ISSN 03062619.

CHARGED Electric Vehicles Magazine. Revolutionary continuous mixing process for producing Li-ion electrode slurries: Lower costs and higher quality. URL `https://chargedevs.com/newswire/the-tech/lower-costs-and-higher-quality-revolutionary-continuous-mixing-process-for-producing-li-ion-electrode-slurries/`. Accessed on May 11, 2022.

F. Cheng, A. A. Small, and L. M. Colosi. The levelized cost of negative CO2 emissions from thermochemical conversion of biomass coupled with carbon capture and storage. *Energy Conversion and Management*, 237:114115, 2021. ISSN 0196-8904.

Z. R. Chong, T. He, P. Babu, J.-n. Zheng, and P. Linga. Economic evaluation of energy efficient hydrate based desalination utilizing cold energy from liquefied natural gas (LNG). *Desalination*, 463:69–80, 2019. ISSN 00119164.

R. E. Ciez and J. F. Whitacre. The cost of lithium is unlikely to upend the price of Li-ion storage systems. *Journal of Power Sources*, 320:310–313, 2016. ISSN 03787753.

R. E. Ciez and J. F. Whitacre. Comparison between cylindrical and prismatic lithium-ion cell costs using a process based cost model. *Journal of Power Sources*, 340:273–281, 2017. ISSN 03787753.

C. Clifford. Charm gets $53 million to turn corn leftovers into oil and inject it into abandoned oil and gas wells. 2023. URL `https://www.cnbc.com/2023/05/18/frontier-signs-first-co2-removal-deal-with-charm-worth-53-million.html`. Accessed on July 29, 2024.

S. Comello and S. Reichelstein. The U.S. investment tax credit for solar energy: Alternatives to the anticipated 2017 step-down. *Renewable and Sustainable Energy Reviews*, 55:591–602, 2016. ISSN 13640321.

S. Comello and S. Reichelstein. The emergence of cost effective battery storage. *Nature communications*, 10(1):2038, 2019.

S. Comello, S. Reichelstein, and A. Sahoo. The road ahead for solar PV power. *Renewable and Sustainable Energy Reviews*, 92:744–756, 2018. ISSN 13640321.

S. Comello, G. Glenk, and S. Reichelstein. Transitioning to clean energy transportation services: Life-cycle cost analysis for vehicle fleets. *Applied Energy*, 285:116408, 2021. ISSN 03062619.

Council of the European Union. "Fit for 55": Council agrees on higher targets for renewables and energy efficiency, 2022. URL `https://www.consilium.europa.eu/en/press/press-releases/2022/06/27/fit-for-55-council-agrees-on-higher-targets-for-renewables-and-energy-efficiency/`. Accessed on May 28, 2023.

R. M. Darling. Techno-economic analyses of several redox flow batteries using levelized cost of energy storage. *Current Opinion in Chemical Engineering*, 37:100855, 2022. ISSN 22113398.

S. B. Darling, F. You, T. Veselka, and A. Velosa. Assumptions and the levelized cost of energy for photovoltaics. *Energy & Environmental Science*, 4(9):3133–3139, 2011. ISSN 1754-5692.

S. M. Datar and M. V. Rajan. *Horngren's cost accounting: a managerial emphasis*. Pearson, 2018.

Die Bundesregierung. Mehr energie aus erneuerbaren quellen, 2023. URL `https://www.bundesregierung.de/breg-de/themen/klimaschutz/energiewende-beschleunigen-2040310`. Accessed on April 27, 2023.

H. Dreger, H. Bockholt, W. Haselrieder, and A. Kwade. Discontinuous and Continuous Processing of Low-Solvent Battery Slurries for Lithium Nickel Cobalt Manganese Oxide Electrodes. *Journal of Electronic Materials*, 44(11):4434–4443, 2015. ISSN 1543-186X.

F. Duffner, M. Wentker, M. Greenwood, and J. Leker. Battery cost modeling: A review and directions for future research. *Renewable and Sustainable Energy Reviews*, 127:109872, 2020. ISSN 13640321.

F. Duffner, N. Kronemeyer, J. Tübke, J. Leker, M. Winter, and R. Schmuch. Post-lithium-ion battery cell production and its compatibility with lithium-ion cell production infrastructure. *Nature Energy*, 6(2):123–134, 2021. ISSN 2058-7546.

Element Energy. Electric Cars: Calculating the Total Cost of Ownership for Consumers: Final report for BEUC (The European Consumer Organisation), 2021.

ENBW. Solarpflicht: Kommt die solarpflicht für alle? https://www.enbw.com/blog/energiewende/solarenergie/solarpflicht-kommt-die-solarpflicht-fuer-alle/, 2022. Accessed on April 11 2023.

O. Erdinc, N. G. Paterakis, I. N. Pappi, A. G. Bakirtzis, and J. P. Catalão. A new perspective for sizing of distributed generation and energy storage for smart households under demand response. *Applied Energy*, 143:26–37, 2015. ISSN 03062619.

D. Eroglu, K. R. Zavadil, and K. G. Gallagher. Critical link between materials chemistry and cell-level design for high energy density and low cost lithium-sulfur transportation battery. *Journal of The Electrochemical Society*, 162(6):A982–A990, 2015. ISSN 0013-4651.

EUPD Research. 89 percent of the solar potential for german single- and two-family houses is still unexploited. https://www.eupd-research.com/en/89-percent-of-the-solar-potential-still-unexploited/, 2021. Accessed on April 11, 2023.

European Environment Agency. Eu greenhouse gas emissions kept decreasing in 2018, largest reductions in energy sector, 2020. URL https://unfccc.int/process-and-meetings/the-paris-agreement. Accessed on May 3, 2023.

European Parliament. "Fit for 55": zero CO2 emissions for new cars and vans in 2035, 2023. URL https://www.europarl.europa.eu/news/en/press-room/20230210IPR74715/fit-for-55-zero-co2-emissions-for-new-cars-and-vans-in-2035. Accessed on May 28, 2023.

A. Evans, V. Strezov, and T. J. Evans. Assessment of utility energy storage options for increased renewable energy penetration. *Renewable and Sustainable Energy Reviews*, 16(6):4141–4147, 2012.

R. Ewert, A. Wagenhofer, and A. Rohlfing-Bastian. *Interne Unternehmensrechnung*. Springer-Gabler, 9 edition, 2023.

Exchange Rates UK. Euro to US Dollar Spot Exchange Rates for 2022, 2022. URL https://www.exchangerates.org.uk/EUR-USD-spot-exchange-rates-history-2022.html. Accessed on November 25, 2022.

D. L. Farrar and F. Woodruff. A model for the determination of optimal electric generating system expansion patterns, 1973.

F. Field, R. Kirchain, and R. Roth. Process cost modeling: Strategic engineering and economic evaluation of materials technologies. *JOM*, 59(10):21–32, 2007. ISSN 1543-1851.

B. A. Franco, P. Baptista, R. C. Neto, and S. Ganilha. Assessment of offloading pathways for wind-powered offshore hydrogen production: Energy and economic analysis. *Applied Energy*, 286:116553, 2021. ISSN 03062619.

J. Frazelle. Battery day. *Communications of the ACM*, 64(5):52–59, 2021. ISSN 0001-0782.

G. Friedl and C. Ann. A cost-based approach for calculating royalties for standard-essential patents (seps). *The Journal of World Intellectual Property*, 21(5-6):369–384, 2018. ISSN 14222213.

G. Friedl and H.-U. Küpper. Historische Kosten oder Long Run Incremental Costs als Kostenmaßstab für die Preisgestaltung in regulierten Märkten? *Zeitschrift für betriebswirtschaftliche Forschung*, 6(64):98–128, 2011.

G. Friedl, C. Hofmann, and B. Pedell. *Kostenrechnung: Eine entscheidungsorientierte Einführung*. Vahlen, 4 edition, 2022. ISBN 978-3-8006-6814-4.

J. Friedmann, Z. Fan, Z. Byrum, E. Ochu, A. Bhardwaj, and H. Sheerazi. Levelized Cost of Carbon Abatement: An Improved Cost-Assessment Methodology for a Net-Zero Emissions World. 2020.

R. Gabbrielli, P. Castrataro, F. Del Medico, M. Di Palo, and B. Lenzo. Levelized cost of heat for linear fresnel concentrated solar systems. *Energy Procedia*, 49:1340–1349, 2014. ISSN 18766102.

K. G. Gallagher, S. Goebel, T. Greszler, M. Mathias, W. Oelerich, D. Eroglu, and V. Srinivasan. Quantifying the promise of lithium–air batteries for electric vehicles. *Energy & Environmental Science*, 7(5):1555, 2014. ISSN 1754-5692.

Y. L. Gamarra and G. Friedl. Declared essential patents and average total R&D expenditures per patent family. *Telecommunications Policy*, 2023. ISSN 0308-5961.

G. Glenk and S. Reichelstein. Economics of converting renewable power to hydrogen. *Nature Energy*, 4(3):216–222, 2019.

G. Glenk and S. Reichelstein. Reversible Power-to-Gas systems for energy conversion and storage. *Nature Communications*, 13(1):2010, 2022a.

G. Glenk and S. Reichelstein. The economic dynamics of competing power generation sources. *Renewable and Sustainable Energy Reviews*, 168:112758, 2022b. ISSN 13640321.

G. Glenk, R. Meier, and S. Reichelstein. Cost dynamics of clean energy technologies. *Schmalenbach Journal of Business Research*, 73(2):179–206, 2021.

G. Glenk, K. Anton, R. Meier, and S. Reichelstein. Cost-efficient pathways to decarbonizing Portland cement production. 2023a.

G. Glenk, P. Holler, and S. Reichelstein. Advances in Power-to-Gas technologies: cost and conversion efficiency. 2023b.

C. Goodall. Fuels from air and water, 2017. URL `https://www.carboncommentary.com/blog/2017/12/13/fuels-from-air-and-water?utm_source=Carbon+Commentary+latest+posts&utm_campaign=81ca6225cb-Carbon_Commentary_latest_posts11_29_2014&utm_medium=email&utm_term=0_f81f6d4f31-81ca6225cb-500845613`. Accessed on April 25, 2022.

A. Grimm, W. A. de Jong, and G. J. Kramer. Renewable hydrogen production: A techno-economic comparison of photoelectrochemical cells and photovoltaic-electrolysis. *International Journal of Hydrogen Energy*, 45(43):22545–22555, 2020. ISSN 03603199.

O. J. Guerra, J. Eichman, J. Kurtz, and B.-M. Hodge. Cost competitiveness of electrolytic hydrogen. *Joule*, 3(10):2425–2443, 2019. ISSN 25424351.

O. J. Guerra, J. Eichman, and P. Denholm. Optimal energy storage portfolio for high and ultrahigh carbon-free and renewable power systems. *Energy & Environmental Science*, 14 (10):5132–5146, 2021. ISSN 1754-5692.

F. J. Günter and N. Wassiliadis. State of the Art of Lithium-Ion Pouch Cells in Automotive Applications: Cell Teardown and Characterization. *Journal of The Electrochemical Society*, 2022. ISSN 1945-7111.

M. Haarmann, D. Grießl, and A. Kwade. Continuous Processing of Cathode Slurry by Extrusion for Lithium–Ion Batteries. *Energy Technology*, 9(10):2100250, 2021. ISSN 2194-4288.

J. B. Habedank, F. J. Günter, N. Billot, R. Gilles, T. Neuwirth, G. Reinhart, and M. F. Zaeh. Rapid electrolyte wetting of lithium-ion batteries containing laser structured electrodes: in situ visualization by neutron radiography. *The International Journal of Advanced Manufacturing Technology*, 102(9-12):2769–2778, 2019. ISSN 0268-3768.

M. Hagen, D. Hanselmann, K. Ahlbrecht, R. Maça, D. Gerber, and J. Tübke. Lithium-sulfur cells: The gap between the state-of-the-art and the requirements for high energy battery cells. *Advanced Energy Materials*, 5(16):1401986, 2015. ISSN 16146832.

C. A. Heck, M.-W. von Horstig, F. Huttner, J. K. Mayer, W. Haselrieder, and A. Kwade. Review—Knowledge-Based Process Design for High Quality Production of NCM811 Cathodes. *Journal of The Electrochemical Society*, 167(16):160521, 2020. ISSN 1945-7111.

H. H. Heimes, A. Kampker, C. Lienemann, M. Locke, C. Offermanns, S. Michaelis, and E. Rahimzei. Lithium-ion battery cell production process, 2018.

J. Hernández-Moro and J. M. Martínez-Duart. Analytical model for solar PV and CSP electricity costs: Present LCOE values and their future evolution. *Renewable and Sustainable Energy Reviews*, 20:119–132, 2013. ISSN 13640321.

L. Hirth. The market value of variable renewables. *Energy Economics*, 38:218–236, 2013. ISSN 01409883.

H. Hotelling. A general mathematical theory of depreciation. *Journal of the American Statistical Association*, 20(151):340–353, 1925. ISSN 0162-1459.

C. A. Hunter, M. M. Penev, E. P. Reznicek, J. Eichman, N. Rustagi, and S. F. Baldwin. Techno-economic analysis of long-duration energy storage and flexible power generation technologies to support high-variable renewable energy grids. *Joule*, 5(8):2077–2101, 2021. ISSN 25424351.

F. Huttner, W. Haselrieder, and A. Kwade. The Influence of Different Post–Drying Procedures on Remaining Water Content and Physical and Electrochemical Properties of Lithium–Ion Batteries. *Energy Technology*, 8(2):1900245, 2020. ISSN 2194-4288.

F. Huttner, A. Diener, T. Heckmann, J. C. Eser, T. Abali, J. K. Mayer, P. Scharfer, W. Schabel, and A. Kwade. Increased Moisture Uptake of NCM622 Cathodes after Calendering due to Particle Breakage. *Journal of The Electrochemical Society*, 168(9):090539, 2021. ISSN 1945-7111.

IEA. Press release: Global electric vehicle outlook 2022. 2022.

IG Metall. Tariftabellen Metall- und Elektroindustrie: ERA - monatsentgelte (in euro), 2018. URL `https://www.igmetall.de/download/MuE_ERA_Entgelte_Juni2018_78d3e1848939887f53dcf9506907870bb637c493.pdf`. Accessed on December 10, 2022.

Intergovernmental Panel on Climate Change. Synthesis report: Of the ipcc sixth assessment report (ar6), 2023.

Ö. İşlegen and S. Reichelstein. Carbon capture by fossil fuel power plants: An economic analysis. *Management Science*, 57(1):21–39, 2011.

M. Z. Jacobson. Clean grids with current technology. *Nature Climate Change*, 6(5):441–442, 2016.

I. Javeed, R. Khezri, A. Mahmoudi, A. Yazdani, and G. M. Shafiullah. Optimal sizing of rooftop pv and battery storage for grid-connected houses considering flat and time-of-use electricity rates. *Energies*, 14(12):3520, 2021.

H. Jin and P. Lienert. Iron man elon musk places his tesla battery bets. *Reuters*, 2022. https://www.reuters.com/business/autos-transportation/iron-man-elon-musk-places-his-tesla-battery-bets-2022-04-27/.

N. Jones. Liquid hydrogen. *Nature Climate Change*, 2(1):23, 2012.

D. W. Jorgenson. Capital theory and investment behavior. *American Economic Review*, 53(2): 247–259, 1963. ISSN 0002-8282.

P. L. Joskow. Comparing the costs of intermittent and dispatchable electricity generating technologies. *American Economic Review*, 101(3):238–241, 2011. ISSN 0002-8282.

V. Jülch. Comparison of electricity storage options using levelized cost of storage (lcos) method. *Applied Energy*, 183:1594–1606, 2016. ISSN 03062619.

V. Jülch, T. Telsnig, M. Schulz, N. Hartmann, J. Thomsen, L. Eltrop, and T. Schlegl. A holistic comparative analysis of different storage systems using levelized cost of storage and life cycle indicators. *Energy Procedia*, 73:18–28, 2015. ISSN 18766102.

K. Kalaga, M.-T. F. Rodrigues, S. E. Trask, I. A. Shkrob, and D. P. Abraham. Calendar-life versus cycle-life aging of lithium-ion cells with silicon-graphite composite electrodes. *Electrochimica Acta*, 280:221–228, 2018. ISSN 00134686.

F. R. Kalhammer, B. M. Kopf, D. H. Swan, V. P. Roan, and M. P. Walsh. Status and prospects for zero emissions vehicle technology. *Report of the ARB Independent Expert Panel*, 1(1): 12–36, 2007.

M. Kane. Rumor mill: VW paying less than $100 per kWh of battery capacity, 2019. URL `https://insideevs.com/news/369923/rumor-mill-vw-cheap-battery/`. Accessed on November 19, 2022.

D. W. Keith, G. Holmes, D. S. Angelo, and K. Heidel. A process for capturing CO2 from the atmosphere. *Joule*, 2(8):1573–1594, 2018.

M. Keppeler, H.-Y. Tran, and W. Braunwarth. The Role of Pilot Lines in Bridging the Gap Between Fundamental Research and Industrial Production for Lithium–Ion Battery Cells Relevant to Sustainable Electromobility: A Review. *Energy Technology*, 9(8):2100132, 2021. ISSN 2194-4288.

K. R. Khalilpour and A. Vassallo. Technoeconomic parametric analysis of PV-battery systems. *Renewable Energy*, 97:757–768, 2016. ISSN 09601481.

Y. Khawaja, D. Giaouris, H. Patsios, and M. Dahidah. Optimal cost-based model for sizing grid-connected PV and battery energy system. In *2017 IEEE Jordan Conference on Applied Electrical Engineering and Computing Technologies (AEECT)*, pages 1–6. IEEE, 2017.

M. Khzouz, E. Gkanas, J. Shao, F. Sher, D. Beherskyi, A. El-Kharouf, and M. Al Qubeissi. Life cycle costing analysis: Tools and applications for determining hydrogen production cost for fuel cell vehicle technology. *Energies*, 13(15):3783, 2020.

M.-H. Kim, D. Kim, J. Heo, and D.-W. Lee. Techno-economic analysis of hybrid renewable energy system with solar district heating for net zero energy community. *Energy*, 187:115916, 2019. ISSN 03605442.

K.-P. Kistner and A. Luhmer. Zur Ermittlung der Kosten der Betriebsmittel in der statischen Produktionstheorie. *Zeitschrift für Betriebswirtschaft*, 51:165–180, 1981.

K. W. Knehr, J. J. Kubal, P. A. Nelson, and S. Ahmed. Battery performance and cost modeling for electric-drive vehicles: A manual for batpac v5.0. 2022.

T. Knoche and G. Reinhart. Electrolyte Filling of Large-Scale Lithium-Ion Batteries: Challenges for Production Technology and Possible Approaches. *Applied Mechanics and Materials*, 794: 11–18, 2015.

C. Kost, S. Shammugam, V. Fluri, D. Peper, A. Davoodi Memar, and T. Schlegl. Levelized cost of electricity: Renewable energy technologies, 2021.

J. Kriegler, M. Binzer, and M. F. Zaeh. Process strategies for laser cutting of electrodes in lithium-ion battery production. *Journal of Laser Applications*, 33(1):012006, 2021. ISSN 1042-346X.

H.-U. Küpper. Investitionstheoretische Fundierung der Kostenrechnung. *Zeitschrift für betriebswirtschaftliche Forschung*, 37(1):26–46, 1985.

A. Kwade, W. Haselrieder, R. Leithoff, A. Modlinger, F. Dietrich, and K. Droeder. Current status and challenges for automotive battery production technologies. *Nature Energy*, 3(4): 290–300, 2018. ISSN 2058-7546.

H.-U. Küpper. Kosten-und entscheidungstheoretische Ansatzpunkte zur Behandlung des Fixkostenproblems in der Kostenrechnung. *Zeitschrift für betriebswirtschaftliche Forschung*, 36:794–811, 1984.

C. S. Lai and M. D. McCulloch. Levelized cost of electricity for solar photovoltaic and electrical energy storage. *Applied Energy*, 190:191–203, 2017. ISSN 03062619.

A. Lajunen and T. Lipman. Lifecycle cost assessment and carbon dioxide emissions of diesel, natural gas, hybrid electric, fuel cell hybrid and electric transit buses. *Energy*, 106:329–342, 2016. ISSN 0360-5442.

L. Lander, T. Cleaver, M. A. Rajaeifar, V. Nguyen-Tien, R. J. Elliott, O. Heidrich, E. Kendrick, J. S. Edge, and G. Offer. Financial viability of electric vehicle lithium-ion battery recycling. *Iscience*, 24(7):102787, 2021.

P. Lebeau, C. Macharis, J. v. Mierlo, and K. Lebeau. Electrifying light commercial vehicles for city logistics? a total cost of ownership analysis. *European Journal of Transport and Infrastructure Research*, 15(4), Sep. 2015.

J.-Y. Lee, M. Yoo, K. Cha, T. W. Lim, and T. Hur. Life cycle cost analysis to examine the economical feasibility of hydrogen as an alternative fuel. *International Journal of Hydrogen Energy*, 34(10):4243–4255, 2009. ISSN 03603199.

M. Lehtveer and A. Emanuelsson. BECCS and DACCS as negative emission providers in an intermittent electricity system: Why levelized cost of carbon may be a misleading measure for policy decisions. *Frontiers in Climate*, 3, 2021.

R. Leithoff, A. Fröhlich, and K. Dröder. Investigation of the Influence of Deposition Accuracy of Electrodes on the Electrochemical Properties of Lithium–Ion Batteries. *Energy Technology*, 8 (2):1900129, 2020. ISSN 2194-4296.

Q. Li, C. Zheng, A. Shirazi, O. Bany Mousa, F. Moscia, J. A. Scott, and R. A. Taylor. Design and analysis of a medium-temperature, concentrated solar thermal collector for air-conditioning applications. *Applied Energy*, 190:1159–1173, 2017. ISSN 03062619.

W. Li, Y.-G. Cho, W. Yao, Y. Li, A. Cronk, R. Shimizu, M. A. Schroeder, Y. Fu, F. Zou, V. Battaglia, et al. Enabling high areal capacity for co-free high voltage spinel materials in next-generation li-ion batteries. *Journal of Power Sources*, 473:228579, 2020.

F. Liao, E. Molin, and B. van Wee. Consumer preferences for electric vehicles: a literature review. *Transport Reviews*, 37(3):252–275, 2017.

J. Liu, X. Chen, H. Yang, and Y. Li. Energy storage and management system design optimization for a photovoltaic integrated low-energy building. *Energy*, 190:116424, 2020. ISSN 03605442.

Z. Liu, J. Song, J. Kubal, N. Susarla, K. W. Knehr, E. Islam, P. Nelson, and S. Ahmed. Comparing total cost of ownership of battery electric vehicles and internal combustion engine vehicles. *Energy Policy*, 158:112564, 2021. ISSN 03014215.

S. Loutatidou and H. A. Arafat. Techno-economic analysis of med and ro desalination powered by low-enthalpy geothermal energy. *Desalination*, 365:277–292, 2015. ISSN 00119164.

W. Lücke. Investitionsrechnungen auf der Grundlage von Ausgaben oder Kosten. *Zeitschrift für handelswissenschaftliche Forschung*, 7(3):310–324, 1955.

A. Luhmer. Fixe und variable Abschreibungskosten und optimale Investitionsdauer - Zu einem Aufsatz von Peter Swoboda. *Zeitschrift für Betriebswirtschaft*, 50(8/1980):898–903, 1980.

A. MacKenzie, D. L. Granatstein, E. J. Anthony, and J. C. Abanades. Economics of CO2 capture using the calcium cycle with a pressurized fluidized bed combustor. *Energy & Fuels*, 21(2): 920–926, 2007. ISSN 0887-0624.

A. Mahlert. *Die Abschreibungen in der entscheidungsorientierten Kostenrechnung*. Opladen: Westdeutscher Verlag, 1976.

C. Mao, S. J. AN, H. M. Meyer, J. Li, M. Wood, R. E. Ruther, and D. L. Wood. Balancing formation time and electrochemical performance of high energy lithium-ion batteries. *Journal of Power Sources*, 402:107–115, 2018. ISSN 03787753.

Massachusetts Institute of Technology. The future of coal, 2007. URL `http://web.mit.edu/coal/`.

S. Matteson and E. Williams. Learning dependent subsidies for lithium-ion electric vehicle batteries. *Technological Forecasting and Social Change*, 92:322–331, 2015. ISSN 00401625.

L. Mauler, F. Duffner, W. G. Zeier, and J. Leker. Battery cost forecasting: a review of methods and results with an outlook to 2050. *Energy & Environmental Science*, 14(9):4712–4739, 2021. ISSN 1754-5692.

S. T. McCoy and E. S. Rubin. Variability and uncertainty in the cost of saline formation storage. *Energy Procedia*, 1(1):4151–4158, 2009. ISSN 18766102.

McKinsey & Company. The net-zero transition: What it would cost, what it could bring, 2022.

McKinsey Center for Future Mobility. Why the automotive future is electric, 2021.

C. Meyer, H. Bockholt, W. Haselrieder, and A. Kwade. Characterization of the calendering process for compaction of electrodes for lithium-ion batteries. *Journal of Materials Processing Technology*, 249:172–178, 2017. ISSN 09240136.

S. Michaelis, E. Rahimzei, A. Kampker, and H. Heimes. Roadmap Batterie-Produktionsmittel 2030 - Update 2020.

M. Minutillo, A. Perna, A. Forcina, S. Di Micco, and E. Jannelli. Analyzing the levelized cost of hydrogen in refueling stations with on-site hydrogen production via water electrolysis in the Italian scenario. *International Journal of Hydrogen Energy*, 46(26):13667–13677, 2021. ISSN 03603199.

M. H. Mostafa, S. H. Abdel Aleem, S. G. Ali, Z. M. Ali, and A. Y. Abdelaziz. Techno-economic assessment of energy storage systems using annualized life cycle cost of storage (LCCOS) and levelized cost of energy (LCOE) metrics. *Journal of Energy Storage*, 29:101345, 2020. ISSN 2352152X.

E. Moyassari, T. Roth, S. Kücher, C.-C. Chang, S.-C. Hou, F. B. Spingler, and A. Jossen. The role of silicon in silicon-graphite composite electrodes regarding specific capacity, cycle stability, and expansion. *Journal of The Electrochemical Society*, 169(1):010504, 2022. ISSN 1945-7111.

U. Mulleriyawage and W. Shen. Optimally sizing of battery energy storage capacity by operational optimization of residential PV-Battery systems: An Australian household case study. *Renewable Energy*, 160:852–864, 2020.

Nat Energy. Editorial: Hydrogen on the rise. *Nature Energy*, 1:16127, 2016.

P. A. Nelson, S. Ahmed, K. G. Gallagher, and D. W. Dees. Cost savings for manufacturing lithium batteries in a flexible plant. *Journal of Power Sources*, 283:506–516, 2015. ISSN 03787753.

P. A. Nelson, S. Ahmed, K. G. Gallagher, and D. W. Dees. Modeling the performance and cost of Lithium-ion batteries for electric-drive vehicles: Third edition. *ANL/CSE-19/2*, (2), 2019.

T. Nemeth, P. Schröer, M. Kuipers, and D. U. Sauer. Lithium titanate oxide battery cells for high-power automotive applications – electro-thermal properties, aging behavior and cost considerations. *Journal of Energy Storage*, 31:101656, 2020. ISSN 2352152X.

Nextmove. Battery day: Tesla stellt 4680er zelle und model s plaid vor, 2020. URL `https://nextmove.de/battery-day-tesla-stellt-neue-4680er-zelle-und-das-model-s-plaid-vor/`. Accessed on July 29, 2022.

A. Nezlobin. Accrual accounting, informational sufficiency, and equity valuation. *Journal of Accounting Research*, 50(1):233–273, 2012.

A. Nezlobin, M. V. Rajan, and S. Reichelstein. Dynamics of rate-of-return regulation. *Management Science*, 58(5):980–995, 2012.

B. Nykvist and M. Nilsson. Rapidly falling costs of battery packs for electric vehicles. *Nature Climate Change*, 5:329–332, 2015. ISSN 17586798.

B. Nykvist, F. Sprei, and M. Nilsson. Assessing the progress toward lower priced long range battery electric vehicles. *Energy Policy*, 124:144–155, 2019. ISSN 03014215.

E. O'Shaughnessy, D. Cutler, K. Ardani, and R. Margolis. Solar plus: Optimization of distributed solar PV through battery storage and dispatchable load in residential buildings. *Applied Energy*, 213:11–21, 2018. ISSN 03062619.

X. Ouyang and B. Lin. Levelized cost of electricity (LCOE) of renewable energies and required subsidies in China. *Energy Policy*, 70:64–73, 2014. ISSN 03014215.

B. Parkinson, P. Balcombe, J. F. Speirs, A. D. Hawkes, and K. Hellgardt. Levelized cost of CO2 mitigation from hydrogen production routes. *Energy & Environmental Science*, 12(1):19–40, 2019. ISSN 1754-5692.

R. L. Parr. *Intellectual Property: Valuation, Exploitation, and Infringement Damages.* John Wiley & Sons, 5 edition, 2018.

G. Patry, A. Romagny, S. Martinet, and D. Froelich. Cost modeling of lithium–ion battery cells for automotive applications. *Energy Science & Engineering*, 3(1):71–82, 2015. ISSN 2050-0505.

I. Pawel. The cost of storage – how to calculate the levelized cost of stored energy (LCOE) and applications to renewable energy generation. *Energy Procedia*, 46:68–77, 2014. ISSN 18766102.

R. Petri, T. Giebel, B. Zhang, J.-H. Schünemann, and C. Herrmann. Material cost model for innovative li-ion battery cells in electric vehicle applications. *International Journal of Precision Engineering and Manufacturing-Green Technology*, 2(3):263–268, 2015. ISSN 2288-6206.

K.-H. Pettinger. Production test procedures. In R. Korthauer, editor, *Lithium-Ion Batteries: Basics and Applications*, pages 237–246. Springer-Verlag, Berlin and Heidelberg, 2018. ISBN 978-3-662-53069-6.

M. Philippot, G. Alvarez, E. Ayerbe, J. van Mierlo, and M. Messagie. Eco-Efficiency of a Lithium-Ion Battery for Electric Vehicles: Influence of Manufacturing Country and Commodity Prices on GHG Emissions and Costs. *Batteries*, 5(1):23, 2019.

C. Pillot. The worldwide rechargeable battery market 2010 – 2025, avicenne energy, 2020.

P. Poonpun and W. T. Jewell. Analysis of the cost per kilowatt hour to store electricity. *IEEE Transactions on Energy Conversion*, 23(2):529–534, 2008. ISSN 0885-8969.

Y. Preger, H. M. Barkholtz, A. Fresquez, D. L. Campbell, B. W. Juba, J. Romàn-Kustas, S. R. Ferreira, and B. Chalamala. Degradation of commercial lithium-ion cells as a function of chemistry and cycling conditions. *Journal of The Electrochemical Society*, 167(12):120532, 2020.

G. A. D. Preinreich. Annual survey of economic theory: The theory of depreciation. *Econometrica: journal of the econometric society*, 6(3):219–241, 1938.

P. C. Psarras, S. Comello, P. Bains, P. Charoensawadpong, S. Reichelstein, and J. Wilcox. Carbon capture and utilization in the industrial sector. *Environmental science & technology*, 51(19):11440–11449, 2017.

M. M. Rahman, A. O. Oni, E. Gemechu, and A. Kumar. Assessment of energy storage technologies: A review. *Energy Conversion and Management*, 223:113295, 2020. ISSN 01968904.

M. V. Rajan and S. Reichelstein. Depreciation rules and the relation between marginal and historical cost. *Journal of Accounting Research*, 47(3):823–865, 2009.

S. Reichelstein and A. Rohlfing-Bastian. Levelized product cost: Concept and decision relevance. *The Accounting Review*, 90(4):1653–1682, 2015. ISSN 0001-4826.

S. Reichelstein and A. Sahoo. Time of day pricing and the levelized cost of intermittent power generation. *Energy Economics*, 48:97–108, 2015.

S. Reichelstein and M. Yorston. The prospects for cost competitive solar pv power. *Energy Policy*, 55:117–127, 2013. ISSN 03014215.

M. Ren, C. R. Mitchell, and W. Mo. Managing residential solar photovoltaic-battery systems for grid and life cycle economic and environmental co-benefits under time-of-use rate design. *Resources, Conservation and Recycling*, 169:105527, 2021. ISSN 09213449.

K. E. Rodby, T. J. Carney, Y. Ashraf Gandomi, J. L. Barton, R. M. Darling, and F. R. Brushett. Assessing the levelized cost of vanadium redox flow batteries with capacity fade and rebalancing. *Journal of Power Sources*, 460:227958, 2020. ISSN 03787753.

W. P. Rogerson. Intertemporal cost allocation and investment decisions. *Journal of Political Economy*, 116(5):931–950, 2008.

M. Rosenthal, R. Adams, and L. Bennett. A comparative evaluation of advanced converters. Technical report, Oak Ridge National Lab., Tenn., 1965.

E. S. Rubin and H. Zhai. The cost of carbon capture and storage for natural gas combined cycle power plants. *Environmental science & technology*, 46(6):3076–3084, 2012.

M. Sadi, K. H. Chakravarty, A. Behzadi, and A. Arabkoohsar. Techno-economic-environmental investigation of various biomass types and innovative biomass-firing technologies for cost-effective cooling in india. *Energy*, 219:119561, 2021. ISSN 03605442.

M. Safoutin, J. McDonald, and B. Ellies. Predicting the future manufacturing cost of batteries for plug-in vehicles for the u.s. environmental protection agency (epa) 2017–2025 light-duty greenhouse gas standards. *World Electric Vehicle Journal*, 9(3):42, 2018.

A. Sakti, J. J. Michalek, E. R. Fuchs, and J. F. Whitacre. A techno-economic analysis and optimization of li-ion batteries for light-duty passenger vehicle electrification. *Journal of Power Sources*, 273:966–980, 2014. ISSN 03787753.

A. Sakti, I. M. Azevedo, E. R. Fuchs, J. J. Michalek, K. G. Gallagher, and J. F. Whitacre. Consistency and robustness of forecasting for emerging technologies: The case of li-ion batteries for electric vehicles. *Energy Policy*, 106:415–426, 2017. ISSN 03014215.

C. Scheller, K. Schmidt, C. Herrmann, and T. S. Spengler. Decentralized planning of lithium-ion battery production and recycling. *Procedia CIRP*, 90:700–704, 2020. ISSN 22128271.

O. Schmidt, S. Melchior, A. Hawkes, and I. Staffell. Projecting the Future Levelized Cost of Electricity Storage Technologies. *Joule*, 3(1):81–100, 2019. ISSN 25424351.

R. Schmuch, R. Wagner, G. Hörpel, T. Placke, and M. Winter. Performance and cost of materials for lithium-based rechargeable automotive batteries. *Nature Energy*, 3(4):267–278, 2018. ISSN 2058-7546.

D. Schneider. *Die wirtschaftliche Nutzungsdauer von Anlagegütern als Bestimmungsgrund der Abschreibungen.* Köln und Opladen, 1961.

S. F. Schneider, C. Bauer, P. Novák, and E. J. Berg. A modeling framework to assess specific energy, costs and environmental impacts of Li-ion and Na-ion batteries. *Sustainable Energy & Fuels*, 3(11):3061–3070, 2019.

J. Schnell, F. Tietz, C. Singer, A. Hofer, N. Billot, and G. Reinhart. Prospects of production technologies and manufacturing costs of oxide-based all-solid-state lithium batteries. *Energy & Environmental Science*, 12(6):1818–1833, 2019. ISSN 1754-5692.

J. Schnell, H. Knörzer, A. J. Imbsweiler, and G. Reinhart. Solid versus liquid—a bottom–up calculation model to analyze the manufacturing cost of future high–energy batteries. *Energy Technology*, 8(3):1901237, 2020. ISSN 2194-4288.

P. Schulze, J. Holstein, A. van den Noort, and J. Knijp. Power-to-Gas in a decarbonized European energy system based on renewable energy sources. *DNV GL*, 2017.

J.-H. Schünemann. *Cost Model to Validate Production Cost of Lithium-Ion Batteries.* PhD thesis, Technische Universität Carolo-Wilhelmina zu Braunschweig, Braunschweig, 2015.

J.-H. Schünemann, H. Dreger, H. Bockholt, and A. Kwade. Smart Electrode Processing for Battery Cost Reduction. *ECS Transactions*, 73(1):153–159, 2016. ISSN 1938-5862.

M. Schweitzer, H.-U. Küpper, G. Friedl, C. Hofmann, and B. Pedell. *Systeme der Kosten-und Erlösrechnung.* Vahlen, 2015.

N. A. Sepulveda, J. D. Jenkins, A. Edington, D. S. Mallapragada, and R. K. Lester. The design space for long-duration energy storage in decarbonized power systems. *Nature Energy*, 6(5): 506–516, 2021.

W. Short, D. J. Packey, and T. Holt. A manual for the economic evaluation of energy efficiency and renewable energy technologies, 1995.

A. J. Simon, N. B. Kaahaaina, S. Julio Friedmann, and R. D. Aines. Systems analysis and cost estimates for large scale capture of carbon dioxide from air. *Energy Procedia*, 4:2893–2900, 2011. ISSN 18766102.

Y. Simsek, C. Mata-Torres, A. M. Guzmán, J. M. Cardemil, and R. Escobar. Sensitivity and effectiveness analysis of incentives for concentrated solar power projects in Chile. *Renewable Energy*, 129:214–224, 2018. ISSN 09601481.

A. Smallbone, V. Jülch, R. Wardle, and A. P. Roskilly. Levelised cost of storage for pumped heat energy storage in comparison with other energy storage technologies. *Energy Conversion and Management*, 152:221–228, 2017. ISSN 01968904.

R. Stanek and B. Konersmann. Tesla battery day 2020 - Technology announcement analysis, 2020.

Statista GmbH. Carbon dioxide (CO2) emissions in the European Union in 2000, 2010 and 2021, by country (in million metric tons), 2022a. URL `https://www.statista.com/statistics/1171389/co2-emissions-european-union`.

Statista GmbH. The Great Lithium Boom, 2022b. URL `https://www.statista.com/chart/28037/lithium-carbonate-price-timeline/`.

T. Steckel, A. Kendall, and H. Ambrose. Applying levelized cost of storage methodology to utility-scale second-life lithium-ion battery energy storage systems. *Applied Energy*, 300: 117309, 2021. ISSN 03062619.

M. Stich, N. Pandey, and A. Bund. Drying and moisture resorption behaviour of various electrode materials and separators for lithium-ion batteries. *Journal of Power Sources*, 364:84–91, 2017. ISSN 03787753.

P. Swoboda. Die Ableitung variabler Abschreibungskosten aus Modellen zur Optimierung der Investitionsdauer. *Zeitschrift für Betriebswirtschaft*, 4(7/1979):563–580, 1979.

S. Tegen, M. Hand, B. Maples, E. Lantz, P. Schwabe, and A. Smith. 2010 cost of wind energy review. Technical report, National Renewable Energy Lab.(NREL), Golden, CO (United States), 2012.

A. Thielmann, M. Wietschel, S. Funke, A. Grimm, T. Hettesheimer, S. Langkau, A. Loibl, C. Moll, C. Neef, P. Plötz, L. Sievers, L. T. Espinoza, and J. Edler. Batteries for electric cars: fact check and need for action, 2020.

M. Thomitzek, N. von Drachenfels, F. Cerdas, C. Herrmann, and S. Thiede. Simulation-based assessment of the energy demand in battery cell manufacturing. *Procedia CIRP*, 80:126–131, 2019. ISSN 22128271.

Z. Tian, B. Perers, S. Furbo, and J. Fan. Thermo-economic optimization of a hybrid solar district heating plant with flat plate collectors and parabolic trough collectors in series. *Energy Conversion and Management*, 165:92–101, 2018. ISSN 01968904.

T. T. Tran and A. D. Smith. Incorporating performance-based global sensitivity and uncertainty analysis into lcoe calculations for emerging renewable energy technologies. *Applied Energy*, 216:157–171, 2018. ISSN 03062619.

C. Vaalma, D. Buchholz, M. Weil, and S. Passerini. A cost and resource analysis of sodium-ion batteries. *Nature Reviews Materials*, 3(4), 2018.

S. Van Renssen. A business case for green fuels. *Nature Climate Change*, 3(11):951–952, 2013.

V. Viswanathan, K. Mongird, R. Franks, X. Li, V. Sprenkle, and R. Baxter. 2022 grid energy storage technology cost and performance assessment, 2022. URL `https://www.pnnl.gov/sites/default/files/media/file/ESGC%20Cost%20Performance%20Report%202022%20PNNL-33283.pdf`. Accessed on May 26, 2023.

M. Vogt, K. Koch, A. Turetskyy, F. Cerdas, S. Thiede, and C. Herrmann. Model-based energy analysis of a dry room HVAC system in battery cell production. *Procedia CIRP*, 98:157–162, 2021. ISSN 22128271.

F. Wang, Y. Deng, and C. Yuan. Design and Cost Modeling of High Capacity Lithium Ion Batteries for Electric Vehicles through A Techno-economic Analysis Approach. *Procedia Manufacturing*, 49:24–31, 2020. ISSN 23519789.

B. Welsch, L. Göllner-Völker, D. O. Schulte, K. Bär, I. Sass, and L. Schebek. Environmental and economic assessment of borehole thermal energy storage in district heating systems. *Applied Energy*, 216:73–90, 2018. ISSN 03062619.

J. Weniger, T. Tjaden, and V. Quaschning. Sizing and grid integration of residential pv battery systems. In *8th International Renewable Energy Storage Conference and Exhibition (IRES 2013), Berlin*, 2013.

J. Weniger, T. Tjaden, J. Bergner, and V. Quaschning. Sizing of battery converters for residential PV storage systems. *Energy Procedia*, 99:3–10, 2016. ISSN 18766102.

M. Wentker, M. Greenwood, and J. Leker. A Bottom-Up Approach to Lithium-Ion Battery Cost Modeling with a Focus on Cathode Active Materials. *Energies*, 12(3):504, 2019.

B. G. Westphal and A. Kwade. Critical electrode properties and drying conditions causing component segregation in graphitic anodes for lithium-ion batteries. *Journal of Energy Storage*, 18:509–517, 2018. ISSN 2352152X.

W. J. Weydanz, H. Reisenweber, A. Gottschalk, M. Schulz, T. Knoche, G. Reinhart, M. Masuch, J. Franke, and R. Gilles. Visualization of electrolyte filling process and influence of vacuum during filling for hard case prismatic lithium ion cells by neutron imaging to optimize the production process. *Journal of Power Sources*, 380:126–134, 2018. ISSN 03787753.

D. L. Wood, J. Li, and C. Daniel. Prospects for reducing the processing cost of lithium ion batteries. *Journal of Power Sources*, 275:234–242, 2015. ISSN 03787753.

D. L. Wood, J. Li, and S. J. AN. Formation challenges of lithium-ion battery manufacturing. *Joule*, 3(12):2884–2888, 2019. ISSN 25424351.

World Economic Forum. Global risks report 2023, 2023.

G. Wu, A. Inderbitzin, and C. Bening. Total cost of ownership of electric vehicles compared to conventional vehicles: A probabilistic analysis and projection across market segments. *Energy Policy*, 80:196–214, 2015. ISSN 03014215.

C. Xie, Y. Li, Y. Ding, and J. Radcliffe. Evaluating levelized cost of storage (LCOS) based on price arbitrage operations: With liquid air energy storage (LAES) as an example. *Energy Procedia*, 158:4852–4860, 2019. ISSN 18766102.

Y. Xu, K. Yang, and J. Yuan. Levelized cost of offshore wind power in China. *Environmental Science and Pollution Research*, 28(20):25614–25627, 2021. ISSN 16147499.

T. Yang, W. Liu, G. J. Kramer, and Q. Sun. Seasonal thermal energy storage: A techno-economic literature review. *Renewable and Sustainable Energy Reviews*, 139:110732, 2021. ISSN 13640321.

G. Yingzhe. CATL aims to mass produce sodium-ion batteries in 2023, 2022. URL `https://www.caixinglobal.com/2022-10-25/catl-aims-to-mass-produce-sodium-ion-batteries-in-2023-101955814.html`. Accessed on July 29, 2024.

C. Yuan, Y. Deng, T. Li, and F. Yang. Manufacturing energy analysis of lithium ion battery pack for electric vehicles. *CIRP Annals*, 66(1):53–56, 2017. ISSN 00078506.

B. Zakeri and S. Syri. Electrical energy storage systems: A comparative life cycle cost analysis. *Renewable and Sustainable Energy Reviews*, 42:569–596, 2015. ISSN 13640321.

G. Zang, J. Zhang, S. Xu, and Y. Xing. Techno-economic analysis of cathode material production using flame-assisted spray pyrolysis. *Energy*, 218:119504, 2021. ISSN 03605442.

Y. Zhang, A. Lundblad, P. E. Campana, F. Benavente, and J. Yan. Battery sizing and rule-based operation of grid-connected photovoltaic-battery system: A case study in sweden. *Energy Conversion and Management*, 133:249–263, 2017. ISSN 01968904.

Y. S. Zhang, N. E. Courtier, Z. Zhang, K. Liu, J. J. Bailey, A. M. Boyce, G. Richardson, P. R. Shearing, E. Kendrick, and D. J. L. Brett. A Review of Lithium–Ion Battery Electrode Drying: Mechanisms and Metrology. *Advanced Energy Materials*, 12(2):2102233, 2022. ISSN 1614-6832.